International Telecommunication Union

ITU-R

Radiocommunication Sector of ITU

Report ITU-R M.2234
(11/2011)

The feasibility of sharing sub-bands between oceanographic radars operating in the radiolocation service and fixed and mobile services within the frequency band 3-50 MHz

M Series

Mobile, radiodetermination, amateur and related satellite services

International Telecommunication Union

Foreword

The role of the Radiocommunication Sector is to ensure the rational, equitable, efficient and economical use of the radio-frequency spectrum by all radiocommunication services, including satellite services, and carry out studies without limit of frequency range on the basis of which Recommendations are adopted.

The regulatory and policy functions of the Radiocommunication Sector are performed by World and Regional Radiocommunication Conferences and Radiocommunication Assemblies supported by Study Groups.

Policy on Intellectual Property Right (IPR)

ITU-R policy on IPR is described in the Common Patent Policy for ITU-T/ITU-R/ISO/IEC referenced in Annex 1 of Resolution ITU-R 1. Forms to be used for the submission of patent statements and licensing declarations by patent holders are available from http://www.itu.int/ITU-R/go/patents/en where the Guidelines for Implementation of the Common Patent Policy for ITU-T/ITU-R/ISO/IEC and the ITU-R patent information database can also be found.

Series of ITU-R Reports

(Also available online at http://www.itu.int/publ/R-REP/en)

Series	Title
BO	Satellite delivery
BR	Recording for production, archival and play-out; film for television
BS	Broadcasting service (sound)
BT	Broadcasting service (television)
F	Fixed service
M	**Mobile, radiodetermination, amateur and related satellite services**
P	Radiowave propagation
RA	Radio astronomy
RS	Remote sensing systems
S	Fixed-satellite service
SA	Space applications and meteorology
SF	Frequency sharing and coordination between fixed-satellite and fixed service systems
SM	Spectrum management

Note*: This ITU-R Report was approved in English by the Study Group under the procedure detailed in Resolution ITU-R 1.*

Electronic Publication
Geneva, 2012

REPORT ITU-R M.2234

The feasibility of sharing sub-bands between oceanographic radars operating in the radiolocation service and fixed and mobile services within the frequency band 3-50 MHz

Summary

This Report presents the results of several sharing studies which were performed prior to WRC-12, in support of Agenda item 1.15 (Resolution 612 (WRC-07)). The studies that were undertaken focused on identifying the interference mechanisms between oceanographic radar systems identified in Recommendation ITU-R M.1874[1] and fixed and mobile systems which are currently operating in the frequency band 3-50 MHz. In this frequency band, interference may potentially occur through both ground-wave and sky-wave propagation. The studies addressed the interference upon oceanographic radars and fixed and mobile systems.

Several administrations have conducted theoretical interference analyses between generic oceanographic radars and fixed and mobile systems. The analyses showed that, interference to a fixed or mobile station could occur as a result of either ground wave or sky-wave propagation, when the fixed or mobile service receive channel falls within the sweep bandwidth of the oceanographic radar.

The results of the ground-wave analysis showed that land path separation distances between the oceanographic radar transmitter and the mobile or fixed receiver varied as a function of noise environment, operational frequency, transmit power, soil type and antenna directionality. The minimum separation distances varied between 40 km to 120 km for “rural” and 50 km to 170 km for “quiet rural” noise environments with an oceanographic radar signal level of 19 dBW e.i.r.p. The analysis did not take into account ground cover, vegetation, buildings and other obstructions or variations in elevation. Taking these factors into account may significantly reduce the required separation distances.

For ground-wave propagation through sea path the minimum separation distances varied between 190 km to 790 km for “rural” and 200 km to 920 km for “quiet rural” noise environments with an oceanographic radar signal of 19 dBW e.i.r.p.

The theoretical studies also showed that sky-wave interference from oceanographic radars to fixed and mobile systems and vice versa can occur as a function of the characteristics which are associated with sky-wave propagation. One study showed that for the situation of globally employed co-channel links, 0.1% to 12.7% of the HF links would be negatively impacted by interference from oceanographic radar, depending on frequency band, propagation conditions and incumbent service characteristics.

Three additional studies evaluated the interference occurrence based on the percentage of time that the interference to noise ratio exceeded –6 dB. The first study examined back-lobe interference within the European region. The duty cycle and the co-channel occurrence time were considered. It was found that I/N= –6 dB was not exceeded for more than 18.4% of the time, for any of the oceanographic radar systems. The second study examined worldwide interference caused by a directional antenna. The interference signal was averaged to account for waveform duty cycle and the co-channel occurrence time. The results show that I/N= –6 dB was not exceeded for more than 1.6% of the time and area. A separate analysis considered omnidirectional antennas and median noise levels; it confirms the increase in interference occurrence when considering main lobe peak interference level as distinct from back lobe average interference level.

These studies show a dependence on the size of the geographic region under study. Sky-wave propagation characteristics suggest strongest interference is expected within the one-hop sky-wave propagation zone, which typically ranges from 1 000 to 3 000 km.

There is currently no ITU-R reference to determine whether these percentages are satisfactory for the fixed or mobile service operating in 3 to 50 MHz.

---

[1] Recommendation ITU-R M.1874 – Technical and operational characteristics of oceanographic radars operating in sub-bands within the frequency range 3-50 MHz.

Results of studies suggest analysis of interference impact depends on antenna gain pattern, geographical regions, and how the interference manifests itself in a receiver from the mobile or fixed service. It is noted that oceanographic radars operate over an emission bandwidth range from 25 to 150 kHz while fixed and mobile receivers operate with bandwidths from 3 to 12 kHz.

In support of the theoretical studies, ground-wave and sky-wave field-strength measurements were conducted. The results of the ground-wave measurements showed that interference to fixed and mobile systems could occur via ground-wave propagation if those systems are operating in a co-channel mode. The measurements were taken within the theoretical study ground-wave maximum separation distances and within the main beam of the oceanographic radar. A preliminary measurement was taken that indicated interference from sky-wave mode also occurs. In addition, spectrum congestion within lower portions of the HF frequency band has also been demonstrated through occupancy measurements that were conducted on the Korean peninsula. These measurements also showed that, for the geography in which the measurements were made, the higher frequencies within the HF frequency band (>20 MHz) were less congested, however it was also noted that this measurement analysis was undertaken during a low sunspot activity period. Theoretical analysis of congestion in the frequency bands up to 50 MHz was not undertaken.

This report also outlines several interference mitigation techniques that could be used to reduce the interference from oceanographic radars to fixed and mobile systems. These include:

1) Reducing ground-wave interference by adhering to the separation distances that have been outlined in Table 6 and Table 8;

2) Implementing time synchronization of multiple radar transmissions within the same swept bandwidth to reuse the frequency;

3) Limiting the e.i.r.p to 25 dBW or less; and

4) Implementing back lobe attenuation on the transmitting antenna.

A more detailed summary of the analyses and the measurements can be found in § 9 of this Report.

1 Introduction

WRC-12 Agenda item 1.15 calls for the consideration of an allocation to the radiolocation service in the 3 to 50 MHz range. These allocations could be used for the operation of oceanographic radars that monitor the sea surface for wave heights, currents and tracking of large objects. These radars have an operational range up to 300 km. Oceanographic radars have been operating in the 3 to 50 MHz range since 1970s on an experimental, non-interference basis. Increased reliance on the data from these systems for maritime safety, oceanographic, climatological, meteorological and disaster response operations have driven the need to improve the regulatory status of oceanographic radars while taking into account the protection of existing allocated services. WRC-12 Agenda item 1.15 was established with the understanding that spectrum would be allocated on a shared basis. Reallocation of spectrum from an existing allocated radio service to the radiolocation services is not the intent.

There is an increasing interest in the ability to accurately measure the currents and waves in coastal waters and to maintain maritime domain awareness. Oceanographic radar systems operating at frequencies higher than 50 MHz are limited in their ability to provide data meeting the combined range, accuracy and resolution requirements. The global oceanography community is planning for the implementation of coastal oceanographic radar networks. The potential benefits to society for improved measurement of coastal currents and sea state include a better understanding of issues like coastal pollution, fisheries management, search and rescue, beach erosion, maritime navigation and sediment transport. Oceanographic radar measurements of the sea surface provide support to meteorological operations through the collection of sea state and dominant ocean wave data. In addition, HF oceanographic radar technology has applications in maritime domain awareness by allowing the long range sensing of surface vessels. This could benefit the safety and security of shipping and ports.[2]

There are two typical paths of propagation for HF radio waves (Report ITU-R F.2087)

– Ground wave: for path up to line-of-sight (LOS) and beyond. This mode is normally used for path lengths up to 50-200 km.
– Sky wave: for beyond LOS path affected via reflection at the ionosphere, 100-350 km above the Earth. Ranges of several thousands of kilometres are common.

The objectives of this Report are to:

1) assess and quantify the potential for the degradation of fixed or mobile services which could occur as the result of oceanographic radar operations when operating co-channel;
2) assess oceanographic radar compatibility with incumbent fixed and mobile service users within the frequency bands;
3) to assess the impact that fixed or mobile service operations could have upon oceanographic radars operating co-channel.

All applicable ITU-R Recommendations regarding ground-wave propagation, sky-wave propagation, noise, point-to-point or line-of-sight propagation, system characteristics and system protection criteria levels for systems that operate in the frequency band 3 to 50 MHz have been used as the basis for the analysis.

Sky-wave propagation is not the desired propagation mode for oceanographic radars because oceanographic radars sense conditions of the coastal ocean surface via ground-wave propagation. However, since the radars typically use simple omnidirectional monopole antennas that radiate energy by means of both ground-wave and sky-wave propagation modes there is the potential for oceanographic radars to interfere with other HF services via the ground-wave and/or the sky-wave mode of propagation. Although there could be situations in which interference from both ground-wave and sky-wave propagation could occur simultaneously, these situations were not addressed in this study.

2 Incumbent service characteristics and protection criteria

The ITU-R provided information about protection criteria and system parameters to be used in the WRC-12 Agenda item 1.15 studies. In particular, The ITU-R suggested using the values contained in Recommendation ITU-R F.339-7 for fixed and mobile systems operating below 30 MHz, corresponding to analogue telephony single sideband suppressed carrier systems and digital 9 600 b/s 64-QAM:

– receiver's bandwidth: 3 kHz;
– signal-to-noise density ratio of 61 dB for analogue telephony single sideband suppressed carrier systems marginally commercial under fading conditions;
– signal-to-noise ratio of 32 dB in 3 kHz for digital data under fading condition.

[2] Use of Coastal Ocean Dynamics Application Radar (CODAR) Technology in U.S. Coast Guard Search and Rescue Planning, David Ullman; James O'Donnell; Christopher Edwards; Todd Fake; David Morschauser; Coast Guard Research And Development Center Groton CT.

The ITU-R states that, the noise figure of a HF receiver being lower than the external noise (which is the dominant limiting factor for HF communications), studies should refer to Recommendation ITU-R P.372-10 for the radio noise values which are appropriate for "quiet rural" and "rural" noise, according to the case, with an I/N ratio of –6 dB as the common preferred protection ratio for mobile and fixed HF systems.

There are also electronic news gathering (ENG) applications in spectrum currently allocated to the fixed and mobile services in the frequency bands below 50 MHz. The characteristics for ENG can be found in Recommendation ITU-R M.1824.

The ITU-R also provided information about protection criteria and system parameters to be used in the WRC 12 Agenda item 1.15 studies with regards to the mobile service operated above 30 MHz. In particular, it suggested using the values contained in Recommendation ITU-R M.1808, containing the protection criteria:

− I/N = –6 dB be used as the interference threshold for land mobile systems;
− I/N = –10 dB be used for applications with greater protection requirements, such as public protection and disaster relief (PPDR).

The ITU-R also suggested that the propagation calculations be based upon the models and methods outlined in Recommendation ITU-R P.1546-4 or Report ITU-R SM.2028-1.

In addition, the following parameters were used:

− receive antenna gain: 0 dBi;
− external noise figure: Rural and Quiet rural (Recommendation ITU-R P.372-10).

3 Characteristics of oceanographic radars

Recommendation ITU-R M.1874 details the characteristics of HF oceanographic radars to be considered in compatibility studies under WRC-12 Agenda item 1.15.

A variety of antenna types are currently used with high-frequency oceanographic radar systems.

Some systems utilize either a 3-element Yagi antenna or a phased-array system to sweep azimuthally with some using multiple sets of Yagi antenna for transmission. The majority of systems use a vertical dipole antenna, either individually or in phased array systems. All of the oceanographic radar systems utilize vertical polarization, so the transmit antenna elevation beam width is limited (35-60 degrees). Whatever the antenna type, the antenna gain for ground-wave propagation is typically 0-2 dBi. The maximum antenna gain for sky-wave propagation varies from 6 to 8 dBi. Therefore the type of propagation studied has to be clearly defined in order to use proper values for antenna gain.

Furthermore, some systems have limited duty cycles and wide emission bandwidth (sweeping width). Thus, the transmitted signals only intercept the receiver's bandwidth of incumbent services for a limited amount of time (e.g. the oceanographic radar system that has 0.5 duty cycle and 150 kHz bandwidth would intercept the incumbent system bandwidth (typically 3 kHz) 1% of time). Some studies used average power whereas others used peak power for the radar. Table 1 summarizes the system characteristics for all existing generic oceanographic radars described in Recommendation ITU-R M.1874.

As an example, characteristics of some generic directional oceanographic radars are summarized in Table 2 and Fig. 1.

TABLE 1

Generic oceanographic radar parameters for compatibility studies

System No.*	Frequency band (MHz)	Peak power (W)	Emission BW (kHz)	Sky-wave propagation				Ground-wave propagation			
				Antenna gain main lobe (dBi)	P main lobe** (dBW)	Antenna gain back lobe (dBi)	P back lobe** (dBW)	Antenna gain main lobe (dBi)	P main lobe** (dBi)	Antenna gain back lobe (dBi)	P back lobe** (dBW)
System 1	5	50	25	8	25/13	8	25/13	2	19/7	2	19/7
System 2	13	50	50	8	25/10	8	25/10	2	19/4	2	19/4
System 3	27	50	100	8	25/7	8	25/7	2	19/1	2	19/1
System 4	42	50	125	8	25/6	8	25/6	2	19/0	2	19/0
System 5	8	30	12.5	8	23/14	–6	9/0	2	17/8	–12	3/–6
System 6	12	30	50	8	23/8	–6	9/–6	2	17/2	–12	3/–12
System 7	16	30	50	8	23/8	–6	9/–6	2	17/2	–12	3/–12
System 8	25	30	75	8	23/6	–6	9/–8	2	17/0	–12	3/–14
System 9	42	30	1000	8	23/–5	–6	9/–19	2	17/–11	–12	3/–25
System 10	9.2	50***	22	6	23/11	–12	5/–7	0	17/5	–18	–1/–13
System 11	24.5	50***	100	15	32/14	–3	14/–4	9	26/8	–9	8/–10
System 12	24.5	50***	100	6	23/5	–12	5/–13	0	17/–1	–18	–1/–19
System 13	41.9	50***	300	6	23/0	–12	5/–18	0	17/–6	–18	–1/–24

* System number shown in the Recommendation ITU-R M.1874.

** Peak power/averaged power: averaged power is considering peak power, emission bandwidth, receiver's bandwidth, duty cycle and transmit antenna gain in interested direction.

*** For systems 10 to 13, power 50 W is used to conduct compatibility studies within the scope of Resolution 612 (WRC-07).

TABLE 2

Radar parameters of FMICW generic directional oceanographic radars

Characteristics			Frequency Band					
			4.5 MHz ±1 MHz	**9 MHz ±1 MHz**	**13 MHz ±1 MHz**	**16 MHz ±1 MHz**	**25 MHz ±3 MHz**	**43 MHz ±4 MHz**
Frequency*		(MHz)	4.5	9	13	16	24.5	43
Modulation			FMICW					
Transmit antenna			3-elements Yagi					
Transmit antenna gain	Front	(dBi)	6.3					
	Rear	(dBi)	–11.2					
	Pattern	–	See Fig. 1					
Peak transmit power into antenna		(W)	50					
Duty ratio		–	0.5					
Sweep bandwidth**		(kHz)	25	22	50	50	100	125

* The centre frequencies of each frequency band are used for the study except for the frequency band 25 MHz ±3 MHz. The frequency of system 12 (24.5 MHz) is used for the frequency band instead.

** The sweep bandwidths are based on Recommendation ITU-R M.1874 except for the frequency band 25 MHz ±3 MHz.
The bandwidth of system 12 (100 kHz) is used for the frequency band.

FIGURE 1

Typical oceanographic radar antenna patterns[3]

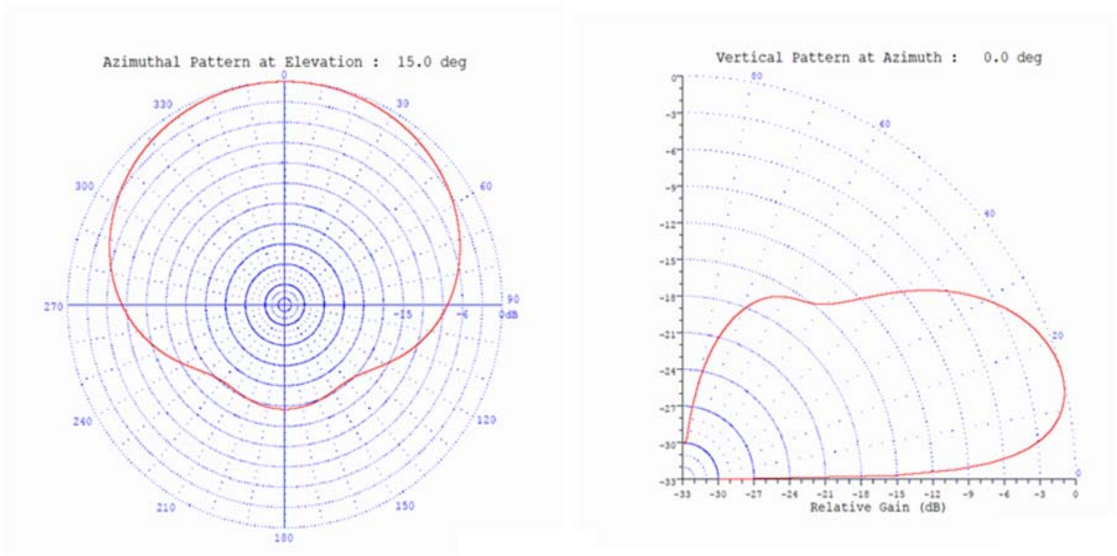

[3] The gain in the horizontal direction depends on the ground coupling.

4 Theoretical ground-wave analysis

4.1 Ground-wave propagation model

A ground wave is a radio wave that propagates close to the surface of the Earth. In this mode the radio wave propagates by interacting with the semi-conductive surface of the earth. The wave "clings" to the surface and thus follows the curvature of the earth. Ground-wave propagation is the required propagation mode for the operation of oceanographic radars.

The ground-wave propagation mode is stable and predictable as described in Recommendation ITU-R P.368-9 for frequencies up to 50 MHz. Measurement data showed a very good correlation between measured propagation losses and losses based on the ground-wave propagation model described in Recommendation ITU-R P.368-9 as seen in Attachment 5. The use of Recommendation ITU-R P.1546-4 was another available option for use in the ground-wave analysis. For the reasons discussed in Attachment 5, and in particular § 4 of the attachment, Recommendation ITU-R P.1546-4 was found to not be an appropriate model for use in these sharing studies.

Recommendation ITU-R P.368-9 provides information on the ground-wave mode over smooth homogeneous Earth for various sets of electrical constants of the ground. A software based implementation of this model, GRWAVE[4], was used for all ground-wave analysis calculations.

4.2 Input parameters for GRWAVE based analysis

The path lengths of a ground-wave signal are usually on the order of 50-200 km where the longer ranges (200 km) occur at lower frequencies. In the ground-wave mode, the ultimate range depends on factors such as transmitter power, frequency (lower frequency gives greater distance) and surface conditions (wet ground gives greater distance, with the best conditions for these frequencies being over seawater). Higher conductivity and permittivity values result in longer propagation ranges. The analysis took these factors into account by setting the relative permittivity and conductivity of the surface of the earth for the worst case:

– for land path, input parameters are set to "land" (i.e. with relative permittivity set to 22 and conductivity set to 0.003 S/m); since the propagation losses along other types of ground such as medium dry, dry and very dry ground are higher (see Table 3 below);
– for sea path, input parameters are set to "average salinity" (i.e. with relative permittivity set to 70 and conductivity set to 5 S/m); since the propagation losses along other types of water are higher.

4.3 Path loss calculation

Let P_r be the radar power in the rear direction. The minimum path loss P_L necessary for each oceanographic system in order not to interfere with the receiver is such that:

$$P_r + P_L < I_{max}$$

where I_{max} is the maximum interference to the incumbent service receiver.

A comparison of free space propagation losses and ground wave above various types of ground ("very dry ground", "dry ground", and "land") at 4 MHz follows in Table 3.

[4] GRWAVE is available through ITU-R SG 3.

TABLE 3

Comparison of propagation losses in dB at 4 MHz for free space loss and ground wave above various types of ground (T=emitter height, R=receiver height) using GRWAVE

	T=3 m, R=2.5 m				T=3, R=5 m
Distance (km)	**FSL**	**Very dry ground**	**Medium ground**	**Land**	**Land**
10	64.5	109.9	98.6	94.3	94.3
20	70.5	122.2	110.8	106.7	
30	74.0	129.5	118.2	114.1	
40	76.5	134.8	123.4	119.3	
50	78.5	139.1	127.7	123.6	123.6
70	81.4	145.8	134.4	130.3	
100	84.5	153.7	142.2	138.1	
150	88.0	164.1	152.6	148.4	
200	90.5	173.1	161.5	157.3	157.2
300	94.0	189.6	177.7	173.4	173.4
350	95.4	205.3	193.3	188.9	188.9

Table 3 shows that:

– for inland propagation, the minimum propagation losses occur for the “land” type;

– the losses are the same whatever the receive antenna height (here 2.5 m and 5 m).

4.4 Derivation of noise and maximum interference levels

4.4.1 External noise calculation

The external noise is a combination of three components: man-made noise, galactic noise, and atmospheric noise. Each will be discussed in the following sections.

4.4.2 Man-made noise

Man-made noise depends on the frequency and the environment.

Section 5 in Recommendation ITU-R P.372-10 details how to derive median values of man-made noise energy N_{man} for a number of environments:

$$N_{man} = c - d \log f - 204 \text{ (dBW/Hz)}$$

where f is the operational frequency expressed in MHz and c and d (Table 4) are dependent on the environment.

TABLE 4

Noise calculation factors

Environmental category	*c*	*d*
Rural (curve C)	67.2	27.7
Quiet rural (curve D)	53.6	28.6

Applying this formula for "rural" and "quiet rural" environments, one can then derive the resulting man-made noise level N_{man}.

4.4.3 Galactic noise

Galactic noise N_{gal} only depends on frequency. The galactic noise component will not be observed at frequencies below the ionospheric f_{oF2} critical frequency (Recommendation ITU-R P.372-10).

Figure 2 further indicates that galactic noise only contributes at high frequencies in the "quiet rural" noise environment.

FIGURE 2

Man-made, galactic, and example atmospheric noise energy models.

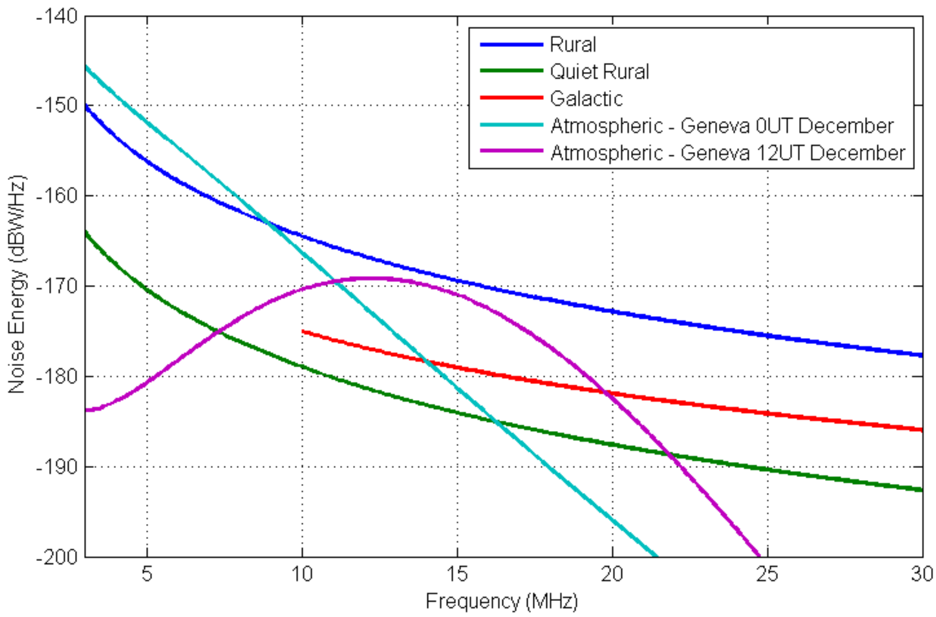

4.4.4 Atmospheric noise

Atmospheric noise N_{atm} depends on frequency, time of day and season.

4.4.5 Resulting external noise calculation

Software NOISEDAT developed by ITU-R enables one to calculate these three components, and therefore the resulting external noise:

$$N=10*\log_{10}(10^\wedge(N_{gal}/10)+10^\wedge(N_{man}/10)+10^\wedge(N_{atm}/10))$$

For instance at 9 MHz:

1) man-made noise is equal to –163.2 and –177.7 dBW/Hz respectively for "rural" and "quiet rural" environments;

2) galactic noise is equal to –173.9 dBW/Hz;

3) atmospheric noise depends on the brightness temperature, with maximum values during the night and minimum values at midday, when the solar elevation angle is the highest. Over Europe, atmospheric noise grossly varies from –175 to –158 dBW/Hz.

Therefore at 9 MHz the external noise varies from –163 dBW/Hz to –157 dBW/Hz for "rural" environment and from –170 to –157 dBW/Hz to for "quiet rural" environment.

The value adopted for the external noise depends on the propagation path:

1) for ground-wave propagation with no time variations, the worst value for N is estimated from the minimum N_{atm} value, thus corresponding to a worst case

2) for sky-wave propagation, with daily, monthly and yearly variations, N is estimated from the N_{atm} value which is at the minimum 80% of the time.

4.5 Maximum interference level

Once the external noise N is known, the maximum interference level into a 3 kHz receiver is:

$$I_{max} = N + (I/N)_{long\ term} + 10*\log_{10}(3000)$$

with

– I_{max} the maximum interference level in the incumbent service receiver;

– $(I/N)_{long\ term} = -6$ dB;

– N the external noise value in dBW/Hz, calculated in "rural" and "quiet rural" environments

The maximum interference level, I_{max}, is derived from the value of the lowest atmospheric noise level. Table 5 provides an estimation of the external noise and the maximum interference levels

TABLE 5

Estimation of external noise and maximum interference level

	Unit	5 MHz	9 MHz	13 MHz	16 MHz	25 MHz	43 MHz
Natm	dBW/Hz	–181.6	–175.4	–179.1	–189.1	–215.7	–252
Ngal	dBW/Hz	–168.1	–173.9	–177.6	–179.7	–184.2	–190
Nman rural	dBW/Hz	–156.2	–163.2	–167.7	–170.2	–175.5	–182
N rural	dBW/Hz	–155.9	–162.6	–167.0	–169.7	–175.0	–181.4
Imax rural(1)	**dBW**	**–127.1**	**–133.8**	**–138.2**	**–140.9**	**–146.2**	**–152.6**
Nman quiet rural	dBW/Hz	–170.4	–177.7	–182.3	–184.8	–190.4	–197
N quiet rural	dBW/Hz	–166.0	–170.6	–174.5	–178.2	–183.3	–189.2
Imax quiet rural (1)	**dBW**	**–137.2**	**–141.9**	**–145.7**	**–149.4**	**–154.5**	**–160.4**

(1) I_{max} calculated for a 3 kHz receiver bandwidth and I/N= –6.

4.6 Results

Separation distances between oceanographic radar systems and systems of the fixed and mobile service shown below are derived from a calculation of the worst case external noise, or minimum value of N.

4.6.1 Land path

Table 6 lists the separation distances which are required in order to stay below the maximum interference level for "rural" and "quiet rural" environments for a land path which is located in the back lobe of the oceanographic radar's antenna.

The results are rounded up to the nearest multiple of 10 km, which explains why some systems with slightly different characteristics lead to similar separation distances.

TABLE 6

Separation distances relative to each oceanographic system ground-wave propagation through land path

	Frequency band (MHz)	e.i.r.p. back lobe* (dBW)	Minimum path loss (dB)		Separation distances (km)	
			rural	quiet rural	rural	quiet rural
System 1	5	19	146.1	156.2	**120**	**170**
System 2	13	19	157.2	164.7	**100**	**110**
System 3	27	19	165.2	173.5	**80**	**100**
System 4	42	19	171.6	179.4	**80**	**90**
System 5	8	3	136.6	144.9	**50**	**70**
System 6	12	3	141.2	148.7	**50**	**60**
System 7	16	3	143.9	152.4	**40**	**60**
System 8	25	3	149.2	157.3	**40**	**60**
System 9	42	3	155.6	163.4	**40**	**60**
System 10	9.2	–1	132.8	140.9	**40**	**60**
System 11	24.5	8	154.2	164.5	**50**	**70**
System 12	24.5	–1	145.2	153.5	**40**	**50**
System 13	41.9	–1	151.6	159.4	**40**	**50**

* E.i.r.p in the horizontal direction. E.i.r.p in the skyward direction is typically higher.

Studies indicate that, for land path propagation and back lobe e.i.r.p. of oceanographic radar systems, separation distances range from 50 km up to 170 km in “quiet rural” environment, and from 40 km up to 120 km in “rural” environment.

Table 7 shows the separation distances via a land path for a “rural” and “quiet rural” environment for various frequency bands and e.i.r.p.

TABLE 7

Ground-wave analysis via a land path using decreasing e.i.r.p.

Frequency band (MHz)		Separation distances for rural (km)			Separation distances for quiet rural (km)			
	19(2) (dBW)	16 (dBW)	10 (dBW)	3 (dBW)	19(2) (dBW)	16 (dBW)	10 (dBW)	3 (dBW)
5	120	110	80	60	170	150	120	90
9	100	80	70	50	130	110	90	70
13	100	80	60	50	110	100	80	60
16(1)	80	70	60	40	100	100	80	60
25(1)	80	70	60	40	100	90	80	60
42(1)	80	70	60	40	100	90	80	60

(1) Values at these frequencies are often similar due to the fact that the calculations round up to the next multiple of 10 km.

(2) The 19 dBW e.i.r.p. corresponds with a 2 dBi transmit antenna gain in the horizontal direction for ground-wave propagation in comparison to the higher gain of 8 dBi and a maximum e.i.r.p of 25 dBW that apply at higher elevation angles and to the sky-wave analysis.

In some circumstances, these separation distances may be reduced by terrain and man-made obstructions behind the radar, and backlobe attenuation.

As shown in Table 7, further reduction of power reduces the separation distance.

4.6.2 Sea path

Table 8 below indicates the separation distance required in order to respect the maximum interference level for “rural” and “quiet rural” environment for a sea path in the main lobe.

The results are rounded up to the next multiple of 10 km, which explains why some systems with slightly different characteristics lead to similar separation distances.

TABLE 8

Separation distances relative to each oceanographic radar system ground-wave propagation through sea path, receiver located on sea

	Frequency band (MHz)	e.i.r.p. main lobe(1) (dBW)	Minimum path loss (dB)		Separation distances (km)	
			rural	quiet rural	rural	quiet rural
System 1	5	19	146.1	156.2	790	920
System 2	13	19	157.2	164.7	480	520
System 3	26	19	165.2	173.5	280	320
System 4	42	19	169.6	179.4	200	230
System 5	8	17	150.6	158.9	580	680
System 6	12	17	155.2	162.7	450	530
System 7	16	17	157.9	166.4	380	450
System 8	25	17	163.2	171.3	270	320
System 9	42	17	167.6	177.4	190	230
System 10	9.2	17	150.8	158.9	570	650
System 11	24.5	26	172.2	182.5	310	350
System 12	24.5	17	163.2	171.5	270	310
System 13	41.9	17	167.6	177.4	190	230

(1) E.i.r.p in the horizontal direction. E.i.r.p in the skyward direction is typically higher.

Studies indicate that, for ground-wave propagation over a sea path, separation distances start from 230 up to 920 km in "quiet rural" environment, and from 190 up to 790 km in "rural" environment.

Table 8 shows the separation distances via a sea path for a "rural" and "quiet rural" environment for various frequency bands and e.i.r.p. As shown in Table 9, a reduction of power reduces the separation distances.

TABLE 9

Ground-wave analysis via sea path using decreasing e.i.r.p.

Frequency band (MHz)	Separation distances for rural (km)				Separation distances for quiet rural (km)			
	19(1) (dBW)	16 (dBW)	10 (dBW)	3 (dBW)	19(1) (dBW)	16 (dBW)	10 (dBW)	3 (dBW)
5	790	750	670	590	920	880	800	710
9	590	560	500	440	670	640	580	510
13	480	440	400	350	520	490	450	400
16	390	370	340	290	450	430	390	350
25	280	270	240	210	320	300	280	250
42	200	190	180	160	230	220	200	180

(1) The 19 dBW e.i.r.p. corresponds with a 2 dBi transmit antenna gain in the horizontal direction for ground-wave propagation in comparison to the higher gain of 8 dBi and a maximum e.i.r.p of 25 dBW that apply at higher elevation angles and to the sky-wave analysis.

5 Frequency dependent rejection analysis

In addition to separation distance, frequency separation can also be used to minimize interference. Conducting an analysis for frequency separation requires performing a frequency dependent rejection (FDR) analysis. The FDR analysis uses transmitter emission masks and receiver selectivity curves. It calculates the amount of rejection applied to the interference power due to non-overlapping regions of the transmitter envelope and receiver selectivity curve.

5.1 Transmitter masks

The oceanographic radars are designed to have adjustable sweep bandwidths so the user can maximize their data resolution while effectively managing their use of the spectrum. As a result, typical sweep bandwidths are much smaller than the system's maximum available value and, in practice; oceanographic radars are rarely operated at or near the maximum sweep bandwidths.

Bandwidths[5] that will be used in the analysis are on the order of; 25 kHz at operational frequencies around 4.5 MHz and 9.0 MHz, 50 kHz at operational frequencies around 13 MHz and 100 kHz at operational frequencies around 26 MHz and 42 MHz.

Figures 3 to 5 contain the plots of the oceanographic radar emission envelopes, derived from measured data, used in the FDR analysis. No measurement data is available for frequencies around 9 MHz, but it is assumed that the envelope would be similar to the envelope at 4.5 MHz. In a similar manner, there is no measurement data available for frequencies near 42 MHz, however it is assumed that the sweep characteristics dictate that the emission envelope would be similar to the plot for 26 MHz.

FIGURE 3

Emission envelope of oceanographic radar operating near 4.5 MHz with a typical sweep bandwidth (~25 kHz)

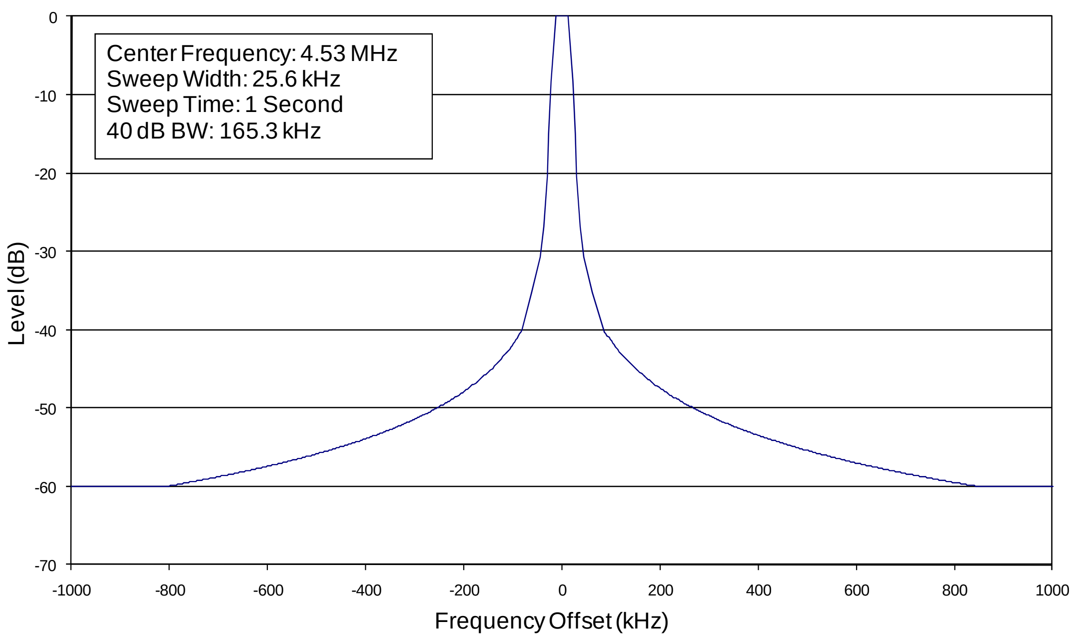

[5] These are typical bandwidths for oceanographic radar systems.

FIGURE 4

Emission envelope of oceanographic radar operating near 13 MHz with a typical sweep bandwidth (~50 kHz)

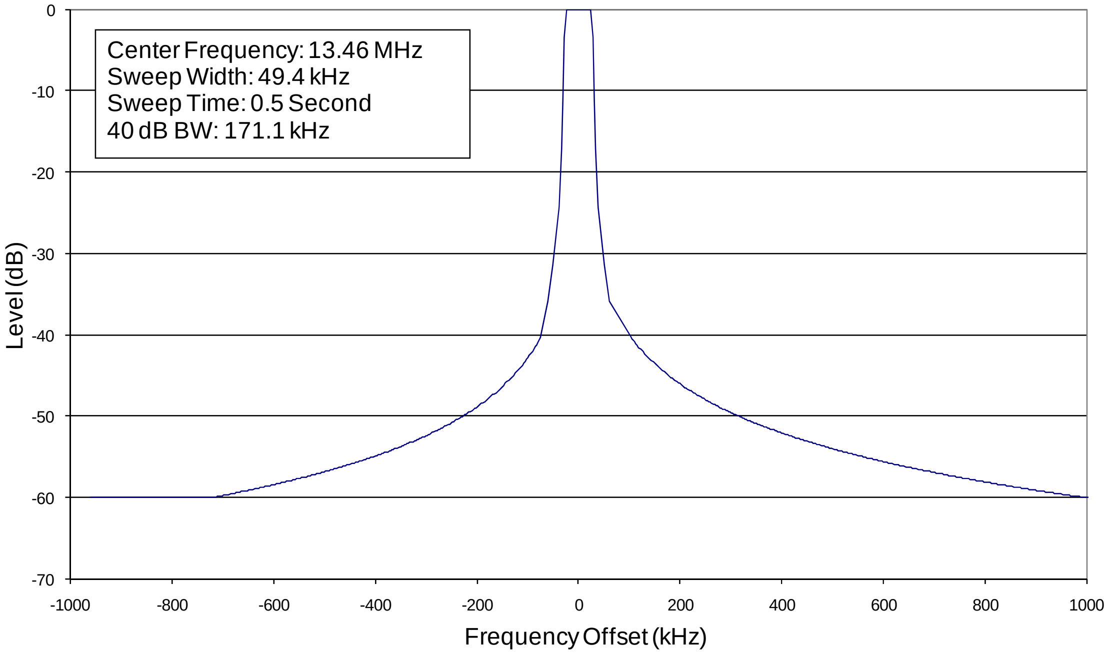

FIGURE 5

Emission envelope of oceanographic radar operating near 26 MHz with a typical sweep bandwidth (~100 kHz)

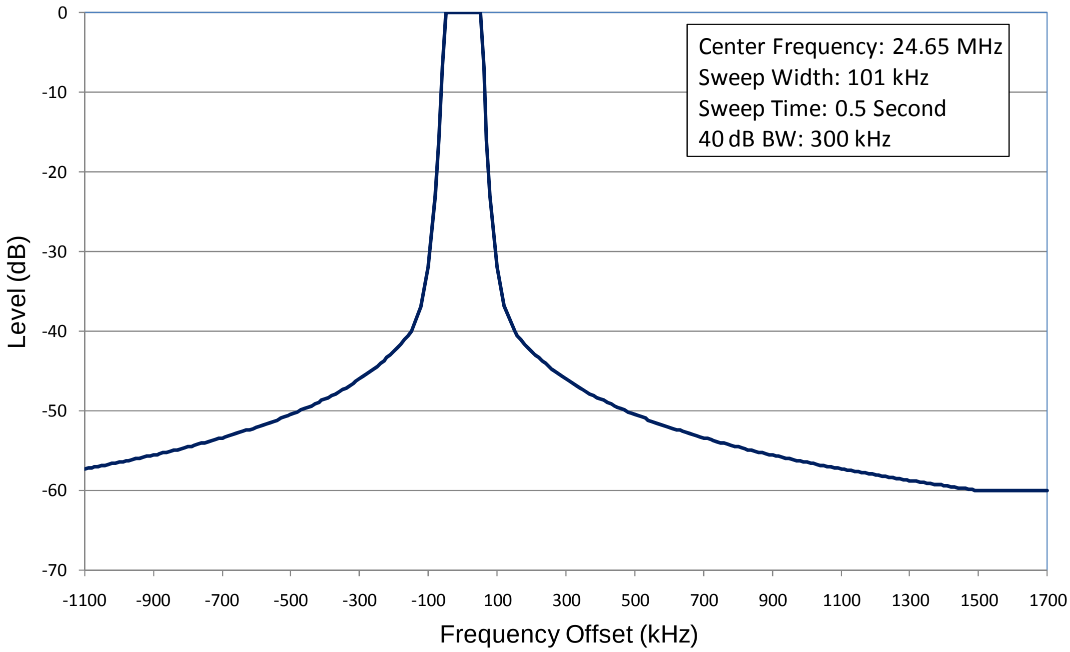

5.2 Receiver selectivity curve

The victim receiver was assumed to operate on a typical 3 kHz bandwidth, with the selectivity dropping 80 dB at a frequency offset of 15 kHz. Figure 6 shows the receiver selectivity curve used for this analysis.

FIGURE 6

Selectivity curve of typical victim receiver

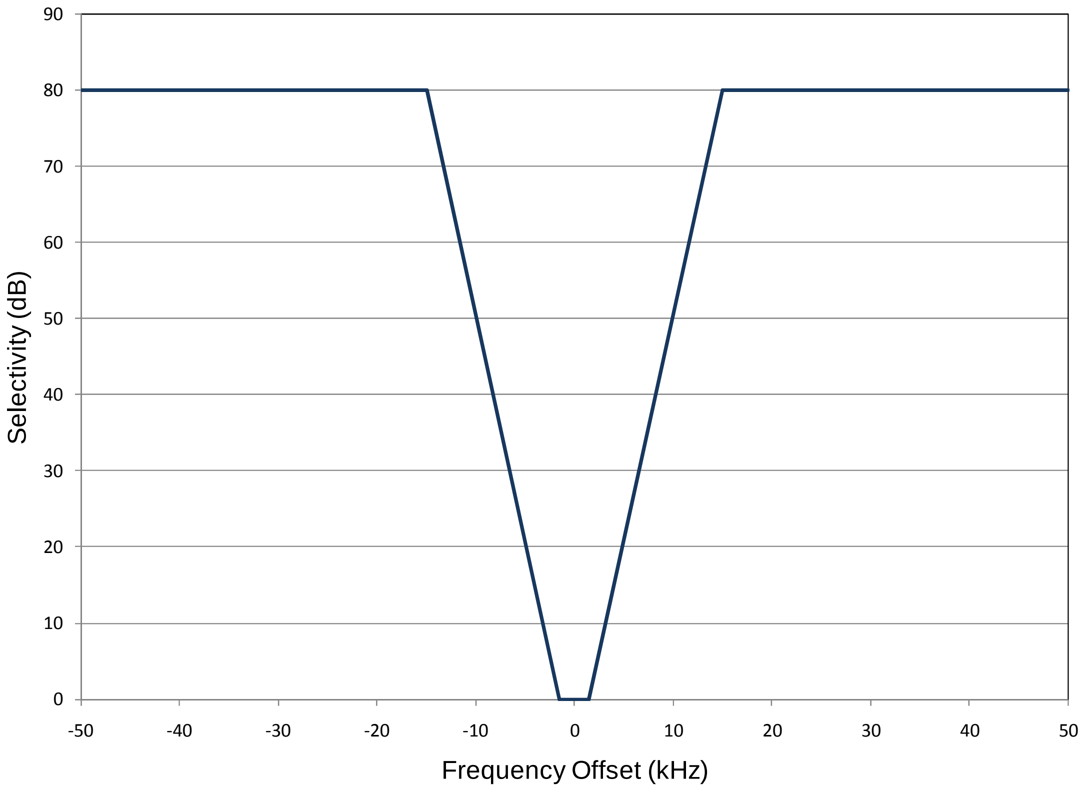

5.3 Frequency separation analysis results

Using the data displayed in the plots in Figs 3 through 6, FDR curves can be plotted that range from co-channel operation to frequency offset of 1 000 kHz or more. Figures 7, 8 and 9 show the curves for frequencies around 4.5 MHz, 13 MHz and 26 MHz

FIGURE 7

Frequency dependent rejection curve for radar operating near 4.5 MHz with typical sweep bandwidth (~25 kHz)

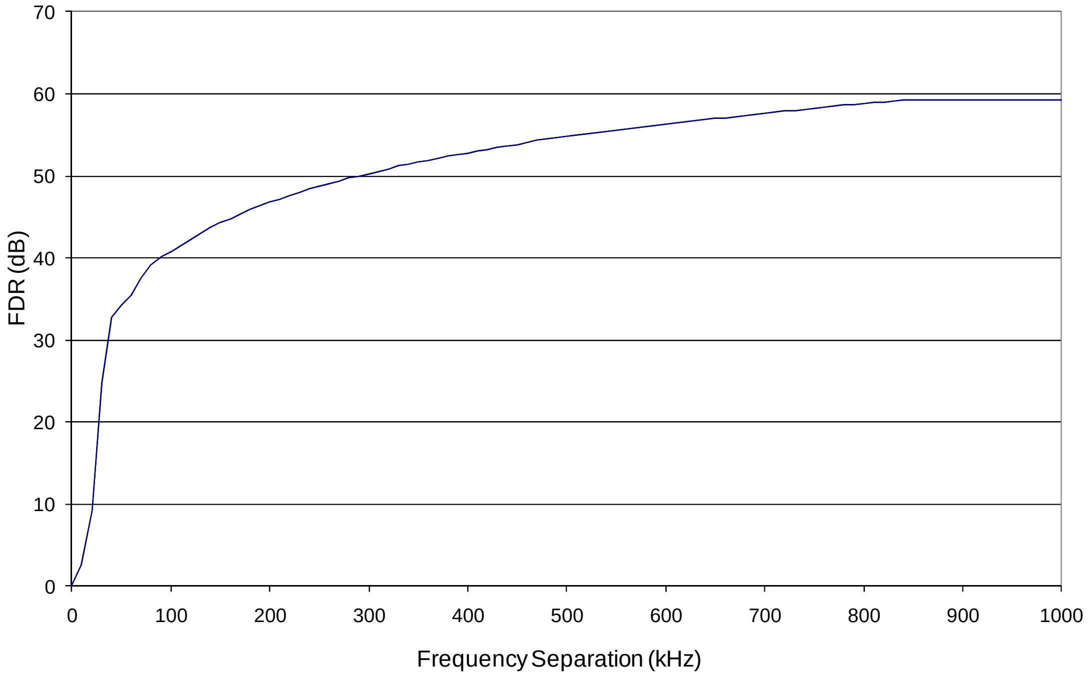

FIGURE 8

Frequency dependent rejection curve for radar operating near 13 MHz with typical sweep bandwidth (~50 kHz)

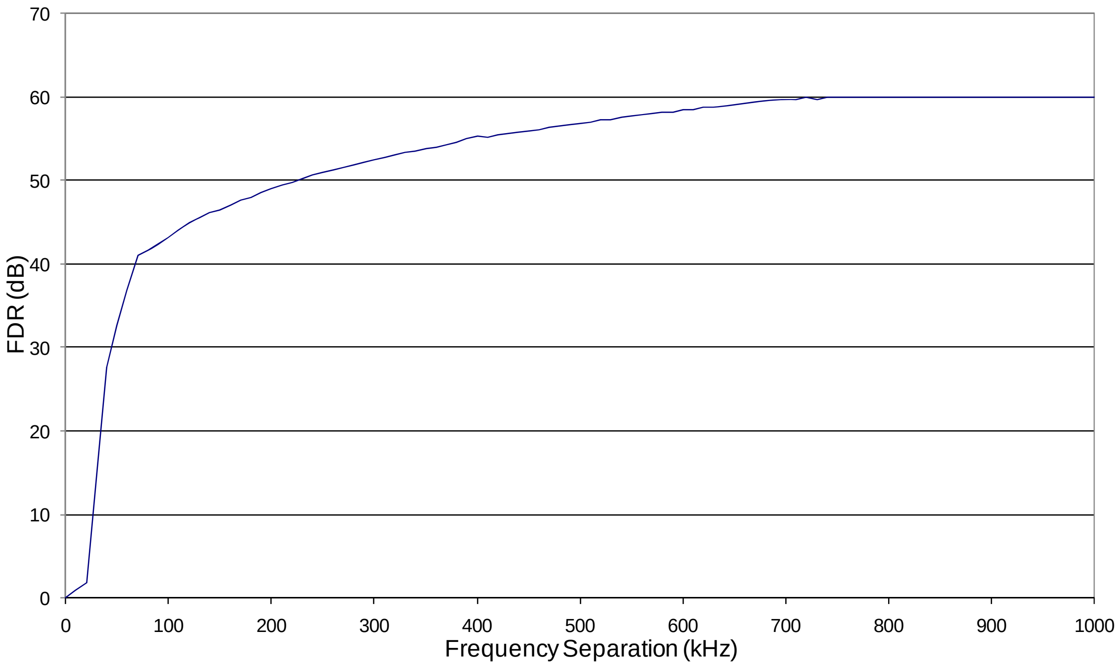

FIGURE 9

Frequency dependent rejection curve for radar operating near 25 MHz with typical sweep bandwidth (~100 kHz)

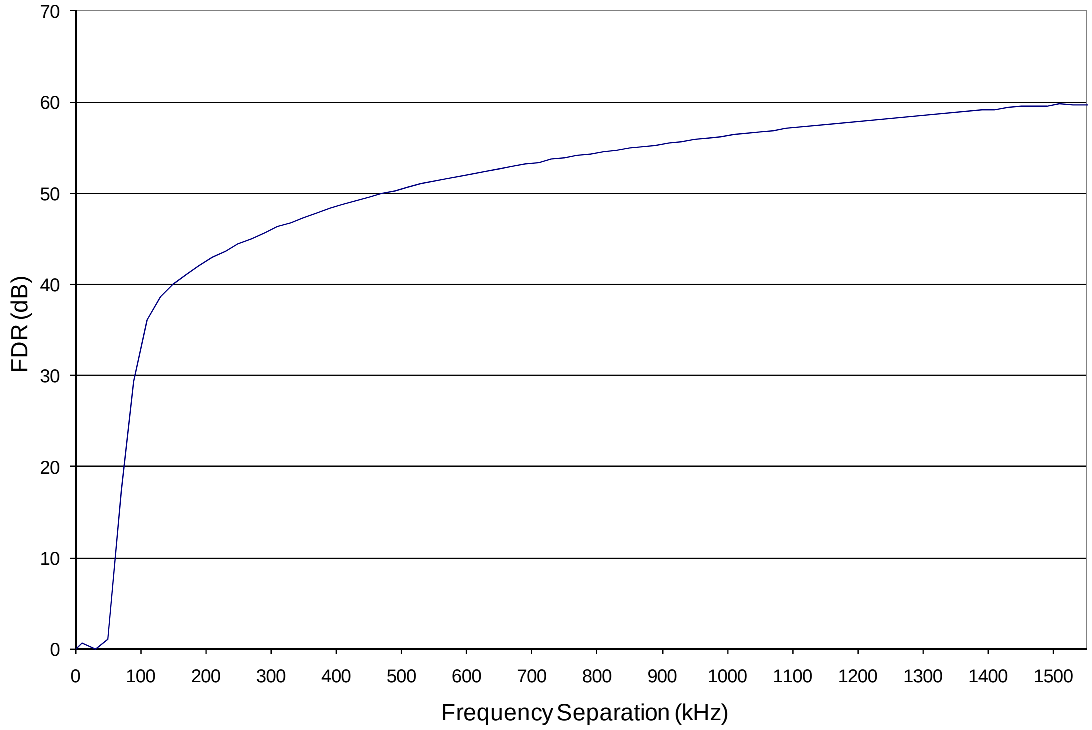

6 Theoretical sky-wave analysis

In the case of sky-wave propagation, the path is beyond line-of-sight (LOS). It is affected by ionospheric factors. Path lengths of several thousands of kilometres are common. Sky-wave propagation is an unwanted propagation mode for oceanographic radars but must be considered due to the fact that the oceanographic radars use antennas which radiate energy that will propagate via both ground-wave and sky-wave.

The key variables that are associated with the sky-wave analysis include; site location (latitude), season, time of day, sunspot activity and frequency of operation. Some relevant studies are described in this section for reference.

The sky-wave interference analysis methodologies that were used in these studies were based upon wanted link analysis and I/N calculations. The calculations were run using the ITS HF REC 533 analysis software and ICEPAC[6]. The REC 533 portion of the ITS software is based upon Recommendation ITU-R P.533-10 for performing propagation calculations. The software provides a mechanism which allows one to define multiple values for a given input variable (time of day, season, sunspot number, etc.). Assignment of multiple values to the various input variables provides a mechanism for taking the variation in the propagation medium into account.

---

6 Ionospheric Communication Enhanced Profile Analysis and Circuit Prediction Program.

6.1 Interference from oceanographic radars to the fixed and mobile services by sky-wave wanted link signal to noise ratio-based analysis

6.1.1 Methodology

This analysis evaluated the effect of interference from unwanted oceanographic radar signals on wanted fixed and mobile links on a global basis. A grid of receive stations was established around the globe spaced at an approximately 500 km × 500 km spacing (Fig. 10).

FIGURE 10

Fixed/mobile service receiver grid

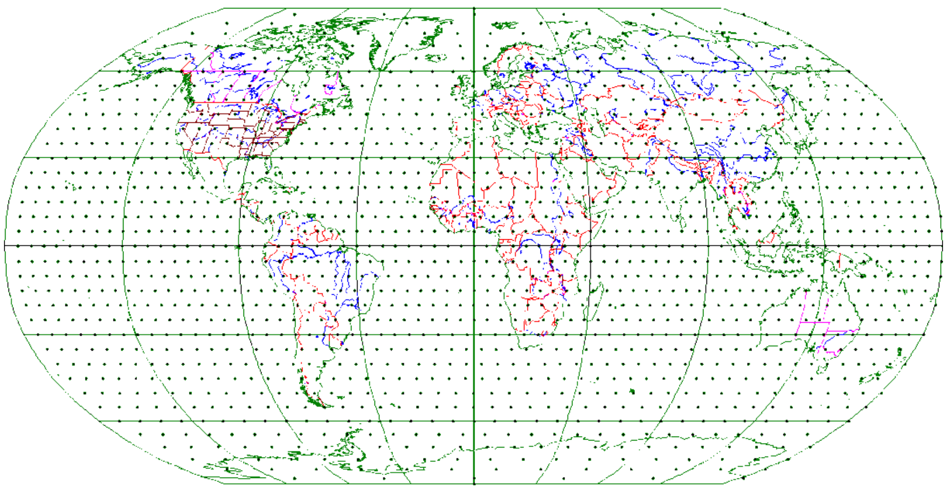

Each of these receive stations has four transmit stations associated with it, forming four wanted links per receive station (Fig. 11).

FIGURE 11

An example configuration of a typical receiver and four associated wanted links

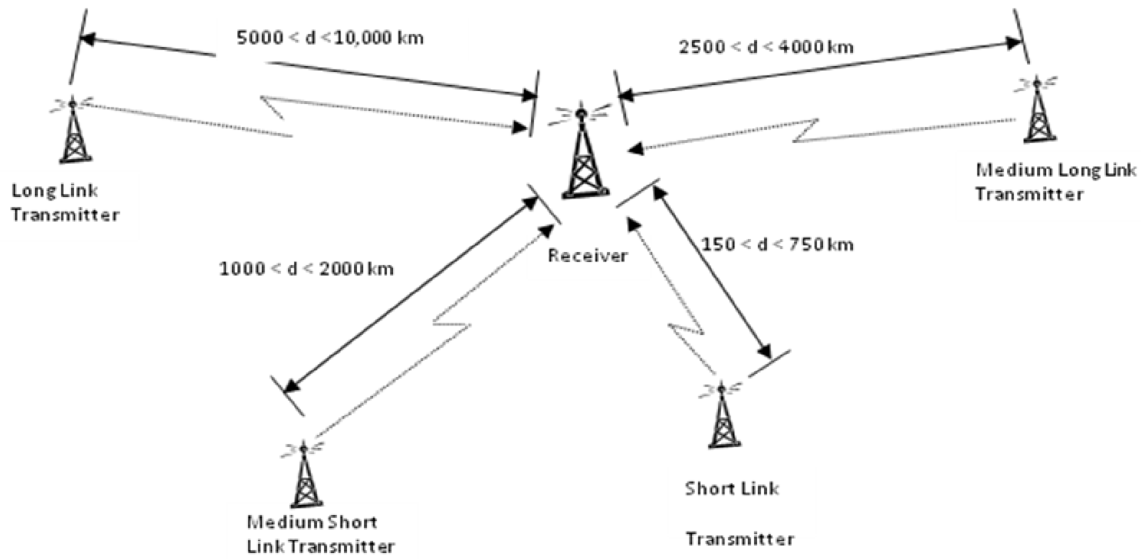

This is not to say that every real receiver operates with four associated transmitters. This scenario is established to produce wanted links at varying distances ranging from as short as 150 km to as long as 10 000 km. The four transmitters associated with each receive station are placed at random azimuths relative to the receive station. The distances between the receive station and its four associated transmitter stations are randomly established within the parameters defined in Table 10.

TABLE 10

Link distance parameters

Desired link distance parameters for random placement			
Link description	**Minimum distance (km)**	**Maximum distance (km)**	**Azimuth**
Short	150	750	Between 0º and 359º
Medium short	1 000	2 000	Between 0º and 359º
Medium long	2 500	4 000	Between 0º and 359º
Long	5 000	10 000	Between 0º and 359º

With the grid of receive locations and the associated groups of four transmitters per receiver established as the wanted links, the links are modelled using the propagation model under various condition of month, time, sunspot number and the four frequency ranges of interest (4.5 MHz, 9 MHz, 13 MHz and 26 MHz). This will provide the S/N for each of the wanted links. Of all the links modelled at the given times, months and frequencies, only a percentage of them will meet the minimum specified S/N performance for the incumbent services under consideration. These results provide a reference point for operation of systems within the incumbent services in an interference free environment[7].

The second aspect of the analysis is to determine the impact of an oceanographic radar signal on the wanted links modelled as discussed in the paragraph above (Fig. 12).

[7] In reality, due to the nature of HF propagation, operation in a purely interference-free environment is rare even without the presence of interference from HF oceanographic radars systems. However, these results will provide a good baseline to which we can compare the effect of signals from oceanographic radars.

FIGURE 12

Link analysis configuration for an oceanographic radar and the receiver and transmitters which are associated with four wanted links

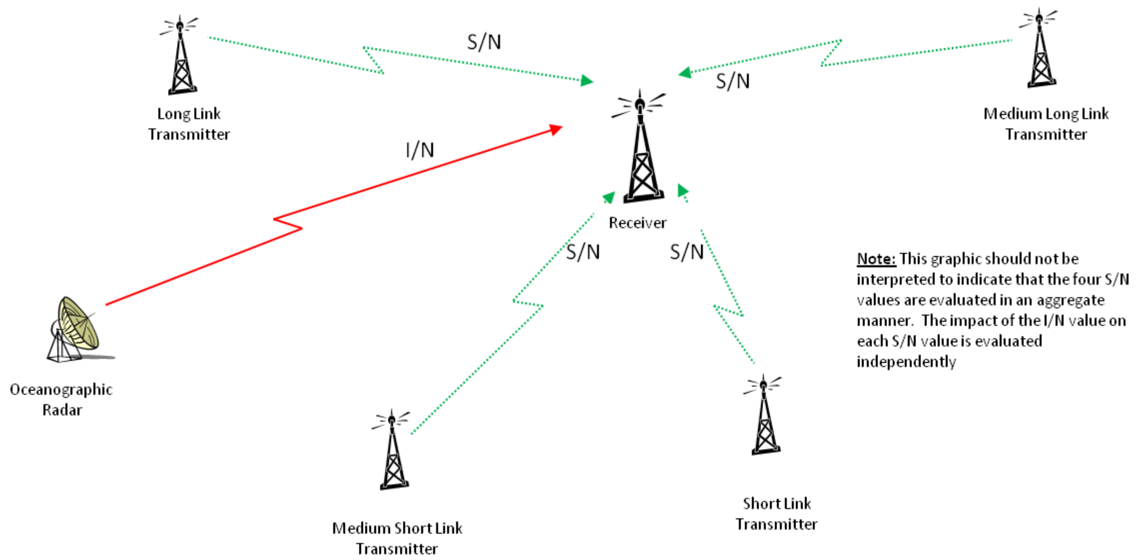

Obviously the wanted links that do not propagate sufficiently to meet minimum operational requirements of the radio service will not improve in the presence of interference and are still unusable. The objective is to evaluate the interference to the links that did propagate sufficiently in the interference-free scenario, to determine if the oceanographic radar unwanted (interfering) signal will propagate sufficiently to degrade the operational links below their minimum performance requirements.

The Recommendation ITU-R P.533-10 based link simulations were created using a set of HF receivers which were distributed on a global basis at spacing of approximately 550 km in longitude and at 5° latitude spacing[8]. This yields 1 660 receive stations distributed around the world on approximately equal density. These receive stations are the potential victim stations when evaluating the interference from the unwanted oceanographic radar signal level. For each of the 1 660 receive stations, four randomly placed transmit stations are placed as described in the previous section, forming four wanted links to each receiver operating at distances ranging from 150 to 10 000 km. Oceanographic radars located at Virginia Beach and Forteleza were selected as the primary unwanted transmission sites. For each oceanographic radar location this methodology results in evaluation of the effect of interference on 6 640 wanted links ranging in length from 150 to 10 000 km, distributed around the world. This is not say that 6 640 wanted links would be operating within the signal bandwidth of the oceanographic radar. Obviously the number of wanted links operating at any given time that would fall within the bandwidth of the oceanographic radar signal would be much lower, but the high density of receive and transmit locations was used to cover all ranges of wanted link distances, unwanted link distances, and the effect of geographic location[9].

---

8 An alternate way to visualize the station spacing is the stations are placed on rings of constant latitude, with the rings spaced at 5 degrees in latitude, where the minimum latitude is −90 degrees and the maximum is +90 degrees. Within each ring, the stations are spaced at approximately 550 km. The spacing deviates from the 550 km value slightly to provide an integer number of stations within a ring.

9 HF propagation at low latitudes is different than propagation at high latitudes.

Times of day, season and sunspot number were varied for each wanted/unwanted link pair. Table 11 shows the values used. Unwanted transmission levels were compared to wanted transmission levels for each receiver point and its associated links. The S/(I + N) was calculated and tabulated as a function of required S/N for the fixed and mobile services.

TABLE 11

Analysis input values

Parameter	Values used
Hour of day	00 through 24 hours, at 1 hour spacing
Month	January, April, July and October
Sunspot number	20 and 100
Noise	–145 dBW (Residential)
Rec. ITU-R P.533-10 reliability	50%
Receiver bandwidth	3 kHz
Oceanographic radar antenna	See Fig. 2
Oceanographic radar power	50 W
Receiver antenna	Link length dependent: See Fig. 13
Wanted link transmitter antenna	Link length dependent: See Fig. 13
Wanted link fixed service transmitter power	Short link: 1 000 W
	Medium short link: 1 000 W
	Medium long link: 10 000 W
	Long link: 10 000 W
Wanted link mobile service transmitter power	50 Watts and 150 W (independent of link length)

FIGURE 13

Fixed and Mobile Service Antenna Patterns for Short, Medium Short, Medium Long and Long Link Analysis

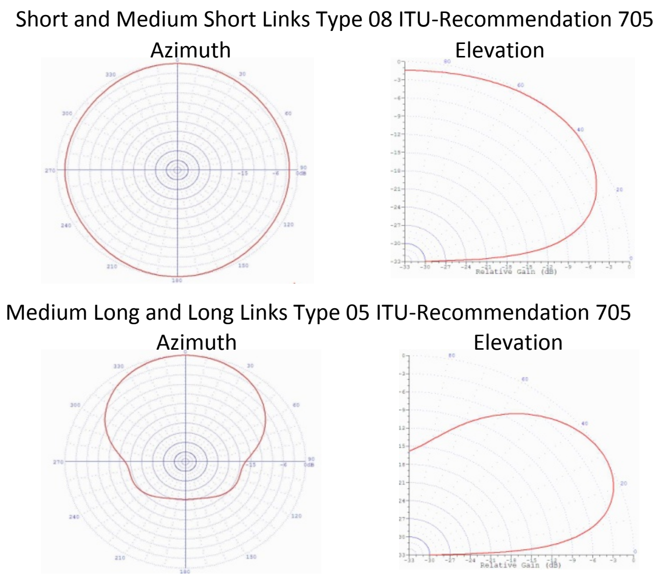

The wanted links were modelled to produce the S/N values and the unwanted links modelled to produce the I/N values[10]. The results were combined in post processing outside the ITS software and are presented in two ways, the percentage of links degraded by interference and the percentage of links degraded by interference where the oceanographic radar frequency is within 5 MHz of the frequency of optimum transmission (FOT) for the wanted link.

6.1.2 Results

The analysis was run with two oceanographic radar locations potentially interfering with 1 660 receiver test points distributed approximately equally around the globe.

Attachment 1 details the following resulting curves at Fortaleza and Virginia Beach for both the fixed and mobile systems:

– Percentage of links degraded by interference: The difference between the percentage of links that meet minimum S/N requirements with and without interference present. This is the percentage of wanted links that are degraded from operational to non-operational due to interference.

– Percentage of links degraded by interference and the oceanographic radar frequency is within 5 MHz of FOT: The difference between the percentage of links that meet minimum S/N requirements with and without interference present and the wanted link FOT is within ±5 MHz of the interfering signal. This is the percentage of wanted links that are degraded from operational to non-operational due to interference, and will need to operate at a frequency near the interfering signal due to limitations imposed by the FOT.

The results show that the S/N of viable wanted links is degraded below minimum performance thresholds for no more than 12.7% of the wanted links, distributed over varying locations and time. Therefore transmissions from oceanographic radars have a minimal impact on the percentage of fixed and mobile links that meet the minimum S/N requirements.

6.1.3 Discussion

6.1.3.1 Limitations of the I/N approach

Unfortunately using a simple I/N threshold does not take into account that some links will be operating with sufficiently high link margins such that an interference level above I/N of –6 dB will not degrade their performance below the minimum S/N threshold. It also does not take into account the fact that even though a signal may propagate to a location where I/N exceeds –6 dB, that the particular frequency under study does not propagate with sufficient reliability for the wanted link. So while the I/N may be exceeded, the receiver would not be operating on the interfering frequency since the frequency cannot support the wanted link operations.

6.1.3.2 S/N to S/(N + I) comparison approach

Many of the wanted links under analysis will operate at some point with an S/N that is above the minimum required S/N giving a positive link margin. Comparing the wanted link S/N to the S/(N + I) is another approach to determining the impact of oceanographic radars on HF fixed and mobile systems. Given the S/N of a wanted link and the I/N of the unwanted link at a given receiver, the S/(I + N) can be calculated:

$$[S/(N+I)]dB = 10Log_{10}\left[\left(10\hat{}\,(SNR/10)\right)/\left(1+(10\hat{}\,(INR/10)\right)\right]$$

[10] ITS REC 533 shows the results of a modeled link as S/N. In the case of the unwanted link, the value associated with the S/N value in the output is I/N.

where:

SNR = the wanted link signal-to-noise ratio (S/N) in dB

INR = the unwanted link interference-to-noise (I/N) ratio at the wanted link receiver in dB.

As with the I/N approach the frequency under analysis may be sufficiently far away from the FOT and that it is unlikely that the wanted link would operate near the frequency under analysis. For this reason, the percentage of links where S/(N + I) is below the 32 dB minimum and the frequency under analysis is within ±5 MHz of the FOT is also presented. The rationale is that if the FOT is more than 5 MHz away from the frequency under analysis, many HF communications operators have at least a small suite of frequencies to use under varying propagation conditions, and the operator would most likely choose a frequency closer to the FOT.

6.2 Sky-wave interference from fixed systems to oceanographic radars

6.2.1 Analysis methodology

The objective of this analysis was to determine the potential of sky-wave interference to oceanographic radar from fixed service transmitters. Ten fixed service sites were selected in order to provide a distribution of sites that would reflect various latitudes, longitudes and distances from the oceanographic radar. The selected sites can be found in Fig. 14.

FIGURE 14

Fixed service transmitter and oceanographic receiver sites

The paths between each fixed service site and the oceanographic radar were analysed using various fixed service transmitter levels and antenna types. The analysis was conducted over a twenty four hour period for the months of January, April, July and October at an SSN of 20. Table 12 lists the variables which were used in this analysis.

TABLE 12

Oceanographic radar location		**Virginia Beach**		
Fixed service transmitter power levels	W	150	1 000	10 000
Fixed service antenna type		Inverted V	Long wire	Log periodic
Antenna gain	dBi	2	7	10
Hours of the day		24 hours/1 hour increment	24 hours/1 hour increment	24 hours/1 hour increment
Months		January, April, July and October	January, April, July and October	January, April, July and October
Sun spot number		20	20	20
Link reliability	%	50%	50%	50%
I/N max	dB	−6 dB	−6 dB	−6 dB
Noise floor: 4.5 MHz (BW: 50 Hz/3 000 Hz)	dBm	−103/−85	−103/−85	−103/−85
Noise floor: 9 MHz (BW: 50 Hz/3 000 Hz)	dBm	−111/−93	−111/−93	−111/−93
Noise floor: 13 MHz (BW: 50 Hz/3 000 Hz)	dBm	−115/−98	−115/−98	−115/−98
Noise floor: 26 MHz (BW: 50 Hz/3 000 Hz)	dBm	−124/−106	−124/−106	−124/−106
Oceanographic radar IF bandwidth	Hz	50	50	50
Fixed service receiver bandwidth	Hz	3 000	3 000	3 000

On a site-by-site and path-by-path basis, the ITS REC533 HF Analysis software was used to determine the received levels of the fixed service transmissions as seen at the oceanographic radar receiver. These levels were compared to the maximum interference level that could be tolerated by an oceanographic radar operating within a residential environment assuming an I/N of –6 dB. Figure 15 is an example of one these plots.

FIGURE 15

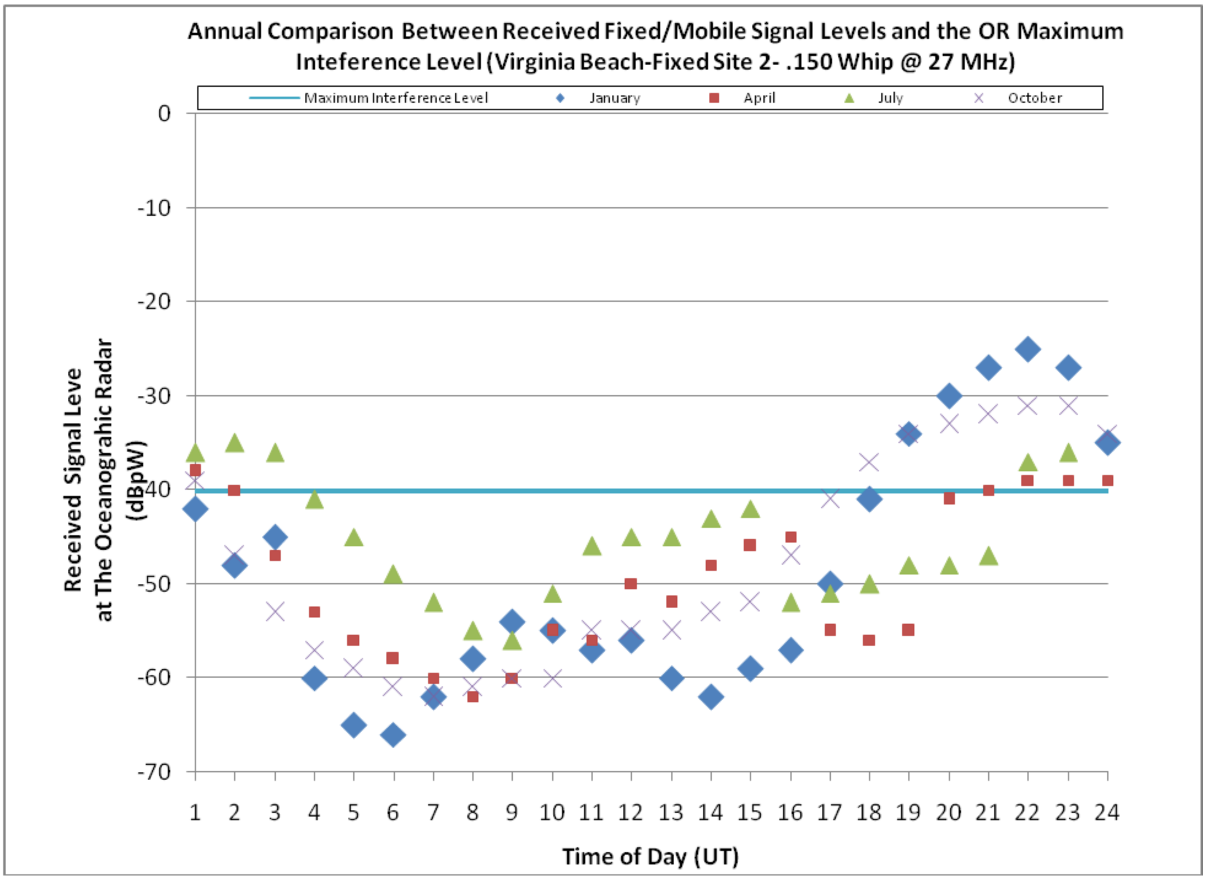

The annualized duration of time during which a fixed service received signal level exceeded the oceanographic radars maximum interference level was derived from this data.

6.2.2 Analysis results

Table 13 lists, as a function of the percentage of time that a fixed or a mobile service is in operation, the percent of time that transmissions from a fixed or a mobile service would exceed an oceanographic radars maximum interference level for an SSN of 20.

TABLE 13

		SSN = 20 Percentage of Time that a Fixed or Mobile System is in Operation					
		100	50	40	30	20	10
Fixed/Mobile Transmitter Power (Kw)	Frequency (MHz)	Percenatge of Time That an Oceanographihc Radar Incurs Interference From A Fixed or Mobile Service Transmission as a function of the percentage of time that a Fixed or a Mobile System is in Operation					
10	4.5	30-60	15-30	12-24	9-18	6-12	3-6
	9	88-90	44-45	35.2-36	26.4-27	17.6-18	8.8-9
	13	96-100	48-50	38.4-40	28.8-30	19.2-20	9.6-10
	27	55-69	27.5-34.5	22-27.6	16.5-20.7	11-13.8	5.5-6.9
1	4.5	28-50	14-25	11.2-20	8.4-15	5.6-10	2.8-2
	9	82-86	41-43	32.8-34.4	24.6-25.8	16.4-17.2	8.2-8.6
	13	86-92	43-46	34.4-36.8	25.8-27.6	17.2-18.4	8.6-9.2
	27	51-66	25.5-33	20.4-26.4	15.3-19.8	10.2-13.2	5.1-6.6
0.15	4.5	22-51	11-25.5	8.8-20.4	6.6-15.3	4.4-10.2	2.2-5.1
	9	61-79	30.5-39.5	24.4-31.6	18.3-23.7	12.2-15.8	6.1-7.9
	13	78-82	39-41	31.2-32.8	23.4-24.6	15.6-16.4	7.8-8.2
	27	32-38	16-19	12.8-15.2	9.6-11.4	6.4-7.6	3.2-3.8

Table 14 lists, as a function of the percentage of time that a fixed or a mobile service is in operation, the percent of time that transmissions from a fixed or a mobile service would exceed an oceanographic radars maximum interference level for an SSN of 100.

TABLE 14

		SSN = 100 Percentage of Time that a Fixed or Mobile System is in Operation					
		100	50	40	30	20	10
Fixed/Mobile Transmitter Power (Kw)	Frequency (MHz)	Percenatge of Time That an Oceanographihc Radar Incurs Interference From A Fixed or Mobile Service Transmission as a function of the percentage of time that a Fixed or a Mobile System is in Operation					
10	4.5	37-60	18.5-30	14.8-24	11.1-18	7.4-12	3.7-6
	9	91-95	45.5-47.5	36.4-38	27.36-28.5	18.2-19	9.1-9.5
	13	98-100	49-50	39.2-40	29.4-30	19.6-20	9.8-10
	27	70-93	35-46.5	28-37.2	21-27.9	14-18.6	7-9.3
1	4.5	21-47	10.5-23.5	8.4-18.8	6.3-14.1	4.2-9.6	2.1-4.7
	9	63-80	31.5-40	25.2-32	18.9-24	12.6-16	6.3-8
	13	81-91	40.5-45.5	32.4-36.4	24.36-27.3	16.2-18.2	8.1-9.1
	27	68-84	34-42	27.2-33.6	20.4-25.5	13.6-16.8	6.8-8.4
0.15	4.5	27-39	13.5-19.5	10.8-15.6	8.1-11.7	5.4-7.8	2.7-3.9
	9	56-72	28-36	22.4-28.8	16.8-21.6	11.2-14.4	5.6-7.2
	13	78-89	39-44.5	31.2-35.6	23.4-26.7	15.6-17.8	7.8-8.9
	27	48-61	24-30.5	19.2-24.4	14.4-18.36	9.6-12.2	4.8-6.1

Although the analysis[11]showed that fixed service transmissions will interfere with oceanographic radars, the potential for interference at any given frequency is limited to the duration of time during which the transmissions are taking place (typically 10 % of the time). In addition, the analysis has assumed that each of the transmitters will be operating on a co-channel basis and that the transmissions from the transmitter sites to the oceanographic radar sites will be correlated in time. From an operational perspective this is an unlikely scenario.

Under these operational conditions the data shows that interference to oceanographic radar could occur between 2 to 10% of the time for the range of sunspot numbers considered (20 and 100).

In addition, the overall potential of interference from a fixed or a mobile system to oceanographic radar is also limited by; the percentage of time a given frequency is actually used by a fixed or mobile service, the percentage of time the interfering antenna will be directed at the oceanographic radar, and the percentage of time that a given link is available.

Given these additional operational considerations, in practice the inference from fixed or mobile services to oceanographic radars will be less than this analysis has shown.

6.3 Aggregate sky-wave interference from multiple oceanographic radars to a fixed system

Six oceanographic radar locations and a single fixed service transmitter site were selected for an aggregate analysis. The sites were selected in order to provide a distribution that would reflect various latitudes, longitudes and distances from the oceanographic radars and the fixed service receiver sites. The selected sites can be found in Fig. 13.

The paths between each oceanographic radar site and fixed service receiver site were analysed using the ITS REC 533 HF Analysis Software. The analysis was conducted over a twenty four hour period for the months of January, April, July and October.

[11] It should be noted that the probability of the co-channel operation, link availability, off-axis antenna pointing and frequency band congestion (e.g. other sources of interference) were not taken into account during this study. Taking these factors into account could result in higher assessments of the potential for interference free operation of either system.

On a site-by-site and path-by-path basis, the ITS REC533 HF Analysis Software was used to determine the received levels of each oceanographic radar transmission as seen at the fixed service receiver site. These levels were converted to absolute power levels, summed and incrementally compared to the maximum interference level that could be tolerated by a fixed service receiver within a "rural" environment assuming an I/N of –6 dB.

The duration of time over a 24 hour period during which the oceanographic radars signal level as detected by the fixed service receiver exceeded the fixed service receivers maximum interference level was derived. The percentage of time during which the fixed service receiver could operate in an interference free environment was calculated from this data. Tables 15 and 16 summarize the results of this analysis.

TABLE 15

Percentage of time during which there is a potential for interference free operation of a fixed service receiving station in the presence of transmissions from multiple oceanographic radars (SSN=20)

	January				April				July				October			
Site Total	4.5 Mhz	9 MHz	13 MHz	27 MHz	4.5 Mhz	9 MHz	13 MHz	27 MHz	4.5 Mhz	9 MHz	13 MHz	27 MHz	4.5 Mhz	9 MHz	13 MHz	27 MHz
1	37.50%	0.00%	8.33%	66.67%	62.50%	0.00%	0.00%	70.83%	83.33%	12.50%	0.00%	70.83%	45.83%	0.00%	0.00%	66.67%
2	8.33%	0.00%	8.33%	66.67%	58.33%	0.00%	0.00%	70.83%	79.17%	0.00%	0.00%	66.67%	8.33%	0.00%	0.00%	66.67%
3	0.00%	0.00%	0.00%	66.67%	45.83%	0.00%	0.00%	33.33%	79.17%	0.00%	0.00%	25.00%	8.33%	0.00%	0.00%	54.17%
4	0.00%	0.00%	0.00%	66.67%	45.83%	0.00%	0.00%	33.33%	79.17%	0.00%	0.00%	20.83%	8.33%	0.00%	0.00%	50.00%
5	0.00%	0.00%	0.00%	66.67%	45.83%	0.00%	0.00%	33.33%	79.17%	0.00%	0.00%	20.83%	8.33%	0.00%	0.00%	50.00%
6	0.00%	0.00%	0.00%	54.17%	16.67%	0.00%	0.00%	29.17%	54.17%	0.00%	0.00%	16.67%	0.00%	0.00%	0.00%	45.83%

TABLE 16

Percentage of time during which there is a potential for interference free operation of a fixed service receiving station in the presence of transmissions from multiple oceanographic radars (SSN=100)

	January				April				July				October			
Site Total	4.5 Mhz	9 MHz	13 MHz	27 MHz	4.5 Mhz	9 MHz	13 MHz	27 MHz	4.5 Mhz	9 MHz	13 MHz	27 MHz	4.5 Mhz	9 MHz	13 MHz	27 MHz
1	41.67%	12.50%	0.00%	50.00%	79.17%	25.00%	0.00%	20.83%	100.00%	29.17%	0.00%	12.50%	54.17%	20.83%	0.00%	37.50%
2	12.50%	0.00%	0.00%	50.00%	79.17%	4.17%	0.00%	12.50%	100.00%	12.50%	0.00%	8.33%	16.67%	0.00%	0.00%	37.50%
3	8.33%	0.00%	0.00%	20.83%	79.17%	0.00%	0.00%	0.00%	100.00%	0.00%	0.00%	0.00%	16.67%	0.00%	0.00%	0.00%
4	8.33%	0.00%	0.00%	20.83%	75.00%	0.00%	0.00%	0.00%	100.00%	0.00%	0.00%	0.00%	16.67%	0.00%	0.00%	0.00%
5	8.33%	0.00%	0.00%	20.83%	75.00%	0.00%	0.00%	0.00%	100.00%	0.00%	0.00%	0.00%	16.67%	0.00%	0.00%	0.00%
6	0.00%	0.00%	0.00%	12.50%	45.83%	0.00%	0.00%	0.00%	83.33%	0.00%	0.00%	0.00%	0.00%	0.00%	0.00%	0.00%

The results of the analysis as summarized in Tables 15 and 16 are consistent with the fact that, during periods of high sunspot activity, propagation at the higher frequencies within the HF band will be more favourable thereby decreasing the potential for interference free operation of the fixed service stations at those higher frequencies. At higher sunspot levels propagation at the lower frequencies within the HF band will be less favourable thereby increasing the potential for interference free operation at those frequencies.

The results of this analysis show that there is a potential for fixed service receiving stations to be degraded by the aggregate effect of interference from multiple oceanographic radars. However given the fact that the oceanographic radar transmit power is comparable to a mobile service transmitter or a low power fixed service transmitter, the aggregate interference should not be any more significant than the inter- and intra-service interference that occurs with the fixed and mobile services.

In addition, the aggregate interference from multiple oceanographic radars on the operation of fixed and/or mobile services can be reduced by ensuring that the sweep patterns of the transmissions from those oceanographic radars are not correlated in time.

Since the transmissions from the various oceanographic radars across multiple locations are not correlated in time, the fixed or mobile service receiver should not see aggregate interference levels that were any higher than the interference level which could be generated by a single system.

As a result the worst case aggregate interference from several oceanographic radar networks that were deployed at various locations around the globe (Fig. 16) would be limited to the strongest uncorrelated sky-wave signal that was received at the site of the fixed or mobile system.

FIGURE 16

6.4 RECAREA sky-wave analysis over Europe

6.4.1 Sky-wave propagation model

The ionospheric sky-wave propagation model which was used in this analysis is described in detail in Recommendation ITU-R P.533-10. The NTIA/ITS HF propagation model RECAREA represents an implementation of the Recommendation in the Area Coverage mode provided by the ITU-R. A PC/Windows-based implementation of this Recommendation, developed and maintained by the NTIA/ITS[12] is available from the United States Department of Commerce. It predicts the expected performance of HF systems for any month, different sunspot activities, hours of the day, and geographic location.

ICEPAC[13]is another application which is available from the United States Department of Commerce. This application package is the same as REC533 but has better accuracy in the polar regions and newer electron density profile structures. In addition, ICEPAC enables one to calculate $L(x, y, f, t)$ the basic transmission loss from point (x, y) to the receiver site as function of solar activity and time of day and year.

Unfortunately, the user interface of ICEPAC only allows sweeping over 9 different combinations of input parameters, which makes it cumbersome to perform comprehensive analyses given the number of input parameters (month, time of day, sunspot number, geomagnetic Q-index and frequency). Taking these parameter combinations into account can easily exceeds 1 000 combinations even with a modest number of alternatives for each parameter.

To overcome this problem, an ITU-R Task Group for another ITU-R issue had developed a high level language computer simulation tool “cumulative PLT tool” which will bypass the ICEPAC user interface and executes the program directly in batch mode for an arbitrarily large number of parameter combinations. The PLT tool performs this by modifying the input files before issuing the DOS command in order to start the ICEPAC program without a user interface.

For this analysis, the computer simulation tool which bypasses the ICEAREA INVERSE was used to execute ICEAREA iteratively for different input parameters in order to calculate the path loss on a gridded area of 30°*30° around the oceanographic radar as shown in Fig. 17.

---

[12] National Telecommunications and Information Administration, Institute for Telecommunication Sciences.

[13] ICEPAC (Ionospheric Communications Enhanced Profile Analysis and Circuit Prediction Program) is part of the HF prediction programs which are considered, according to Recommendation ITU-R F.1611, as related models to that contained in Recommendation ITU-R P.533-10. ICEPAC is available for download from: http://www.itu.int/ITU-R/index.asp?category=documents&link=rsg3&lang=en.

FIGURE 17

Area considered for the sky-wave loss calculations (note the distortion in latitude due to the projection)

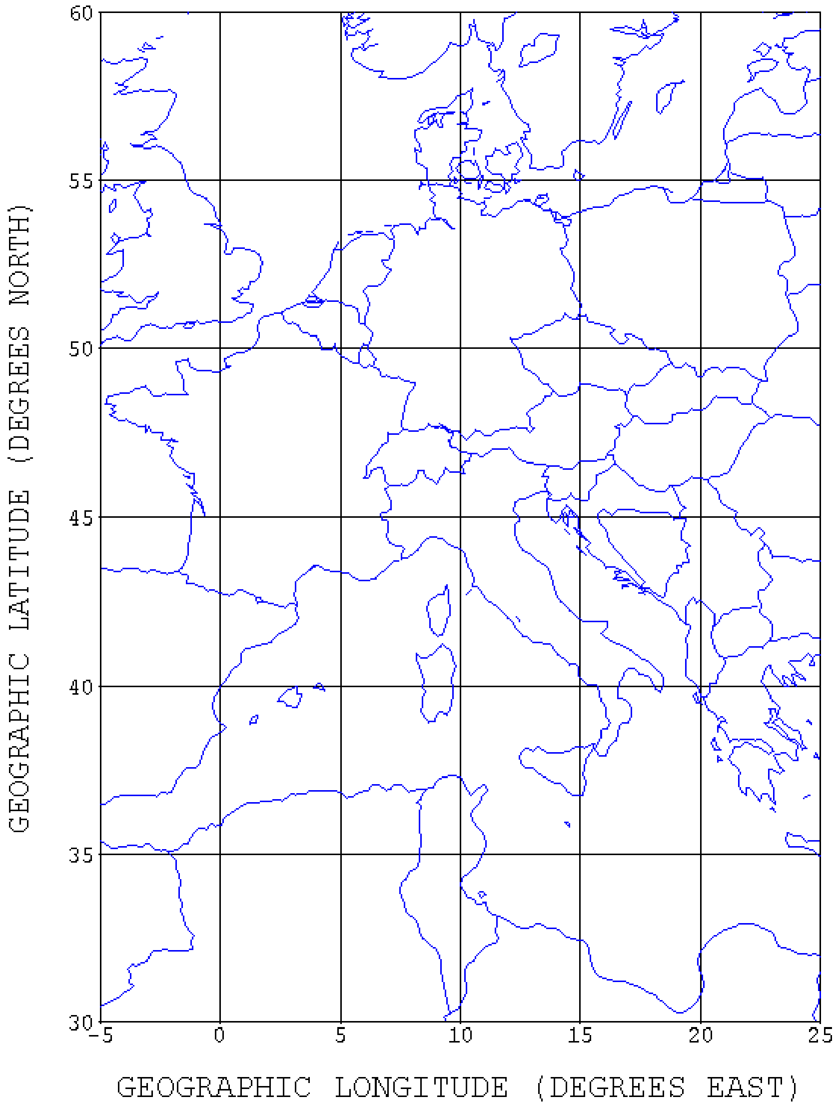

Figure 18 shows sky-wave path loss daily cycles at 13 MHz for each month (average over the area represented figure above) for a sunspot number of 100.

When considering the daily cycle for sky-wave path loss for each month (averaged over the European area) in Fig. 18, it can be noted that:

1) maximum losses occur during the night, and decreases from January to July;

2) minimum losses occur in the afternoon;

3) the night losses are maximum in January, they decrease until July, then increase back;

4) the day losses are quite constant. At 13 MHz (Fig. 18), the losses around 16UT stay between 140 and 145 dB.

FIGURE 18

Sky-wave path loss daily cycles at 13 MHz for each month (average over the area represented above)

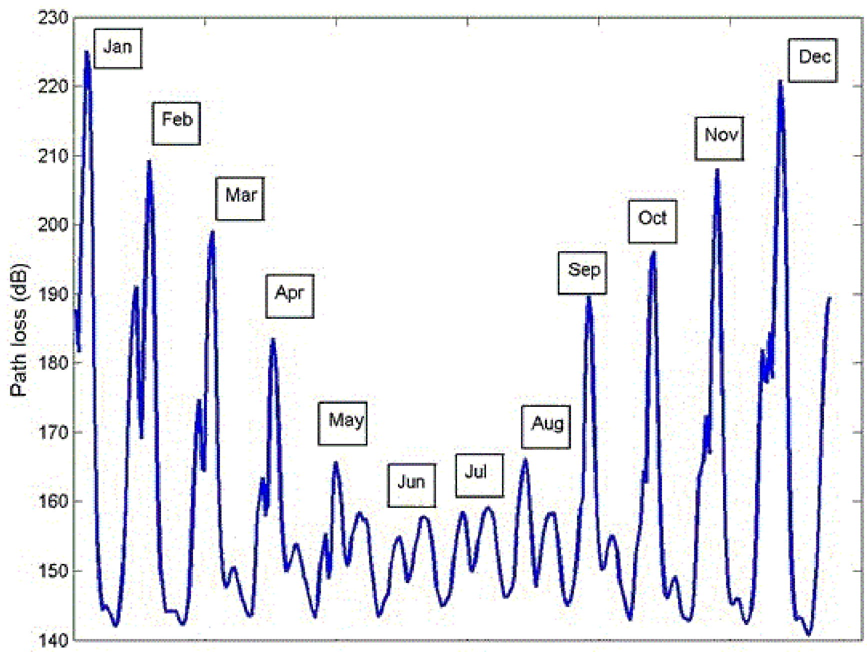

Since the path loss values are the lowest at about 16UT, the calculations for the worst case (minimum path loss) were performed using this hour.

6.4.2 Methodology

The purpose of the analysis is to determine, for a fixed or mobile service receiver, the duration of time during which an I/N < –6 dB is maintained. The computer simulation tool based on ICEPAC was used for all of the calculations and the analysis was conducted using the following parameters:

1) transmitter (oceanographic radar) located in Brest (Brittany, France, western Europe);
2) sunspot number equal to 100;
3) geomagnetic index set to 1.

For each frequency (5, 9, 13, 16, 25, 45 MHz), the steps for checking for each oceanographic radar operating at the selected frequency, whether the protection criterion is respected are:

1) path loss calculation over a 30°*30° grid with 0.25 degrees resolution in both directions, for all hours and all months;
2) for each season (months 1, 4, 7, 10) at 16UT, determination of the location (L,G)1, (L,G)4, (L,G)7, (L,G)10 were the path losses is minimum (worse cases);
3) for each location (L,G)i;
4) calculation of N;
5) for each oceanographic radar system;
6) calculation of Imax;
7) calculation of the cumulative histogram of the interference level for all hours and all months, taking into account the short term interference ratio (receiver to chirp bandwidth ratio);

8) determination of I20, the interference level which is exceeded 20% of the time, for the oceanographic systems operating at the selected frequency. The protection criterion is respected if I20 < Imax;

9) for the location (L,G)i_worst corresponding to the location where I20 is the highest (lowest path losses, thus it is independent of the oceanographic system) and for each oceanographic radar system;

10) calculation of the overall interference time probability T (time ratio when I > Imax).

For a given oceanographic system, T < 20% means that the long term interference protection criterion is respected for the worst case (location where path losses are the minimum), and thus the signal from the oceanographic radar resulting from ionospheric reflection is not considered detrimental to any receiver located in the area.

A detailed description of the parameters (external noise calculations, short-term interfering and long-term interfering time) that have been considered in this analysis can be found in the following sections and in Attachments 2 and 3.

6.4.3 External noise calculation

The value that was used for external noise, N, was estimated from the atmospheric noise, N_{atm}, which is at a minimum for 80% of the time. N_{20} represents the 20% of time that N_{atm} is exceeded.

For each frequency band, the calculations of external noise N_{20} at different locations are detailed in Attachment 3. The results are summarized in Table 17.

TABLE 17

External noise levels in dBW/Hz for "quiet rural" and "rural" environments used in the sky-wave propagation study

Frequency band	Quiet rural	Rural
5 MHz	–151.7	–150.4
9 MHz	–161.7	–159.6
13 MHz	–167.9	–164.9
16 MHz	–169.9	–167.4
25 MHz	–183	–175

6.4.4 Short-term interfering time

An important factor to consider when conducting the analysis is that a receiver from the mobile or fixed service only "sees" the signal from the oceanographic radar from time to time as shown in Fig. 19 below.

FIGURE 19

Time ratio between oceanographic radar emitter and receiver

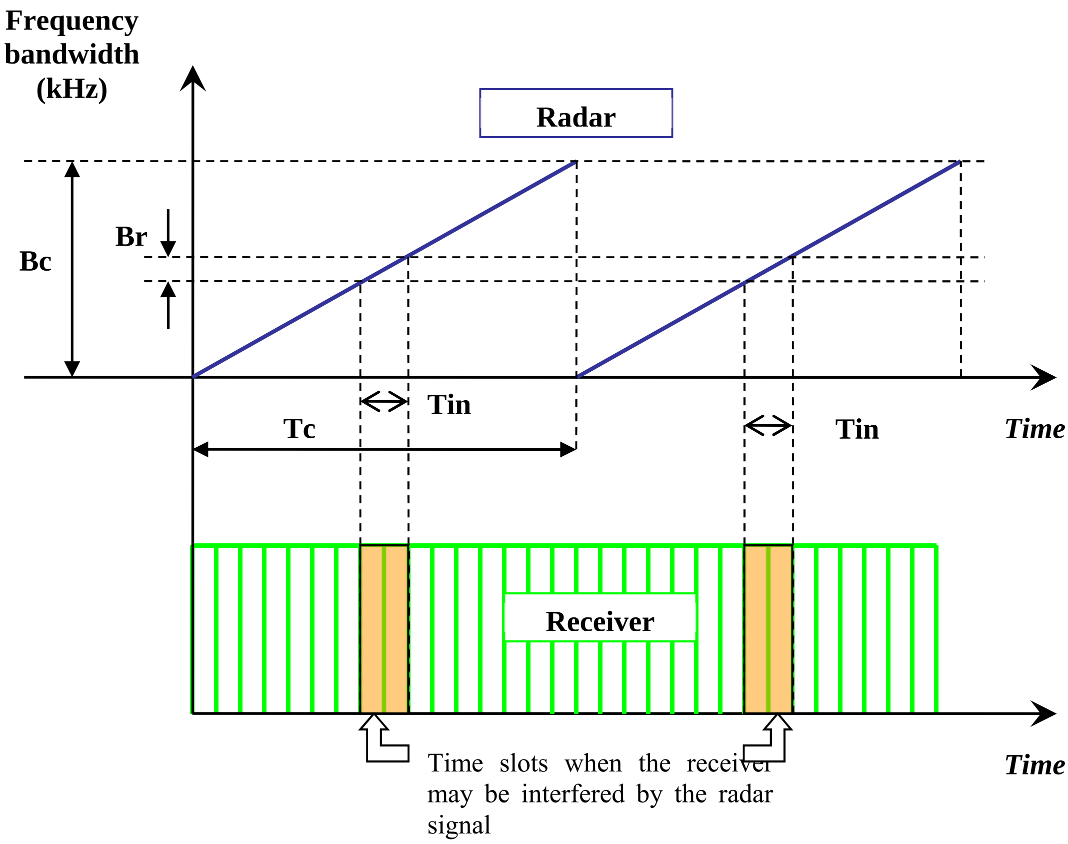

The fixed or mobile receiver detects the oceanographic radar signal according to a time ratio which is equal to T_{in}/T_c.T_{in} is the amount of time that the oceanographic radar FMCW signal is present within a bandwidth B_r. T_c is the chirp time. Given that:

$$T_{in}=T_c*B_r/B_c,$$

the time ratio becomes:

$$B_r/B_c,$$

the ratio of the receiver bandwidth to the chirp bandwidth.

For each oceanographic system, a time ratio equal to B_r/B_c (receiver to chirp bandwidth ratio) must be taken into account when estimating the time during which the receiver is interfered by the oceanographic radar chirp signal.

6.4.5 Long-term interfering time

Variations in the atmospheric path loss, which, for a given frequency, is dependent upon the hour of the day, the month of the year, and the level of solar activity results in variations in the interference level which is seen by a fixed or mobile service receiver. These interfering level variations due to the ionospheric propagation can be evaluated using ICECAP (see § 6.4.1): for a given frequency of operation, ICEPAC is run over a wide area where some oceanographic radar signal resulting from the ionospheric reflection is likely to occur, with input parameters varying iteratively in order to estimate a cumulative histogram of the path loss and thus the interference level.

The histogram (presented in Attachment 2) provides the probability of occurrence of interference level into the receiver. Therefore the percentage of time when the interference level from oceanographic radars is higher than the interference limit I_{max} determined for "rural" and "quiet rural" environments can be estimated.

6.4.6 Results

Calculations of the interfering time for each system are detailed in Attachment 2. The results of those calculations are summarized in Table 18.

TABLE 18

Results from sky-wave propagation studies

Frequency band[(1)]	System	Percentage of time interference occurs	Information about elevation angles[(2)]
5 MHz	S1	12	45-50° by 16UT 60° by 4UT
9 MHz	S5	18.4	Around 35° at 16UT Around 45° at 4UT
	S10	11.5	
13 MHz	S2	5	Between 10° and 37
	S6	4.4	
16 MHz	S7	3.9	Between 8° and 31°
25 MHz	S3, S8 S11, S12	less than 2.2	Between 2° and 18°

(1) Systems operating in the frequency band 45 MHz are not listed since sky wave propagation is limited to frequencies up to 30 MHz.

(2) Elevation angles are incident elevation angles from oceanographic radars which arrive at the receiver by sky-wave propagation. This parameter is provided by ICEPAC for any location of the area grid.

The analysis results show that the interfering time ratio never exceeds 18.4% of time.

It should be noted that that the path loss calculations were carried out with sunspot number set to 100.

Table 18 also contains information about elevation angles. This information was provided in order to provide a perspective of the elevation of incident oceanographic radar signals reaching the location considered. It is interesting to note that the higher the frequency of operation, the lower the elevation angle of oceanographic radar signals reaching the receiver. If the oceanographic radar is backed up by obstacles (obstructions, terrain, trees, buildings, …) then it is likely that at low elevations (below 20°) the signal radiated will have reduced gain in the backlobe direction. The choice of antenna configuration will determine objective gain at low elevations in both the forward and backward directions. As a consequence signals from systems at 25 MHz, and to a lesser extent at 16 MHz, are less likely to reach fixed or mobile receivers by ionospheric reflection. This is all the more likely as oceanographic radar antenna are placed close to or at sea level and are not optimized for ionospheric propagation.

6.5 Worldwide RECAREA sky-wave analysis

6.5.1 Sky-wave propagation model

In this section, ionospheric sky-wave propagation model RECAREA was used.

6.5.2 Methodology

The scheme for determination of overall interference time probability is the same as shown in § 6.4.2.

The interfering oceanographic radar transmitter is placed in Japan and 180 x 180 receivers are distributed worldwide as shown in Fig. 20.

Calculation conditions are set as shown in Table 19. The transmitting system is a FMICW generic directional oceanographic radar facilitated with 3 element vertical Yagi for transmitting antenna, and peak power 50 W (equivalent to 19 dBW e.i.r.p.).

FIGURE 20

Area considered for the sky-wave loss calculations and positions of interfering transmitter

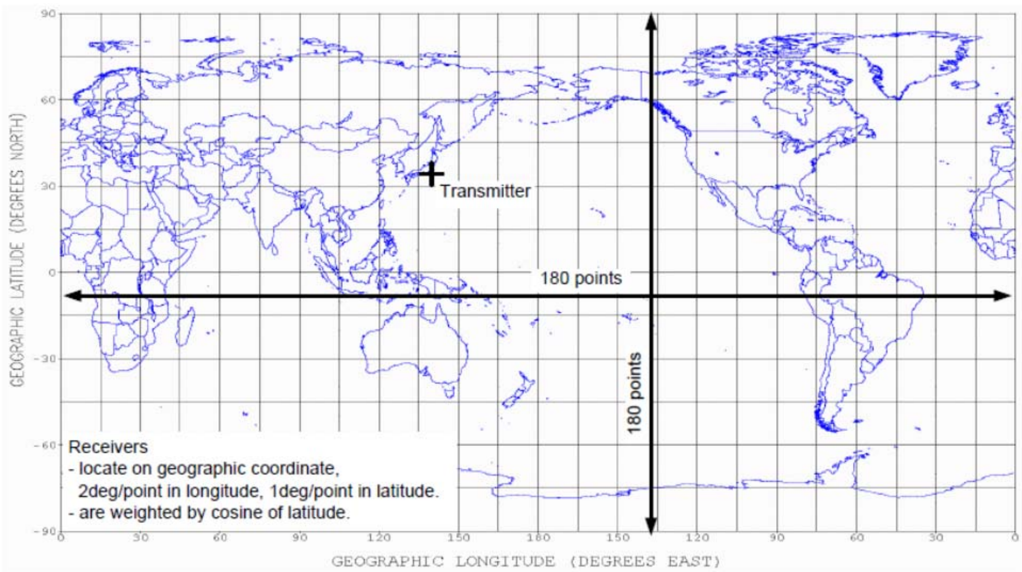

TABLE 19

Input parameters for sky-wave analysis (RECAREA) of FMICW generic directional oceanographic radars

<table>
<tr><th colspan="2" rowspan="2">Item
(RECAREA parameters)</th><th rowspan="2">Unit</th><th colspan="5">Frequency band</th></tr>
<tr><th>4.5 MHz</th><th>9 MHz</th><th>13 MHz</th><th>16 MHz</th><th>25 MHz</th></tr>
<tr><td colspan="2">Path</td><td>–</td><td colspan="5">Short</td></tr>
<tr><td colspan="2">Coefficients</td><td>–</td><td colspan="5">CCIR(Oslo)</td></tr>
<tr><td rowspan="2">Transmitter</td><td>Latitude</td><td>(Degrees)</td><td colspan="5">35.57</td></tr>
<tr><td>Longitude</td><td>(Degrees)</td><td colspan="5">140.09</td></tr>
<tr><td rowspan="4">Groups</td><td>Month</td><td>–</td><td colspan="5">1,2,3,4,5,6,7,8,9,10,11,12</td></tr>
<tr><td>Sunspot number</td><td>–</td><td colspan="5">100</td></tr>
<tr><td>Time, Hour of day</td><td>JST</td><td colspan="5">0,3,6,9,12,15,18,21</td></tr>
<tr><td>Frequency</td><td>(MHz)</td><td>4.5</td><td>9.0</td><td>13.0</td><td>16.0</td><td>24.5</td></tr>
<tr><td rowspan="5">System</td><td>Man-made noise level at 4 MHz</td><td>–</td><td colspan="5">4 (Remote)</td></tr>
<tr><td>Minimum take off angle</td><td>(Degrees)</td><td colspan="5">3</td></tr>
<tr><td>Required circuit reliability</td><td>(%)</td><td colspan="5">10</td></tr>
<tr><td>Required S/N ratio</td><td>(dB)</td><td colspan="5">–6</td></tr>
<tr><td>Receiver bandwidth</td><td>(Hz)</td><td colspan="5">3 000</td></tr>
<tr><td rowspan="4">Tx antenna</td><td>Transmit antenna</td><td>–</td><td colspan="5">3 element vertical Yagi</td></tr>
<tr><td>Design frequency</td><td>–</td><td colspan="5">0</td></tr>
<tr><td>Main beam</td><td>(Degrees)</td><td colspan="5">0 (poleward), 180 (equatorward)</td></tr>
<tr><td>Tx power 50W peak</td><td>(W) average</td><td>1.5</td><td>1.5</td><td>1.5</td><td>1.5</td><td>0.8</td></tr>
<tr><td rowspan="3">Rx antenna</td><td>Receive antenna</td><td>–</td><td colspan="5">CCIR.000 (isotrope)</td></tr>
<tr><td>Bearing</td><td>(Degrees)</td><td colspan="5">0</td></tr>
<tr><td>Gain</td><td>(dB)</td><td colspan="5">0</td></tr>
</table>

6.5.3 Worldwide RECAREA sky-wave analysis results

Calculations of the interfering time for each system are detailed in Attachment 4. The results of those calculations are summarized in Table 20.

TABLE 20

Result of sky-wave analysis: integrated spatial and temporal ratio, that the median I/N exceed the threshold, for variable transmit power

Beam direction	Tx power	Frequency Band				
		4.5 MHz	9 MHz	13 MHz	16 MHz	24.5 MHz
Poleward	Peak 50W	0.016	0.013	0.007	0.004	0.000
Equatorward	Peak 50W	0.003	0.007	0.007	0.006	0.000

7 Results of field measurements

7.1 Spectrum occupancy

Experimental study based on spectrum observation was carried out to analyse the possibility of compatibility between systems operating in the RLS and systems in other existing services in the frequency band 3-50 MHz. The study was conducted within the Korean Peninsula and during a low part of the sunspot cycle (July to September 2009).

The objectives of this study were to:

1) assess and quantify the potential for interference between oceanographic radars and allocated services when operating co-channel within frequency bands 4.5 MHz ± 1 MHz, 9 MHz ± 2 MHz, 13 MHz ± 1 MHz, 16 MHz ± 2 MHz, 26 MHz ±4 MHz and 43 MHz ± 4 MHz;
2) review compatibility of oceanographic radars with incumbent allocated users within the above frequency bands.

In order to investigate spectrum occupancy a mobile measuring system was used for observing the radio environment in the frequency band 3-50 MHz.

The results are detailed in Attachment 6. They show that in the geographic area of study there appeared to be sufficient spectrum availability within existing allocations above 20 MHz that could accommodate allocations to the RLS to meet the needs of oceanographic radars. However below 20 MHz an extensive use of the frequency bands by other services was observed in the measurement area.

7.2 Ground-wave interference measurements

Attachment 7 gives an overview of measurements regarding the interference of oceanographic radars to the mobile service in the frequency band 10 to 13.5 MHz. The objectives of the campaign were:

1) to detect oceanographic radar signals;
2) to measure the field strength;
3) to record the influence on a HF mobile radio communication link.

Two oceanographic radar systems were studied (System 6 Recommendation ITU-R M.1874). They were located in the North Sea. The measurements were taken from July to September 2010.

The FMCW signal and the signal of the incumbent service were measured with a wideband monitoring receiver and an active antenna in the time domain and transformed by FFT into the frequency domain. In addition, the audio signal of a voice transmission and the influence of the oceanographic radar were recorded.

Results detailed in Attachment 7 show that:

1) The tests have shown that a receiver with a bandwidth of 3 kHz experience repetitive interference above the background noise level within the ground-wave separation distance range (see Table 7);
2) Incumbent systems operating within the oceanographic radar sweep bandwidth could be degraded;
3) The oceanographic radar signal manifests itself as repetitive interference to the 3 kHz received signal; this indicates that the peak signal level may be important as the source of interference.

7.3 Sky-wave measurements

Attachment 8 illustrates observations of the physical presence of sky-wave signals. The effect on HF receivers could not be quantified at this time.

8 Interference mitigation techniques

Attachment 9 examines potentially interfering signals produced by coastal oceanographic radars used for continuous, real-time, operational ocean-current monitoring. This subject was examined from three standpoints:

1) consider and examine possible methods that might be used to mitigate interference effects;
2) how effective are these likely to be in eliminating interference into other receivers;
3) what are their impact on performance effectiveness of the oceanographic radar network.

The most effective interference mitigation techniques are already being practiced. These include:

1) minimizing sweep bandwidth, without compromising the performance of the oceanographic radar mission, will reduce possible interference by reducing demand on the spectrum;
2) use of GPS to synchronize signal modulation allows many oceanographic radars to operate on the same frequency at the same time; this greatly reduces the spectral occupancy of networks;
3) keeping radiated power as low as possible without compromising data product utility;
4) use of pulse shaping and layers of filtering to reduce out-of-band interference;
5) using transmit antenna arrays to reduce gain in the back lobe over land (where susceptible receivers are located) was examined in light of the requirement that the seaward sector must be covered as uniformly as possible;
6) a "listen-before-transmit" operating mode for oceanographic radars was examined, so that multiple users with different missions could share the same channels. Several schemes were considered, including the ability of another licensed user to shut down co-channel oceanographic radars while transmitting needed messages. In all cases, compromises in performance to both the incumbent systems and the oceanographic radar user community was deemed unacceptable.

9 Summary

This section summarizes the results of several compatibility studies which were performed prior to WRC-12 in support of Agenda item 1.15. The studies that were undertaken focused on identifying the interference mechanisms between oceanographic radar systems[14] and fixed and mobile systems which are currently operating in the frequency band 3-50 MHz would have upon one another.

The studies addressed the effect of interference upon the oceanographic radars and fixed and mobile systems from a separation distance perspective for ground-wave interference paths. For sky-wave interference paths some studies evaluated link availability and a percentage of time during which interference can occur, and another study evaluated the percentage of a number of globally distributed links that could be degraded.

---

[14] New Recommendation ITU-R M.1874 – Technical and operational characteristics of oceanographic radars operating in sub-bands within the frequency range 3 to 50 MHz.

9.1 Ground-wave analysis

All studies were in general agreement on the separation distances required for protection of the incumbent services over ground-wave interference paths. Ground-wave interference from oceanographic radars to fixed and mobile systems and vice versa can be mitigated by adhering to the separation distances that have been outlined in Table 6 and Table 8. The separation distances can be reduced further by limiting the transmitting power of the oceanographic radar as shown in Tables 7 and 9 of this Report.

9.1.1 Results for frequencies below 30 MHz

The results of the ground-wave analysis (see § 4) showed that land path separation distances between the oceanographic radar transmitter and the mobile or fixed receiver varied, as a function of noise environment, operational frequency, transmit power, soil type and antenna directionality. The minimum separation distances varied between 40 km to 120 km for “rural” and 50 km to 170 km for “quiet rural” noise environments at 19 dBW e.i.r.p. The analysis did not take into account ground cover, vegetation, buildings and other obstructions or variations in elevation. Taking these factors into account may further reduce the required separation distances.

For sea path the minimum separation distances varied between 270 km to 790 km for “rural” and 310 km to 920 km for “quiet rural” noise environments at 19 dBW e.i.r.p.

Further measurement studies are described in § 9.4.2.

9.1.2 Results for frequencies above 30 MHz

Signal strength and path loss measurements at 40 and 43 MHz showed a strong correlation between the path loss values as predicted by Recommendation ITU-R P.368-10 and the measured data. Recommendation ITU-R P.368-10 provides a reliable and accurate assessment of path losses up to 43 MHz and as such should be used for any interference or compatibility studies where the systems that are under investigation have low antenna heights and low terrain angles (e.g. oceanographic radars).

For land path, the minimum separation distances at frequencies above 30 MHz varied between 40 km to 80 km for “rural” and 50 km to 90 km for “quiet rural” noise environments at 19 dBW e.i.r.p. The analysis did not take into account ground cover, vegetation, buildings and other obstructions or variations in elevation. Taking these factors into account may further reduce the required separation distances.

For sea path the minimum separation distances are about 200 km for “rural” and 230 km for “quiet rural” noise environments at 19 dBW e.i.r.p.

9.2 Sky-wave analysis

Five theoretical sky-wave studies were conducted and are contained in Attachments 1 through 4, and 10.

One study (Attachment 1) showed that the S/N of viable HF fixed and mobile service wanted links are degraded below minimum performance thresholds for no more than 12.7% of the wanted links, distributed over varying locations and time. The study showed that the effect that transmissions from oceanographic radars have on the percentage of fixed and mobile links at a given frequency is significantly reduced when the FOT of the wanted link is taken into account relative to the oceanographic radar frequency under study. However, some fixed and mobile service operators may find they need to operate at frequencies in less than optimum propagation conditions and may be required to operate close to the oceanographic radar signal. In contrast, it is also assumed that any wanted link signal with ideal propagation near the oceanographic radar frequency will be degraded by interference, which may not always be the case. These assumptions were necessary to simplify the analysis to a manageable level.

The analysis also showed that fixed service transmissions will interfere with oceanographic radars for between 2 and 10% of the time, and the potential for interference at any given frequency is limited to the duration of time during which the transmissions are taking place (typically 10% of the time). It should be noted that the analyses were run with fixed service systems at transmit power levels of 150, 1 000 and 10 000 W. Some fixed stations may operate at lower power levels, around 25 W in some cases. In addition, the overall potential of interference from a fixed or a mobile system to oceanographic radar is also limited by; the percentage of time a given frequency is actually used by a fixed or mobile service, the percentage of time the interfering antenna will be directed at the oceanographic radars, and the percentage of time that a given link is available.

The study also showed that there is a potential for fixed service receiving stations to be degraded by the aggregation of power from multiple oceanographic radars. It should be noted that the aggregate impact of multiple oceanographic radars to fixed and mobile systems was studied only for six operating oceanographic radar locations as shown in Fig. 16.

Three studies (Attachments 2, 4, and 10) evaluated interference occurrence based on the percentage of time that the interference to noise ratio exceeded –6 dB. Attachments 2 and 4 considered the generic oceanographic radar systems in the HF frequency band, and used a three component environmental noise model ("quiet rural" man-made noise, galactic noise and the 80^{th} percentile atmospheric noise). The first study examined back-lobe interference within the European region. The duty cycle and the co-channel occurrence time (ratio of receiver bandwidth to chirp bandwidth) were taken into account for the derivation of the interfering time ratio. It was found that I/N= −6 dB was not exceeded for more than 18.4% of the time, for any of the oceanographic radar systems. The second study examined worldwide interference caused by a directional antenna. The interference signal was averaged to account for waveform duty cycle and the co-channel occurrence time (ratio of receiver bandwidth to chirp bandwidth). The results show that I/N= −6 dB was not exceeded for more than 1.6% of the time and area. Attachment 10 considered omnidirectional antennas and median noise levels; it confirms the increase in interference occurrence when considering main lobe peak interference level as distinct from back lobe average interference level.

These studies show a dependence on the size of the geographic region under study. Sky-wave propagation characteristics suggest strongest interference is expected within the one-hop sky-wave propagation zone, which typically ranges from 1 000 to 3 000 km.

9.3 Frequency dependent rejection analysis

In addition to separation distance, frequency separation can also be used to minimize interference. Conducting an analysis for frequency separation requires performing a FDR analysis. The FDR analysis uses transmitter emission masks and receiver selectivity curves. It calculates the amount of rejection applied to the interference power due to non-overlapping regions of the transmitter envelope and receiver selectivity curve.

The analysis showed that, based on a 3 kHz receiver bandwidth and a typical oceanographic radar emission curve, an additional 40 to 60 dB of rejection of oceanographic radar transmissions can be obtained by operating the oceanographic radars at frequency offsets of 100 kHz or more (see § 5.3).

9.4 Field measurements

9.4.1 Spectrum occupancy measurements

An experimental study based on spectrum observation was carried out to analyse the possibility of compatibility between systems operating in the RLS and systems in mobile and fixed services in the frequency band 3-50 MHz. The study was conducted within a limited geographical area and during a low sunspot activity part of the cycle.

The results showed that there appeared to be sufficient spectrum availability within existing allocations above 20 MHz that could accommodate allocations that would meet the needs of oceanographic radars. However below 20 MHz it was observed that there was extensive use of the frequency bands in the measurement area. Spectrum occupancy observations will change as sunspot activity varies.

9.4.2 Groundwave interference measurements

Measurements on the impact of oceanographic radars to the mobile service in the frequency band 10 to 13.5 MHz were carried out during a low sunspot activity period (2010). The objectives of the campaign were:

1) to detect oceanographic radar signals;
2) to measure the field strength;
3) to record the interference effect on a HF radio communication link.

A receiver from the land mobile service was located on land in the direction of the main beam of the oceanographic radar within the separation distance (about 80 km, sea path) as determined in the theoretical study (about 400-500 km, for a "rural" environment and 10 dBW e.i.r.p.).

Results showed that:

1) The tests have shown that a receiver with a bandwidth of 3 kHz experience repetitive interference above the background noise level within the ground-wave separation distance range (see Table 7);
2) Incumbent systems operating within the oceanographic radar sweep bandwidth could be degraded;
3) The oceanographic radar signal manifests itself as repetitive interference to the 3 kHz received signal; this indicates that the peak signal may be important as the source of interference.

9.4.3 Sky-wave measurements

Attachment 8 illustrates observations of the physical presence of sky-wave signals. The effect on HF receivers could not be quantified at this time.

9.5 Experimental analysis

An experimental study in Attachment 11 investigated interference effects to establish the necessary set of operating parameters to enable the simultaneous operation of the oceanographic radar and digital data systems within the same radio spectrum.

The measured bit error ratio (BER) degradation observed for the digital data link was from 1×10^{-5} to less than 3×10^{-5} when the oceanographic radar interference peak level was set to I/N = –6 dB with results within experimental error margins for the three oceanographic radar centre frequencies used. The experiment was repeated using the average of the oceanographic radar signal instead of the peak signal level for I/N = –6 dB setting. The observed BER increased to 1×10^{-1}, which is very severe degradation for digital data links, for all three oceanographic radar centre frequencies.

This attachment indicates that compatibility studies between HF digital data links and oceanographic radars should use the waveform's peak signal levels for interference calculations. In addition, degradation should not be scaled with the bandwidth ratio of data and oceanographic radar waveforms.

9.6 Interference mitigation

Potentially interfering signals produced by oceanographic radars used for continuous, real-time, operational ocean-current monitoring were examined from three points of view:

1) consider and examine possible methods that might be used to mitigate interference effects;
2) how effective are these likely to be in eliminating any interference into others' receivers;
3) is the effect on performance effectiveness of the oceanographic radar network.

Some of the following interference mitigation techniques are already being practiced:

1) provided that the oceanographic radar mission is not compromised, sweep bandwidth could be reduced, thus reducing possible interference and demand on the spectrum;
2) use of GPS to synchronize signal modulation, allowing many oceanographic radars to operate on the same frequency at the same time; which greatly reduces the spectral occupancy of networks;
3) keeping radiated power as low as possible without compromising data product utility;
4) use of pulse shaping and layers of filtering to reduce out-of-band interference;
5) using transmit antenna arrays to reduce gain in the backlobe over land (where susceptible receivers are located), noting that the seaward sector must be covered as uniformly as possible.

In addition, a "listen-before-transmit" operating mode for oceanographic radars was examined, so that multiple users with different missions could share the same channels. Several schemes were considered, including the ability of another licensed user to shut down co-channel oceanographic radars while transmitting needed messages. In all cases, compromises in performance to both the incumbent users and the oceanographic radar community were deemed unacceptable.

10 Conclusions

Oceanographic radars have been operating in the 3 MHz to 50 MHz range since the 1970's on an experimental non-interfering basis. There is an increased reliance on the data from these systems for maritime safety, oceanographic, climatological and meteorological and disaster response.

Several administrations have conducted theoretical interference analyses between generic oceanographic radars and fixed and mobile systems. The analyses showed that interference to a fixed or mobile station could occur as a result of either ground-wave or sky-wave propagation, when the fixed or mobile system is receiving within the sweep bandwidth of the oceanographic radar.

Interference via the ground-wave path could be managed by respecting separation distances provided in Tables 7 and 10. Interference via the sky-wave path is highly variable, depending on sunspot activity, season, time of the day, and frequency. Recognizing the requirement for multiple frequency bands ranging from 4.5 to 43 MHz, the studies show that the opportunities for sharing generally improve with an increase in frequency. In general, spectrum congestion increases and sharing becomes more problematic below 20 MHz, however sharing may be achievable.

It was found that mitigation techniques can be used to facilitate spectrum sharing. Potentially implementing time synchronization of multiple oceanographic radar transmissions within the same swept bandwidth could facilitate frequency reuse and reduce overall spectrum requirements.

Attachment 1

Results from the sky-wave signal to noise ratio-based link analysis

This Attachment presents the results of the study presented in § 7.1.

Data presented in the Figs 1-1 through 1-13 is summarized as follows:

– Percentage of links degraded by interference: The difference between the percentage of links that meet minimum S/N requirements with and without interference present. This is the percentage of wanted links that are degraded from operational to non-operational due to interference.

– Percentage of links degraded by interference and oceanographic radar frequency is within 5 MHz of FOT: The difference between the percentage of links that meet minimum S/N requirements with and without interference present and the wanted link FOT is within ±5 MHz of the interfering signal. This is the percentage of wanted links that are degraded from operational to non-operational due to interference, and will need to operate at a frequency within 5 MHz of the interfering signal due to limitations imposed by the FOT.

– Link lengths are defined in Table 10 of § 6.1.1.

The results of the analysis for mobile systems at Fortaleza and Virginia Beach are summarized in Figs 21 through 28.

The results of the analysis for fixed systems at Fortaleza and Virginia Beach are summarized in Figs 29 through 36.

The results show that the S/N of viable wanted links is degraded below minimum performance thresholds for no more than 12.7% of the wanted links, distributed over varying locations and time.

The dashed lines in each figure, assumed that wanted links which Recommendation ITU-R P.533-10 shows will propagate best at frequency more than 5 MHz away from the oceanographic radar signal (wanted link FOT > radar frequency ±5 MHz) will not be degraded. However, some fixed and mobile service operators may find they need to operate at frequencies in less than ideal propagation conditions and may be required to operate closer than 5 MHz to the oceanographic radar signal even though the FOT is more than 5 MHz away. In contrast, it is also assumed that any wanted link signal with a FOT within 5 MHz of the oceanographic radar frequency will be degraded by interference, which is not necessarily true. These assumptions were necessary to simplify the analysis to a manageable level. In the first case, interference may occur to wanted links that are assumed to be interference free (i.e. ±5 MHz away). In the second case, wanted links that are assumed to be degraded could actually be sufficiently separated from the oceanographic radar signal to avoid interference.

FIGURE 21

Oceanographic radar interference effects on short mobile service links (Fortaleza)

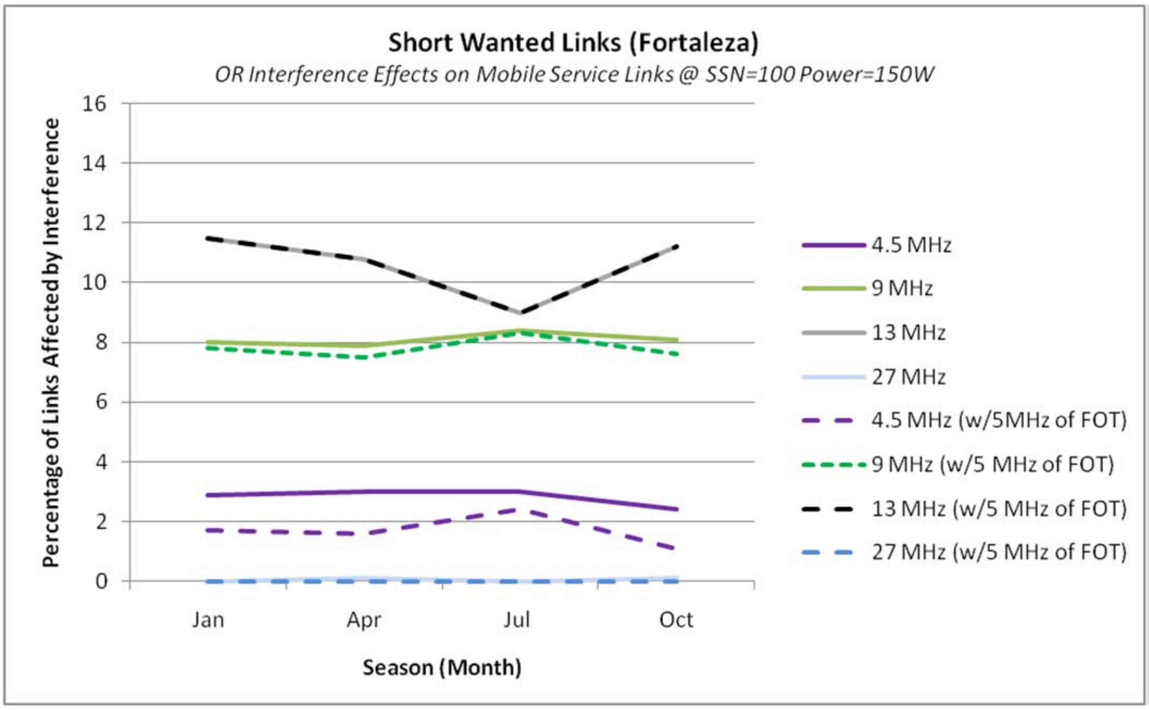

FIGURE 22

Oceanographic radar interference effects on short mobile service links (Fortaleza)

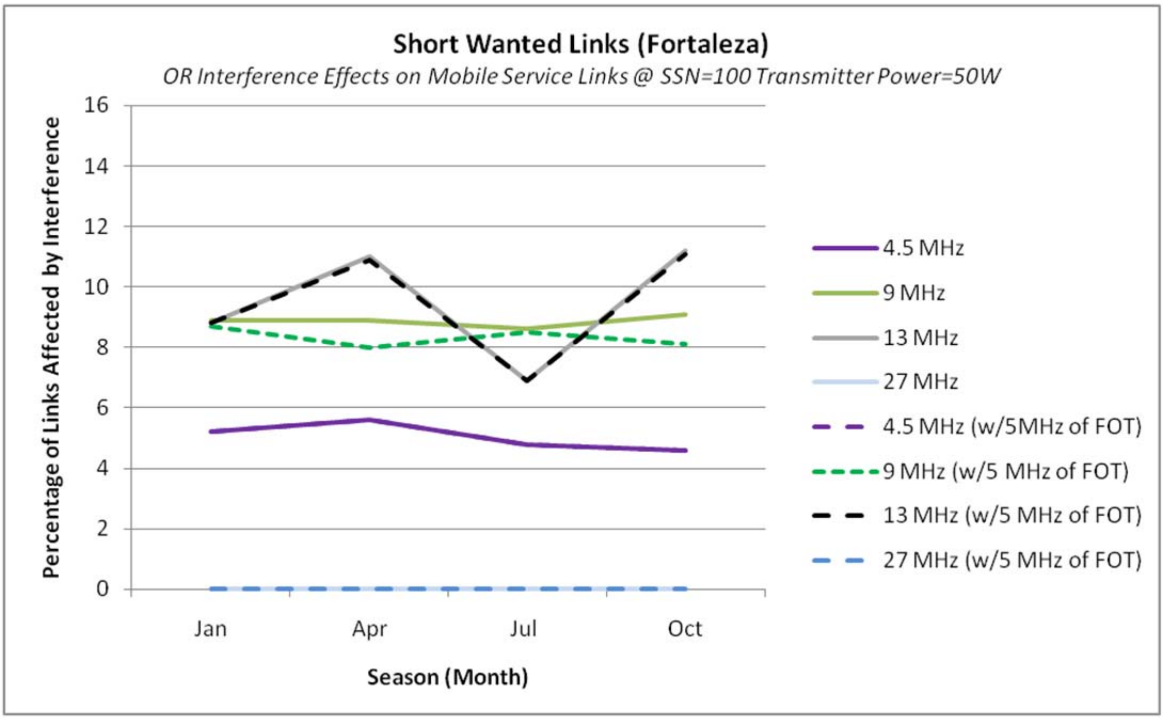

FIGURE 23

Oceanographic radar interference effects on short mobile service links (Virginia Beach)

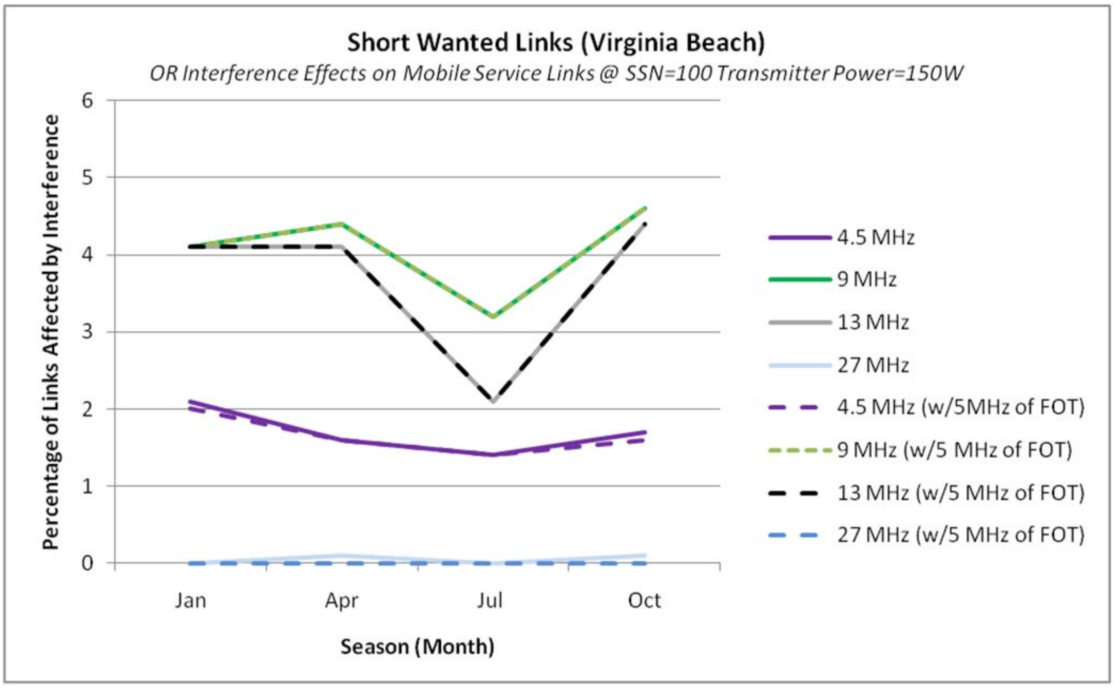

FIGURE 24

Oceanographic radar interference effects on short mobile service links (Virginia Beach)

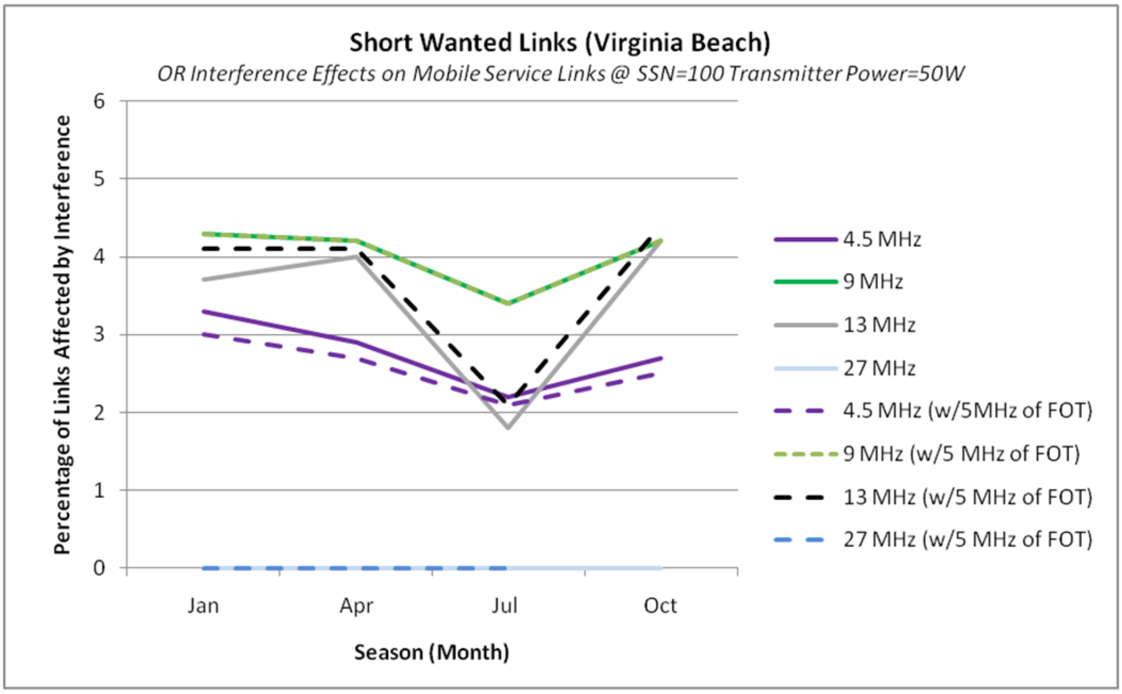

FIGURE 25

Oceanographic radar interference effects on med-short mobile service links (Fortaleza)

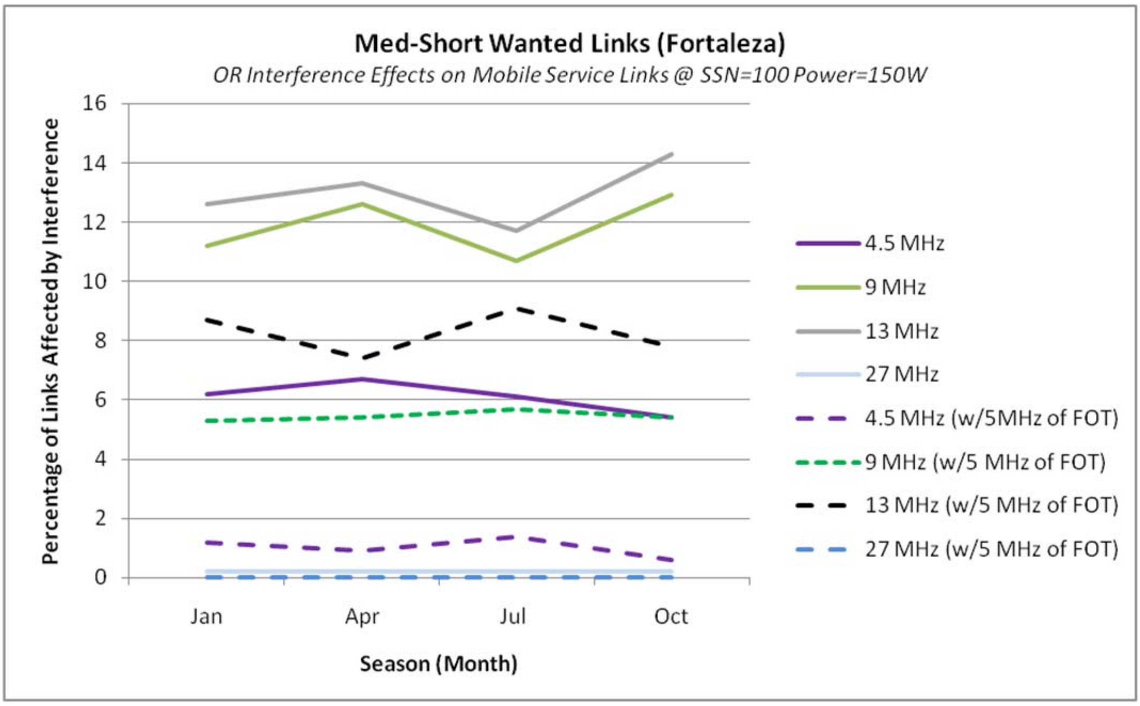

FIGURE 26

Oceanographic radar interference effects on med-short mobile service links (Fortaleza)

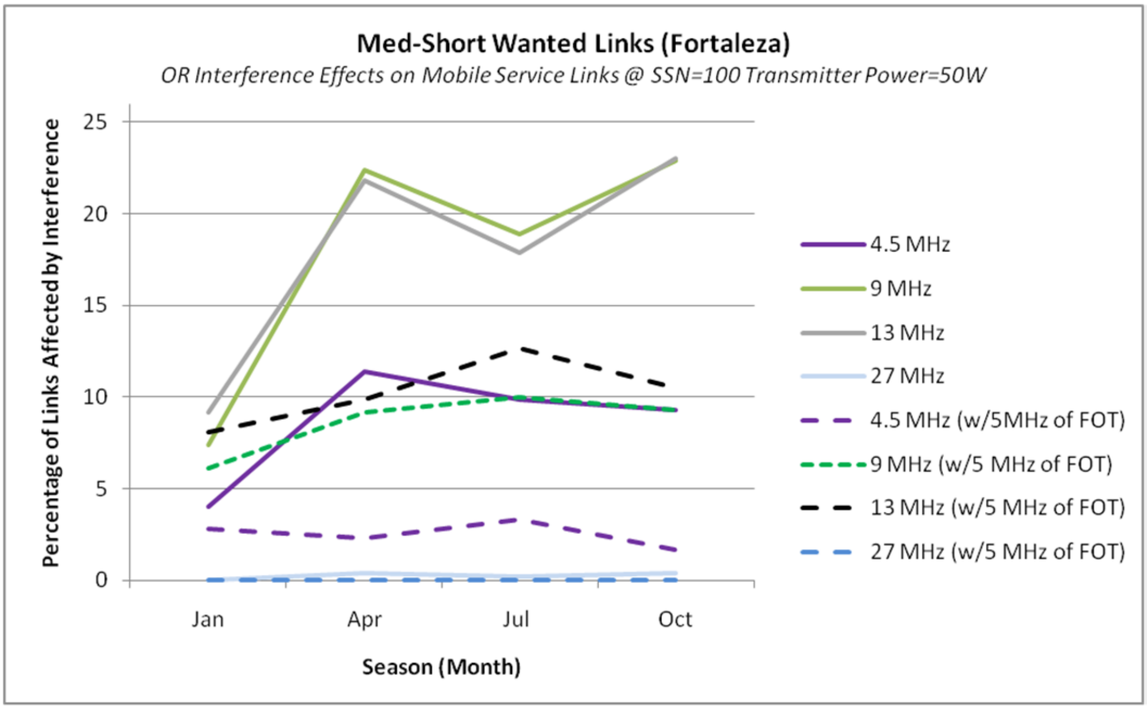

FIGURE 27

Oceanographic radar interference effects on med-short mobile service links (Virginia Beach)

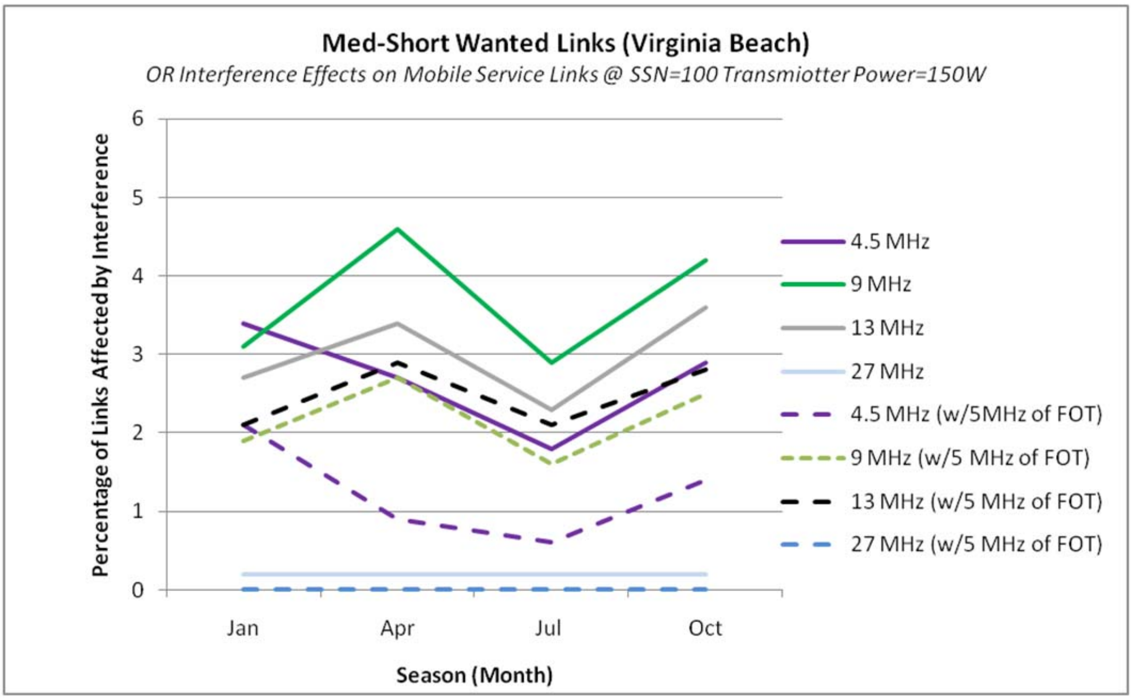

FIGURE 28

Oceanographic radar interference effects on med-short mobile service links (Virginia Beach)

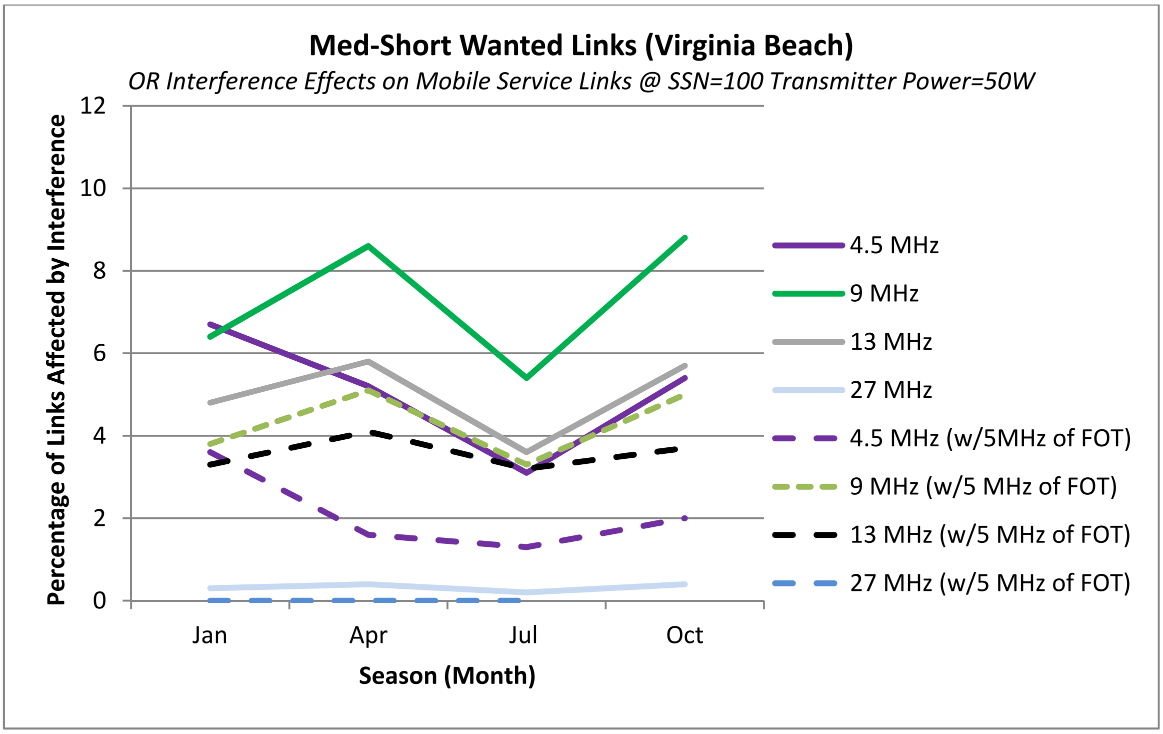

FIGURE 29

Oceanographic radar interference effects on short fixed service links (Fortaleza)

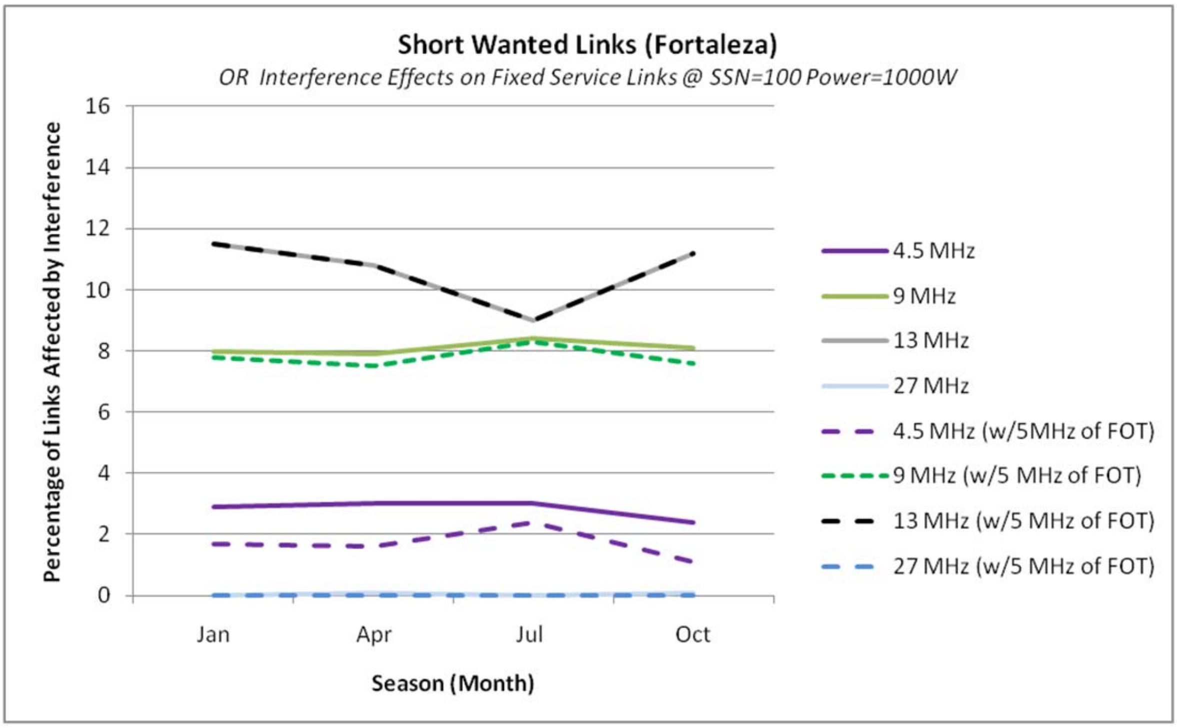

FIGURE 30

Oceanographic radar interference effects on short fixed service links (Virginia Beach)

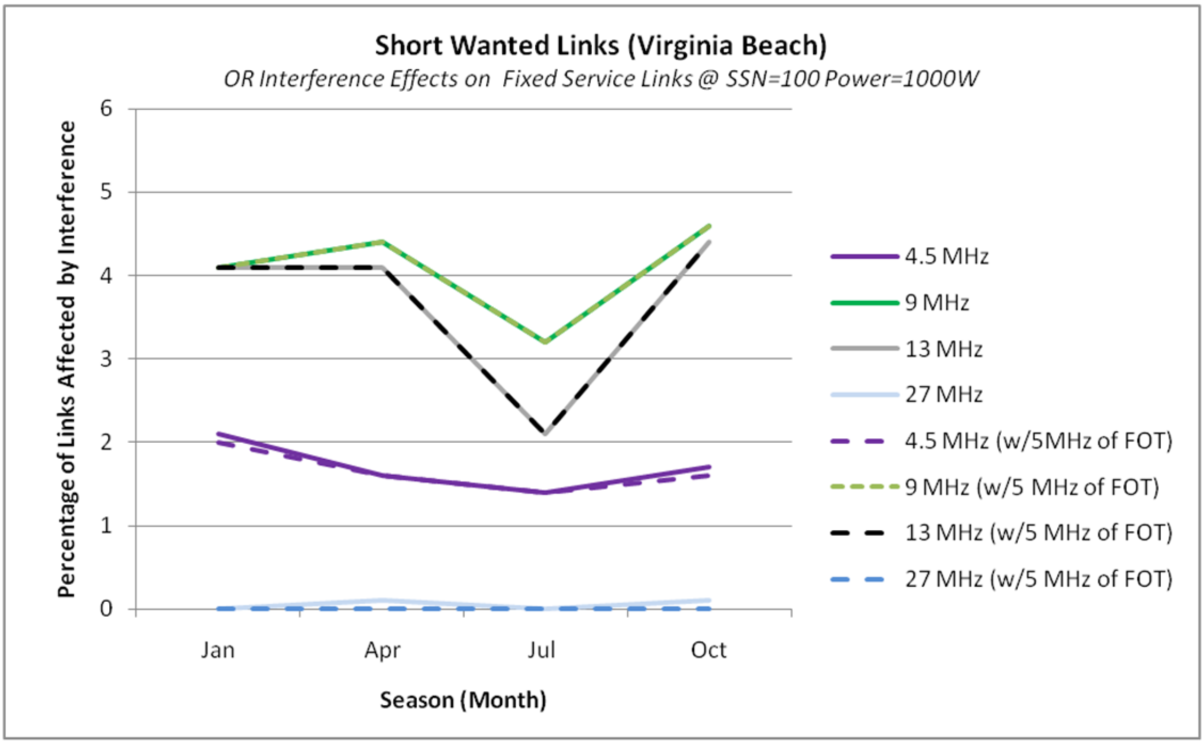

FIGURE 31

Oceanographic radar interference effects on med-short fixed service links (Fortaleza))

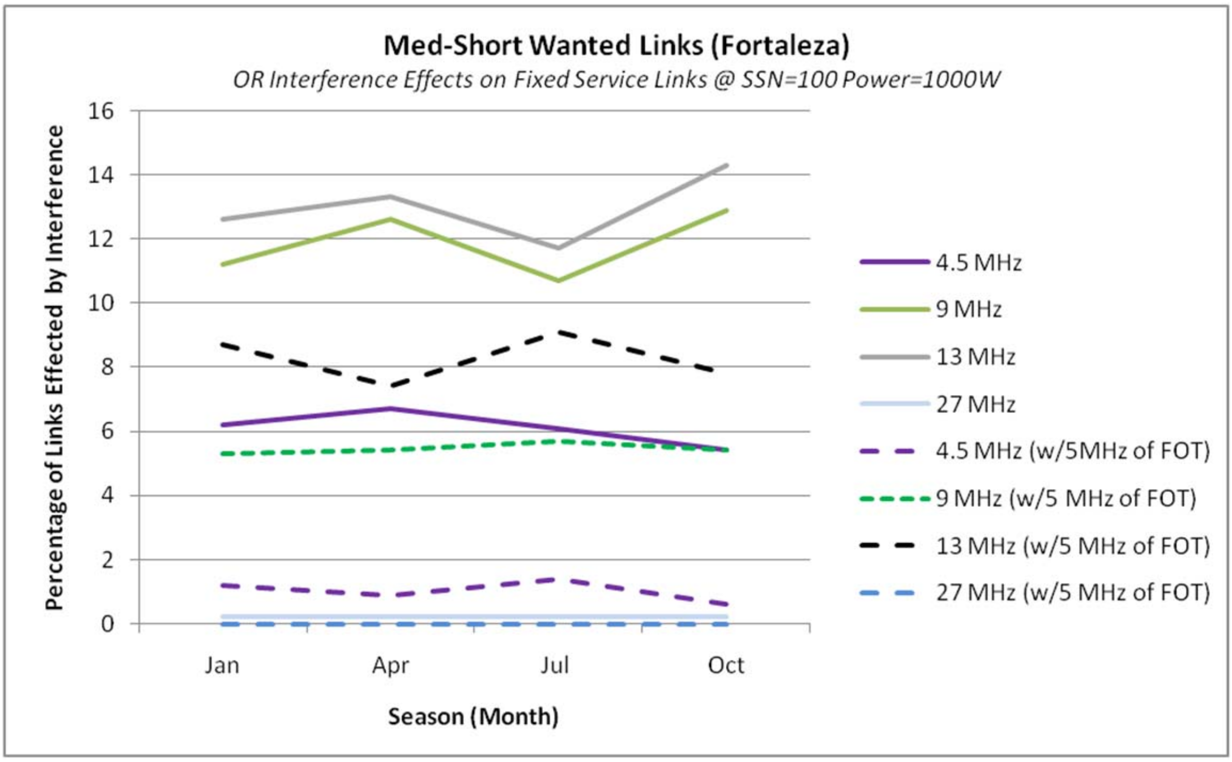

FIGURE 32

Oceanographic radar interference effects on med-short fixed service links (Virginia Beach)

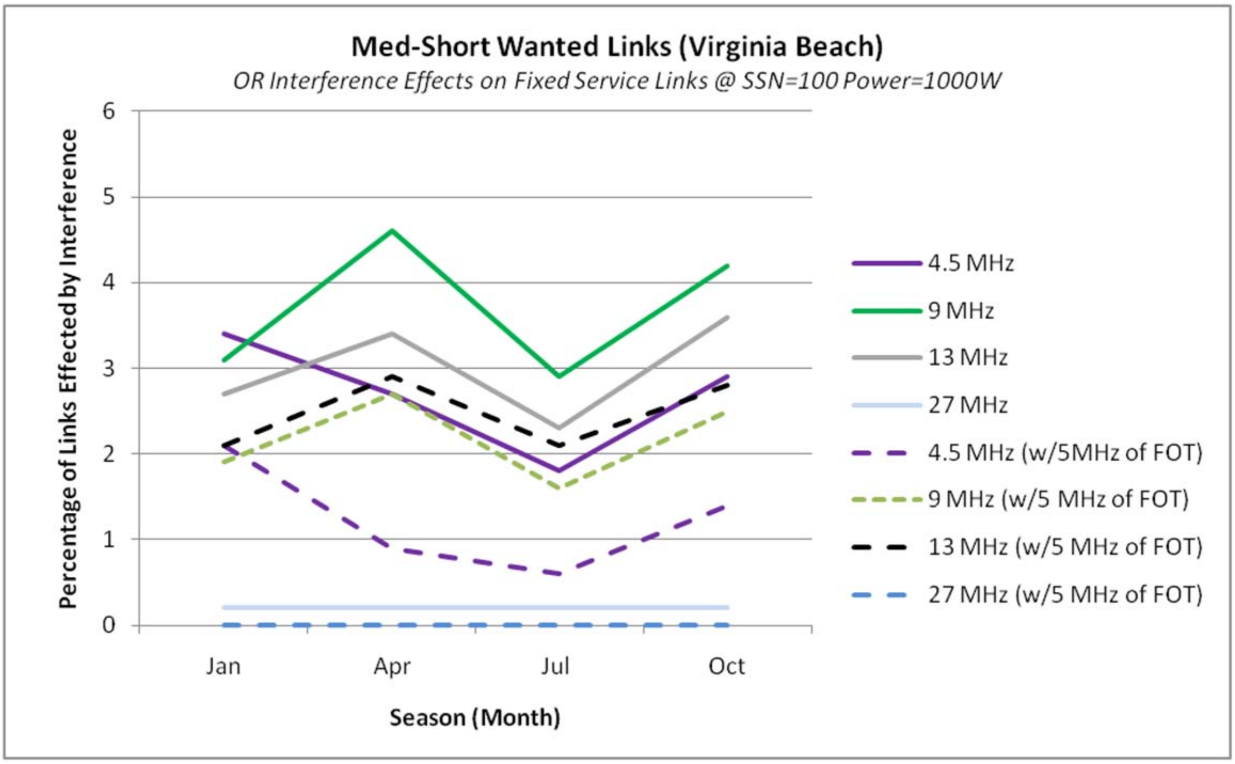

FIGURE 33

Oceanographic radar interference effects on med-long fixed service links (Fortaleza)

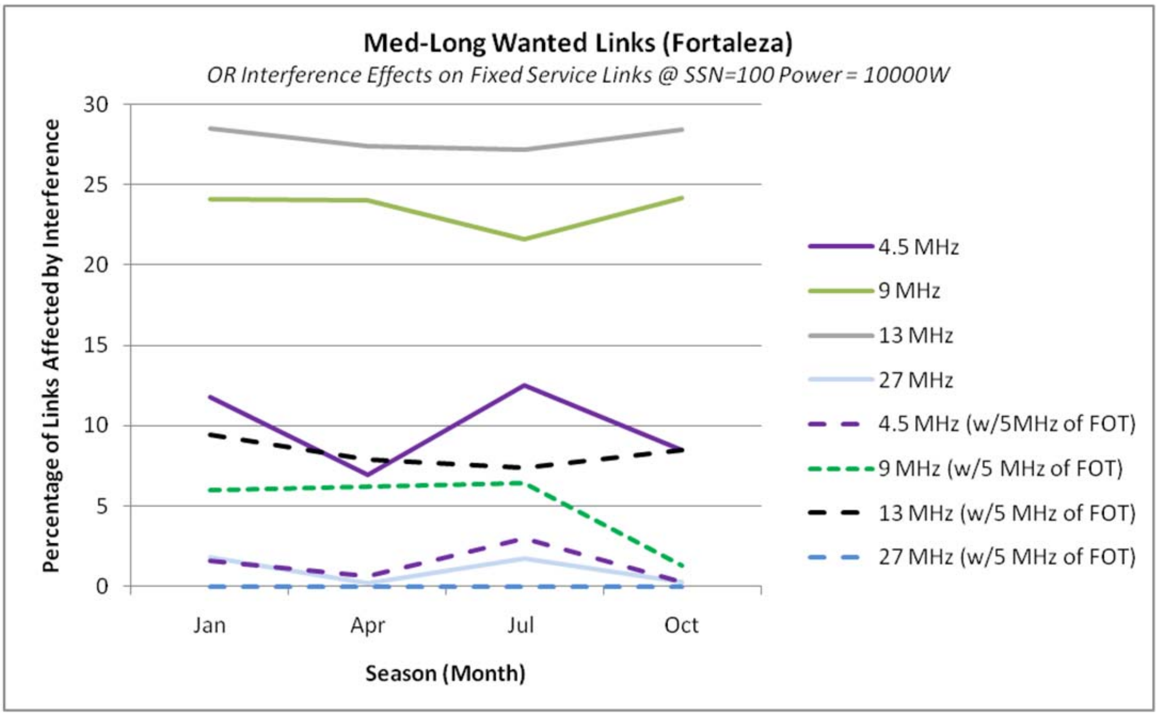

FIGURE 34

Oceanographic radar interference effects on med-long fixed service links (Virginia Beach)

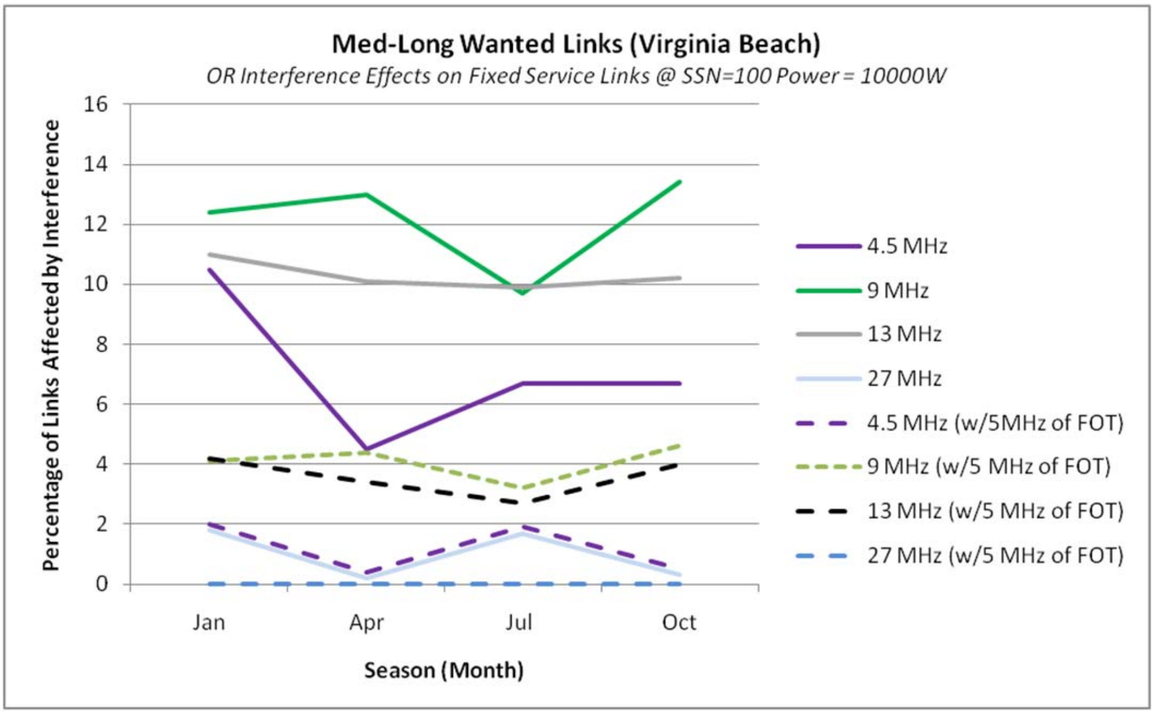

FIGURE 35

Oceanographic radar interference effects on long fixed service links (Fortaleza)

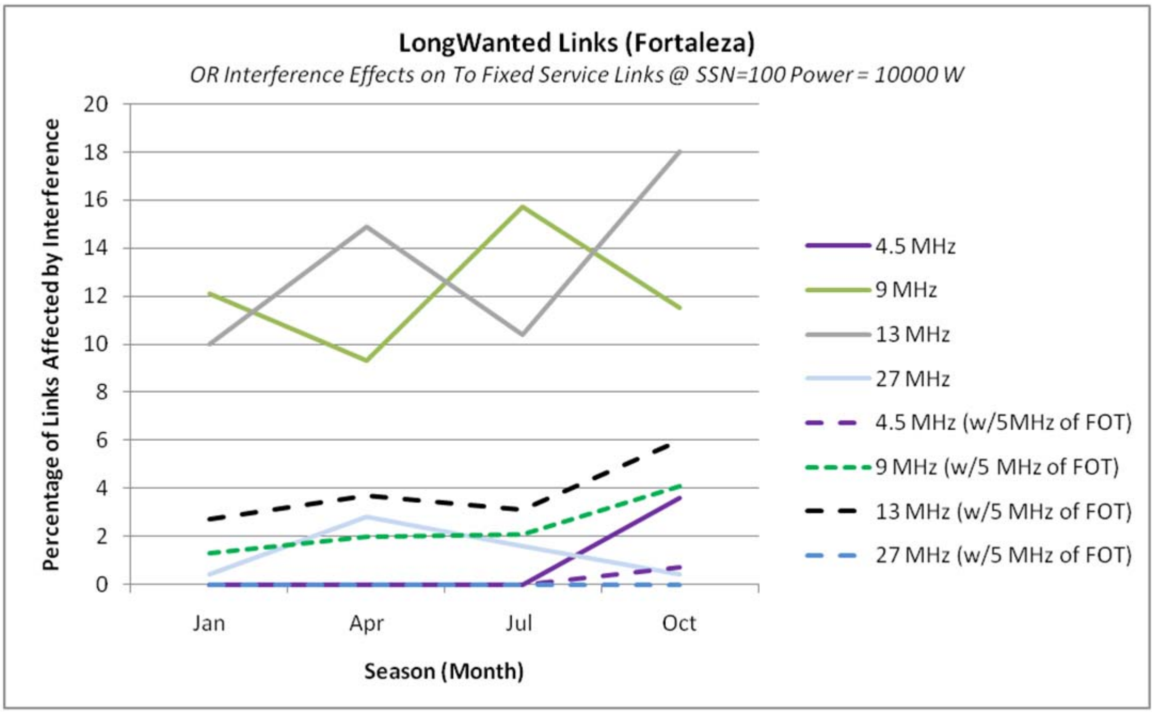

FIGURE 36

Oceanographic radar interference effects on long fixed service links (Virginia Beach)

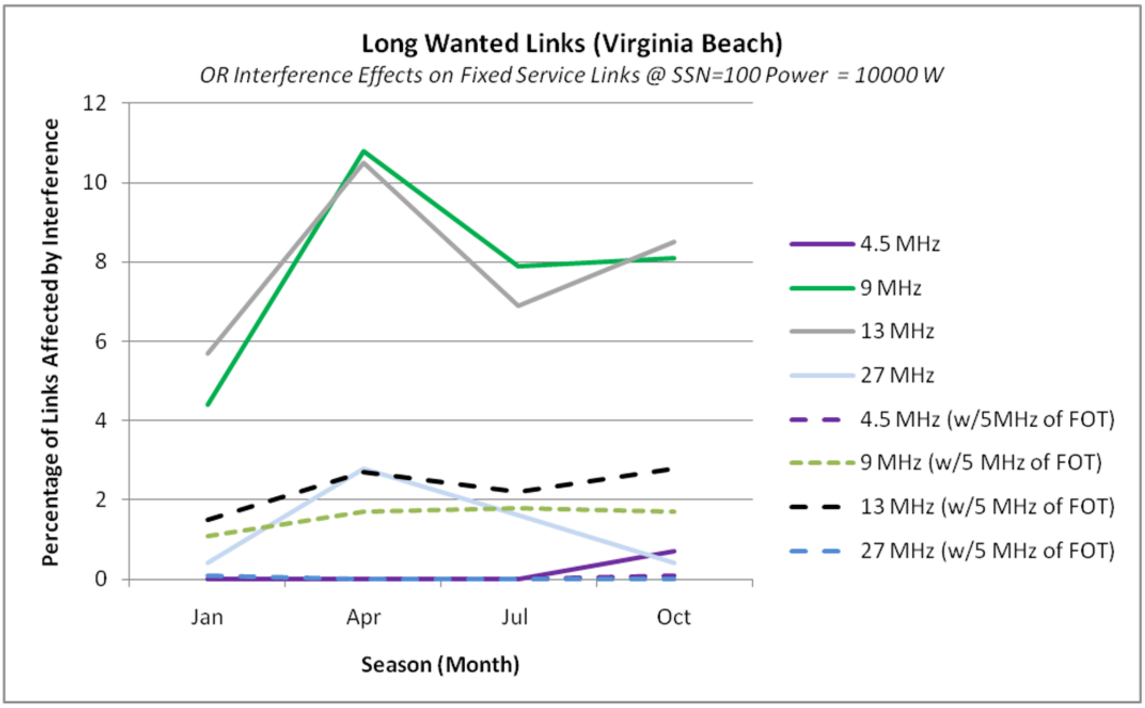

Attachment 2

Calculation of the interfering time ratio for oceanographic radars in each frequency band

2-1 5 MHz (System 1, Table 1)

At 5 MHz, the locations where the path losses are lowest are:

$(L,G)_1$=(0°E, 49.75°N) → Normandy coast, France

$(L,G)_4$=(5°W, 51.5°N) → Mer de la Manche

$(L,G)_7$=(0.25°W, 49.75°N) =L1

$(L,G)_{10}$= (1.25°E, 49.75°N) → Normandy coast, France

Therefore the location (0.5°E, 50°N) is used for these calculations. This location is in coastal Northern Normandy, France, where N_{20} equal to –150.4 and –151.7 dBW/Hz for "rural" and "quiet rural" respectively.

For a 3 kHz bandwidth receiver, I_{max} is equal to –121.6 and –122.9 dBW respectively for "rural" and "quiet rural" environment.

Figure 37 below represents the cumulative histogram representing the interference level from System 1.

FIGURE 37

Cumulative histogram of external noise (dBW/Hz) at 5 MHz at (0.5°E, 50°N) for System 1

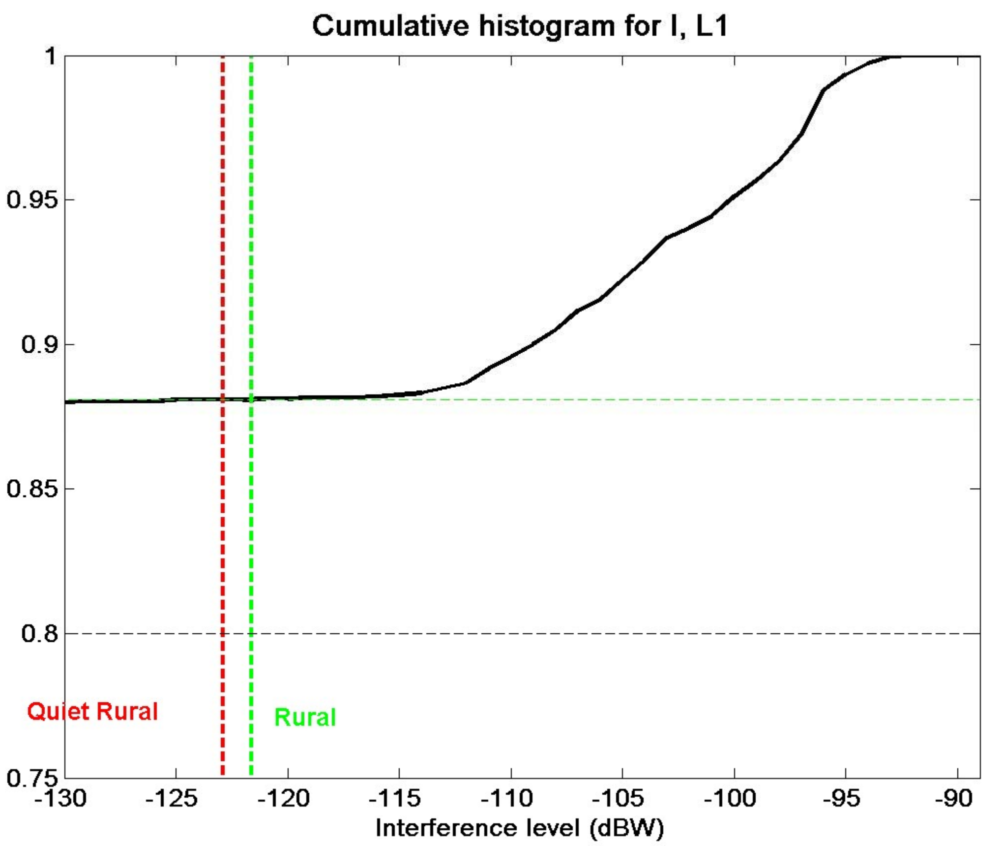

The cumulative histograms show that the interference level is below the “quiet rural” limit 88% of the time for System 1.

The long-term interference criterion in the “quiet rural” environment is exceeded no more than 12% of time for system 1 over the whole area.

When considering the ICEPAC output parameter “elevation angle”, the elevation angle of the signal radiated from the oceanographic radar towards a given location, the results at 5 MHz for the studied location at 16UT and 4UT in January (M1) and July (M7) can be found in Table 21.

TABLE 21

Elevation angle of the signal radiated from the oceanographic radar towards a given location

	16UT		**4UT**	
	M1	**M7**	**M1**	**M7**
L1, L7, L10	52°	42°-50°	N/A	60°
L4	N/A	48°	N/A	N/A

As seen in Table 21, the elevation angles of oceanographic radar signals reaching the location are between 40° and 60° and may be attenuated by the oceanographic radar antenna gain.

2-2 9 MHz (Systems 5 and 10, Table 1)

At 9 MHz, the location where the path losses are lowest remains unchanged whatever the season:

$(L,G)_1$=((3.25°E, 50.25°N)

$(L,G)_4$=(4°E, 50°N)

$(L,G)_7$=(5°E, 50.75°N))

$(L,G)_{10}$= (3.75°E, 50.5°N).

Therefore the location (4°E, 50°N) is used for these calculations. This location is in Belgium.

N_{20} equal to –159.6 and –161.7 dBW/Hz for “rural” and “quiet rural” respectively (see Fig. 43, Attachment 3).

For a 3 kHz bandwidth receiver, I_{max} is equal to –130.8 and –132.9 dBW respectively for “rural” and “quiet rural” environment.

Figure 38 represents the cumulative histogram representing the interference level from Systems 5 and 10.

FIGURE 38

Cumulative histogram of external noise (dBW/Hz) at 9 MHz in location (4°E, 50°N) for System 5 (blue) and System 10 (black)

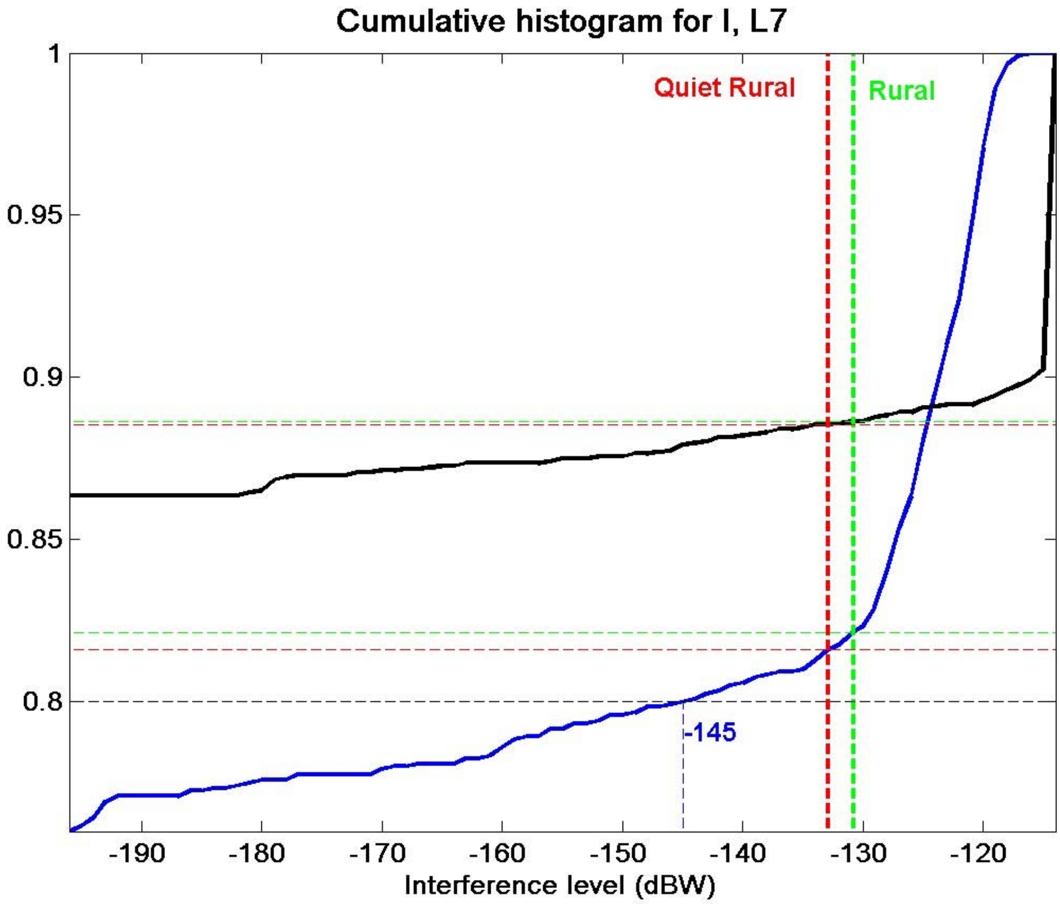

The cumulative histograms show that the interference level is below the "quiet rural" limit 81.6% and 88.5% of the time for systems 5 and 10 respectively.

The long term interference criterion in the "quiet rural" environment is exceeded no more than 18.4% of time for system 5 and 11.5% of time for system 10 over the whole area.

When considering the ICEPAC output parameter "elevation angle", the elevation angle of the signal radiated from the oceanographic radar towards a given location, the results for points located in Belgium are in the order of 35° at 4UT in January and July as well as 16UT in July, and 35° at 16UT in January.

2-3 13 MHz (Systems 2 and 6, Table 1)

At 13 MHz, the location where the path losses are the lowest are:

(L,G)1=(8°E, 51.25°N) → western Germany

(L,G)4= (16°E, 51.25°N) → south west Poland

(L,G)7= (11.25°E, 41.5°N) → mid-path northern Sardinia/Italy

(L,G)10= (8°E, 47°N) → Northern Switzerland.

For a 3 kHz bandwidth receiver, I_{max} is equal to –136.1 and –139.1 dBW respectively for "rural" and "quiet rural" environment.

Figure 39 shows the cumulative histograms for systems 2 and 6 at location L7 (worst case).

FIGURE 39

Cumulative histogram of external noise (dBW/Hz) at 13 MHz at location L7. System 2 in blue and System 6 in black

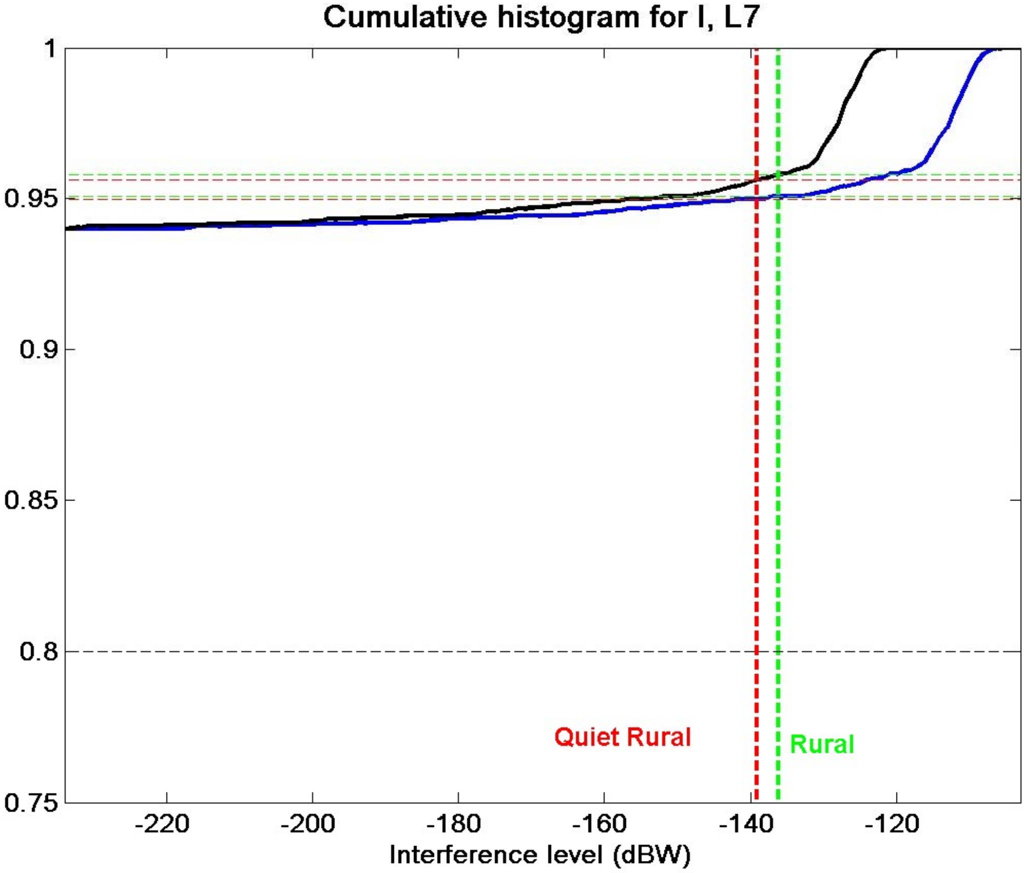

The cumulative histograms in Fig. 39 for the worst location (L7) show that the interference level is below the “quiet rural” limit 95% and 95.6% of the time for systems 2 and 6 respectively.

The long-term interference criterion in the “quiet rural” environment is exceeded no more than 5% of time for system 2 and 4.4% of time for system 6 over the whole area.

When considering the ICEPAC output parameter “elevation angle”, the elevation angle of the signal radiated from the oceanographic radar towards a given location, the results at 13 MHz for the studied location at 16UT and 4UT in January (M1) and July (M7) can be found in Table 22.

TABLE 22

	16UT		**4UT**	
	M1	**M7**	**M1**	**M7**
L1	30°	10°	37°	36°
L4	16°	22°	25°	24°
L7	16°	23°	24°	24°
L10	30°	16°	38°	37°

2-4 16 MHz (System 7, Table 1)

At 16 MHz, the locations where the path losses are lowest are the following:

$(L,G)_1$=(5°E, 40.5°N) → NE Minorque (Baleares Islands)
$(L,G)_4$= (19°E, 49.75°N) → Southern Poland
$(L,G)_7$= (17.5°E, 41.75°N) → Adriatic Sea
$(L,G)_{10}$= (3.5°E, 40.25°N) → North Baleares Islands

The considered values for N_{20} are:

– L1 and L10: −163.7 dBW/Hz for "rural" and −164.7 dBW/Hz for "quiet rural" environment;
– L4 and L7: −167.4 dBW/Hz for "rural" and −169.9 dBW/Hz for "quiet rural" environment.

The N_{20} values presented on the second line correspond to a worse case than those on the first line. The lowest path attenuation occurs at Location L7.

Therefore only the worst case of location L7 is considered, with I_{max} for a 3 kHz bandwidth receiver equal to −138.6 dBW for "rural" and −141.1 dBW for "quiet rural" environment.

Figure 40 shows the cumulative histogram for I in L7.

FIGURE 40

Cumulative histogram of interference from System 7 at location 7 (worst case)

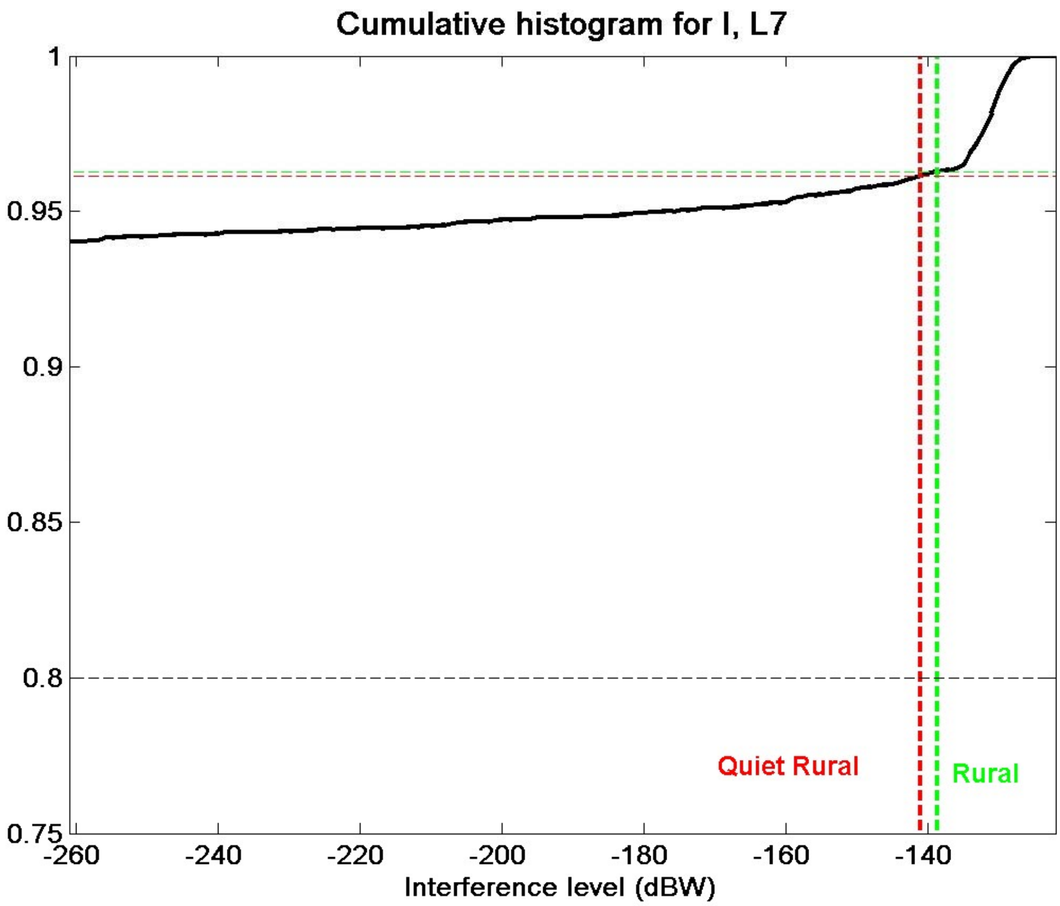

Figure 40 shows that the interference level is below the "quiet rural" limit 96.1% of the time.

The long-term interference criterion in the "quiet rural" environment is exceeded no more than 3.9% of time for system 7, over the whole area.

When considering the ICEPAC output parameter "elevation angle", the elevation angle of the signal radiated from the oceanographic radar towards a given location, the results at 16 MHz for the studied location at 16UT and 4UT in January (M1) and July (M7) can be found in Table 23.

TABLE 23

	16UT		**4UT**	
	M1	**M7**	**M1**	**M7**
L1	27°	8°	31°	
L4	14°	20°	20°	
L7	12°	17°	18°	
L10	28°	9°	32°	

If the oceanographic radar is backed up by natural obstacles (obstructions, terrain, trees …) then it is likely that at elevations below 20° the signal radiated will have reduced gain in the backlobe direction.

2-5 25 MHz (Systems 3, 8, 11, and 12, Table 1)

At 25 MHz, the locations where the path losses are the lowest are the following:

$(L,G)_1$=(5.5°E, 32.25°N) → Algeria

$(L,G)_4$= $(L,G)_1$

$(L,G)_7$= (22.75°E, 32,25°N) → Libya

$(L,G)_{10}$= (17,75°E, 41,5°N) → Adriatic Sea.

Whatever the location, N_{20} is −175 and −183 dBW/Hz respectively for "rural" and "quiet rural" environments.

For a 3 kHz bandwidth receiver, I_{max} is equal to −146.2 and −154.2 dBW respectively for "rural" and "quiet rural" environment.

The lowest path attenuation occurs at location L7, and Fig. 41 below shows the cumulative histograms for Systems 3 and 8 at this location.

FIGURE 41

Cumulative histogram of interference at location 7 (worst case). System 3 in blue, system 8 in black, system 11 in magenta, system 12 in yellow

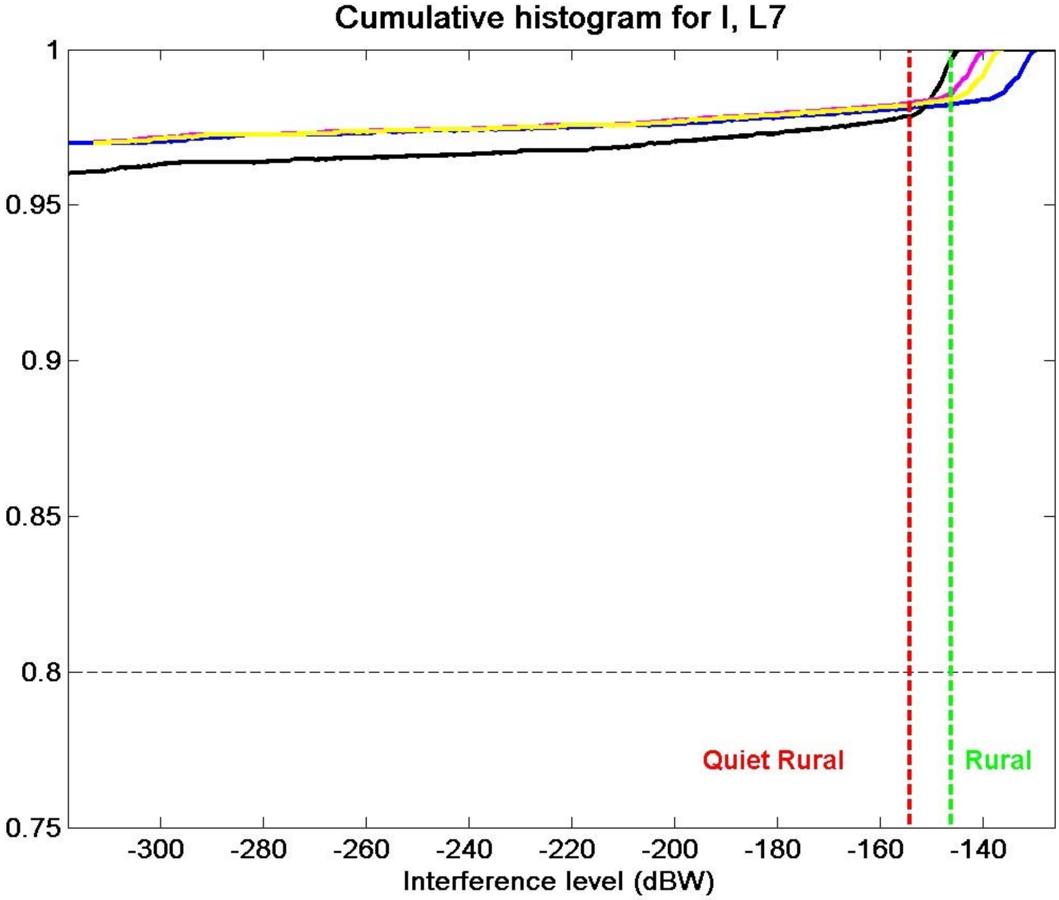

Figure 41 shows that the interference level is below the "quiet rural" limit 98.1%, 97.8%, 98.3% and 98.2% of the time for systems 3, 8, 11 and 12 respectively.

The long-term interference criterion in the "quiet rural" environment is exceeded no more than 2.2% of time for Systems 3, 8, 11, 12 operating in this frequency band, over the whole area.

When considering the ICEPAC output parameter "elevation angle", the elevation angle of the signal radiated from the oceanographic radar towards a given location, the results at 25 MHz for the studied location at 16UT and 4UT in January (M1) and July (M7) are in the following (Table 24):

TABLE 24

Elevation angles

	16UT		4UT	
	M1	M7	M1	M7
L1-L4	14°	2°	17°	
L7	7°	9°	9°	
L10	15°	3°	18°	

If the oceanographic radar is backed up by natural obstacles (obstructions, terrain, trees …) then it is likely that at elevations below 20° the signal radiated will have reduced gain in the backlobe direction.

2-6 45 MHz (Systems 4 and 13, Table 1)

Sky-wave propagation software can only be used for frequencies up to 30 MHz. Sky-wave propagation was not considered at 45 MHz.

Attachment 3

Calculation of external noise levels in the different frequency bands

3-1 5 MHz

At 5 MHz, considering an oceanographic radar emitter in western Brittany, France, the location where the sky-wave propagation losses are lowest is around (0.5° E, 50° N), which is located in coastal Normandy.

At this location, the atmospheric noise follows the values as indicated Table 25.

TABLE 25

Atmospheric noise (dBW/Hz) at 5 MHz in location (0.5°E, 50°N)

Time block	Winter	Spring	Summer	Autumn
0000-0400	−151.9	−151.1	−151.2	−151.5
0400-0800	−154.3	−164.9	−162.4	−158.0
0800-1200	−181.5	−181.4	−180.5	−178.8
1200-1600	−180.3	−180.2	−178.7	−177.3
1600-2000	−158.8	−163.2	−163.3	−158.2
2000-2400	−152.7	−151.2	−152.3	−150.3

Man-made noise is −170.4 dBW/Hz for the "quiet rural" environment and −156.2 dBW/Hz for the "rural" environment The galactic noise is –168.1 dBW/Hz.

Figure 42 shows the cumulative histogram of the resulting external noise for the "rural" (green) and the "quiet rural" (red) environments.

Since the receivers from systems of the fixed and mobile services are expected to work 80% of the time whatever the conditions, it seems justified to consider an external noise threshold value that is not exceeded 80% of time.

The values exceeded by N 20% of the time (N_{20}) are highlighted in Fig. 42.

N_{20} is equal to −150.4 and −151.7 dBW/Hz for the "rural" and the "quiet rural" environments respectively.

FIGURE 42

Cumulative histogram of external noise (dBW/Hz) at 5 MHz in location (0.5°E, 50°N)

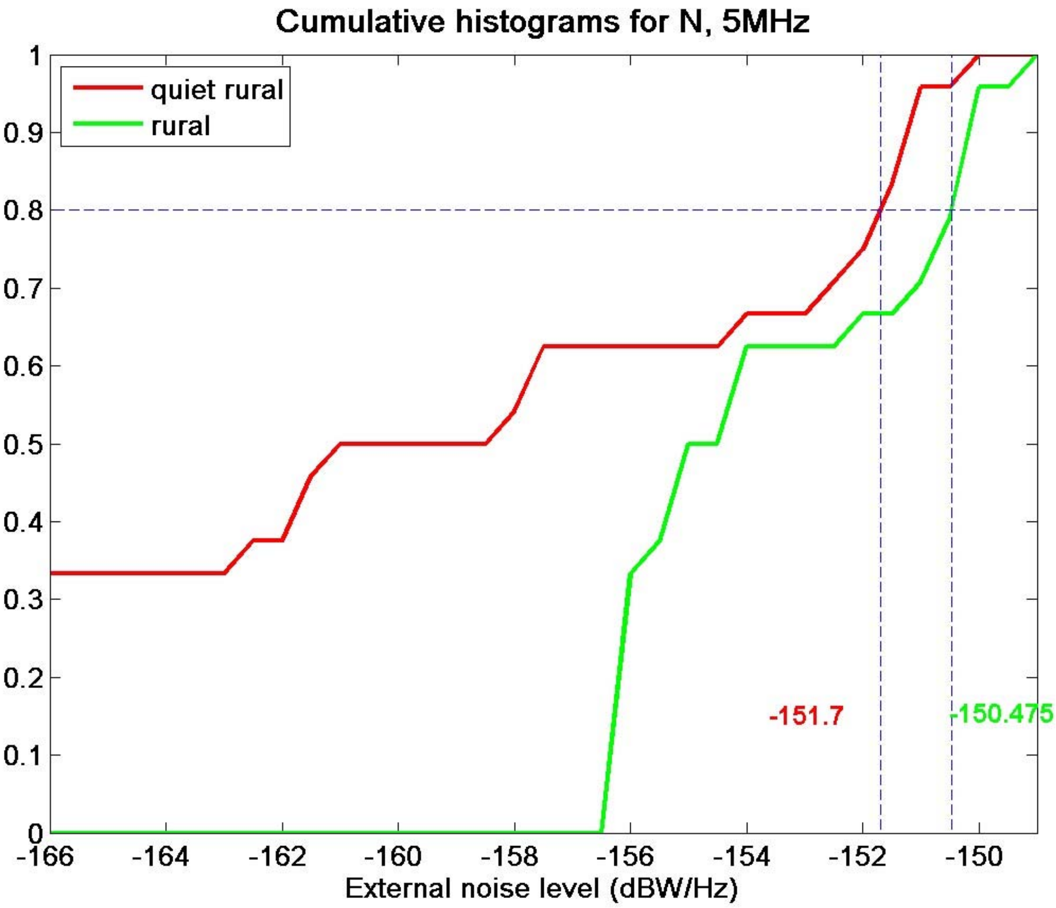

3-2 9 MHz

At 9 MHz, considering an oceanographic radar emitter in western Brittany, France, the location where the sky-wave propagation losses are lowest is around (4° E, 50° N), which is located in Belgium.

At this location, the atmospheric noise follows the values as indicated Table 25.

TABLE 25

Atmospheric noise (dBW/Hz) at 9 MHz in location (5°E, 51°N)

Time block	Winter	Spring	Summer	Autumn
0000-0400	−164.5	−162.5	−160.4	−164.0
0400-0800	−163.7	−167.2	−164.6	−167.2
0800-1200	−173.1	−174.1	−174.6	−173.4
1200-1600	−171.3	−172.7	−172.4	−171.5
1600-2000	−163.4	−162.3	−161.8	−162.8
2000-2400	−161.9	−160.1	−159.2	−159.8

Man-made noise is −177.7 dBW/Hz for “quiet rural” environment and −163.2 dBW/Hz for “rural” environment. The galactic noise is −173.9 dBW/Hz.

Figure 43 shows the cumulative histogram of the resulting external noise for “rural” (green) and “quiet rural” (red) environment.

Since the receivers from systems of the fixed and mobile services are expected to work 80% of the time whatever the conditions, it seems justified to consider an external noise threshold value that is not exceeded 80% of time.

The values exceeded by N 20% of the time (N_{20}) are highlighted in Fig. 43.

N_{20} is equal to −159.6 and −161.7 dBW/Hz for “rural” and “quiet rural” respectively.

FIGURE 43

Cumulative histogram of external noise (dBW/Hz) at 9 MHz in location (5°E, 51°N)

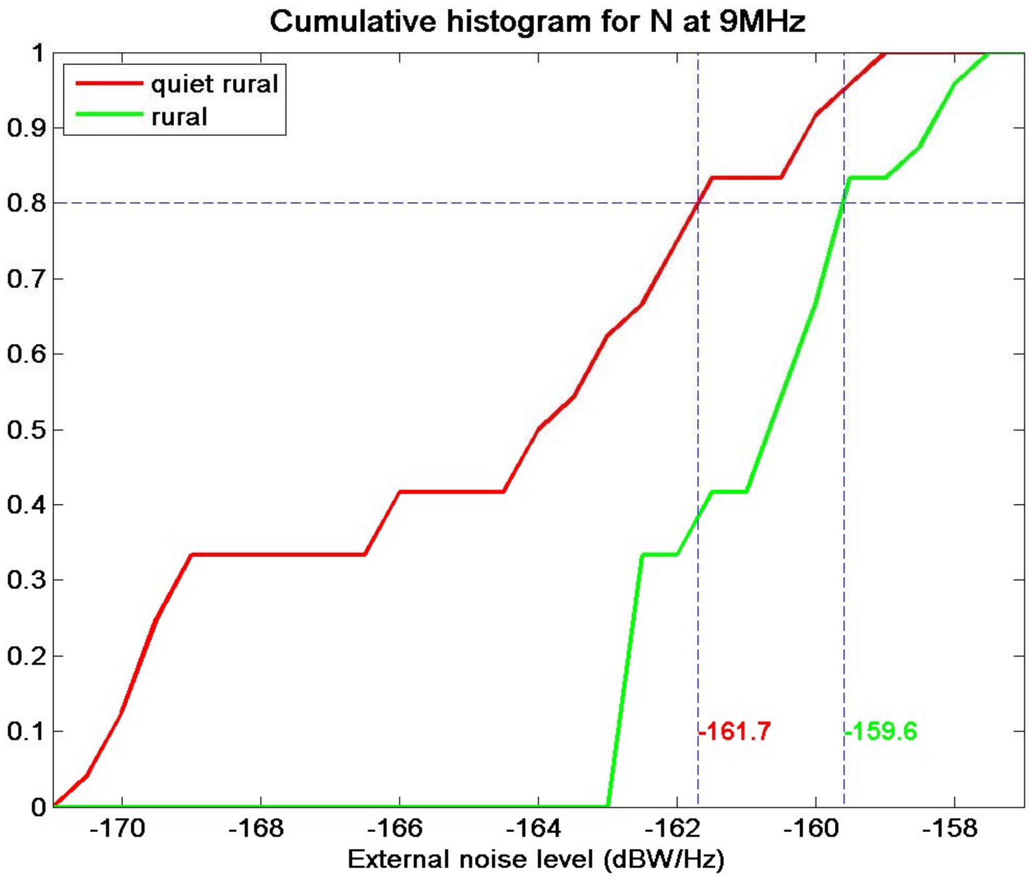

3-3 13 MHz

At 13 MHz, considering an oceanographic radar emitter in western Brittany, France, the location where the sky-wave path losses are lowest depends on the season.

$(L,G)_1$=(8°E, 51.25°N)

$(L,G)_4$= (16°E, 51.25°N)

$(L,G)_7$= (11.25°E, 41.5°N)

$(L,G)_{10}$= (8°E, 47°N).

At this location, the median atmospheric noise follows the values indicated Table 26.

NOTE – Values for L4 have been disregarded since they were smaller than 30 dB. It is recognized that, under certain rare circumstances, ICEPAC predicts path losses smaller than 30 dB from certain regions to the receiver site. This is physically not possible, and is likely due to a flaw in ICEPAC.

TABLE 26

Atmospheric noise (dBW/Hz) at 13 MHz for L1, L7 and L10 (L4 values were incorrect)

Time block	Winter	Spring	Summer	Autumn
L1				
0000-0400	−177.8	−175.0	−171.8	−177.3
0400-0800	−174.6	−175.3	−172.7	−178.5
0800-1200	−172.2	−174.2	−175.4	−174.0
1200-1600	−167.9	−170.7	−172.2	−169.9
1600-2000	−168.9	−165.9	−165.5	−168.1
2000-2400	−171.9	−169.8	−168.1	−169.2
L7				
0000-0400	−179.3	−173.5	−172.1	−176.0
0400-0800	−175.1	−173.2	−172.9	−176.4
0800-1200	−172.1	−173.9	−175.7	−173.0
1200-1600	−167.7	−170.4	−173.4	−169.4
1600-2000	−170.4	−164.8	−165.0	−165.0
2000-2400	−171.9	−169.3	−167.4	−168.0
L10				
0000-0400	−177.9	−174.6	−172.4	−176.9
0400-0800	−174.9	−174.3	−172.7	−177.6
0800-1200	−172.1	−174.0	−175.4	−173.0
1200-1600	−167.7	−170.4	−172.4	−169.7
1600-2000	−169.6	−165.2	−165.0	−167.0
2000-2400	−171.4	−170.1	−168.0	−168.7

Man-made noise is −182.3 dBW/Hz in “quiet rural” environment and −167.7 dBW/Hz in “rural” environment. The galactic noise is −177.6 dBW/Hz.

Figure 44 shows the cumulative histograms of the resulting external noise for the “rural” (green) and the “quiet rural” (red) environments. It must be noted that histograms are quite similar for the 3 considered locations.

The value for N_{20} is −164.9 and −167.9 dBW/Hz respectively for the “rural” and the “quiet rural” environments.

FIGURE 44

Cumulative histogram of external noise (dBW/Hz) at 13 MHz for 3 locations (from bottom to top, N20 values for L1, L7, L10)

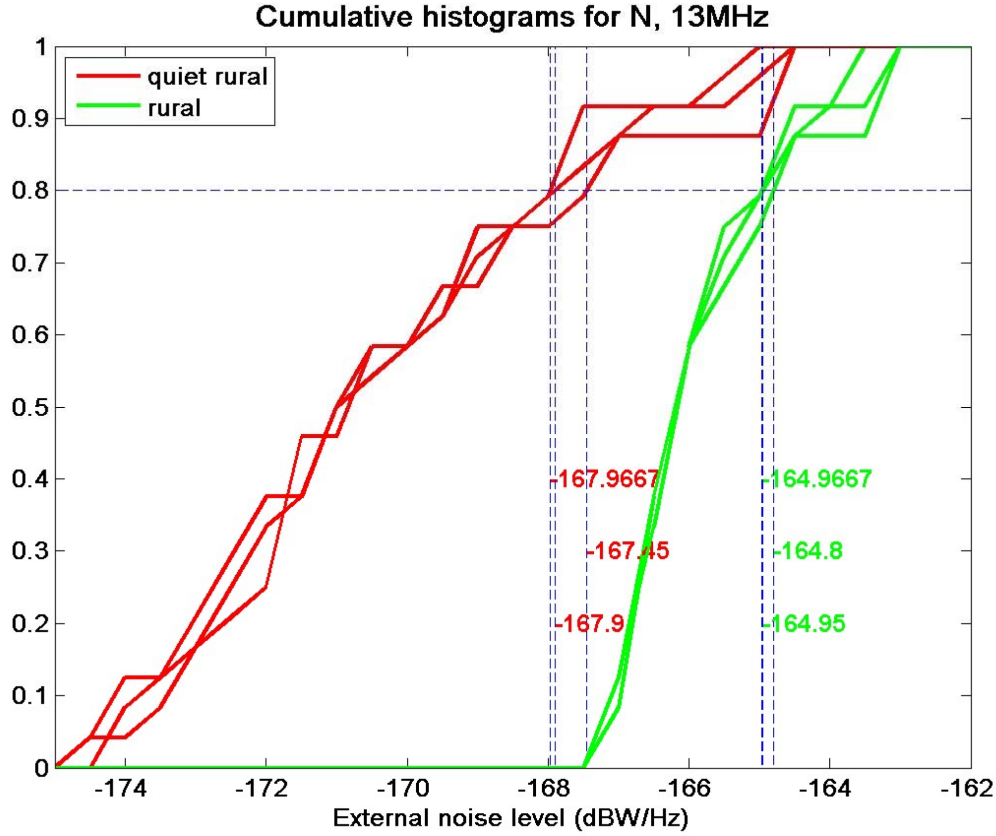

3-4 16 MHz

At 16 MHz, considering an oceanographic radar emitter in western Brittany, France, the locations where the path losses are lowest are the following:

$(L,G)_1$=(5°E, 40.5°N)

$(L,G)_4$= (19°E, 49.75°N)

$(L,G)_7$= (17.5°E, 41.75°N)

$(L,G)_{10}$= (3.5°E, 40.25°N)

At this location, the median atmospheric noise follows the values indicated Table 27.

TABLE 27

Atmospheric noise (dBW/Hz) at 16 MHz for the 4 locations

Time block	Winter	Spring	Summer	Autumn
L1				
0000-0400	−189.3	−170.5	−172.1	−171.4
0400-0800	−183.2	−174.9	−175.9	−171.0
0800-1200	−175.2	−171.8	−176.5	−169.0
1200-1600	−168.2	−164.7	−170.0	−162.9
1600-2000	−170.9	−164.6	−166.5	−157.5
2000-2400	−183.0	−164.0	−169.0	−159.9
L4				
0000-0400	−192.4	−176.0	−176.9	−180.6
0400-0800	−181.7	−178.7	−179.5	−177.8
0800-1200	−177.2	−179.6	−179.7	−177.4
1200-1600	−172.1	−169.5	−171.1	−167.9
1600-2000	−176.0	−169.0	−168.6	−166.1
2000-2400	−186.8	−170.3	−174.0	−171.3
L7				
0000-0400	−196.3	−176.9	−176.1	−181.0
0400-0800	−182.5	−178.3	−178.9	−178.5
0800-1200	−178.1	−179.1	−179.4	−177.9
1200-1600	−173.0	−170.2	−171.1	−167.1
1600-2000	−179.2	−169.4	−168.0	−165.5
2000-2400	−191.3	−171.4	−173.3	−171.1
L10				
0000-0400	−187.8	−170.0	−172.9	−170.9
0400-0800	−183.1	−174.4	−176.1	−170.5
0800-1200	−174.5	−170.7	−176.6	−168.0
1200-1600	−167.2	−164.0	−170.4	−162.5
1600-2000	−168.8	−164.1	−166.9	−157.1
2000-2400	−181.1	−163.3	−169.8	−159.3

Man-made noise is −184.8 dBW/Hz in “quiet rural” environment and −170.2 dBW/Hz in “rural” environment. The galactic noise is −179.7 dBW/Hz.

Figure 27 shows the cumulative histograms of the resulting external noise for the “rural” (green) and the “quiet rural” (red) environments. It must be noted that histograms are quite similar for locations 1 and 10 on one side, and for locations 4 and 7 on the other side.

The considered values for N_{20} are:

− for L1 and L10: −163.7 and −164.7 dBW/Hz respectively for the “rural” and the “quiet rural” environments;

− for L4 and L7: −167.4 and −169.9 dBW/Hz respectively for the "rural" and the "quiet rural" environments.

FIGURE 45

Cumulative histogram of external noise (dBW/Hz) at 16 MHz for the 4 locations (N20 values for L1 to 10 respectively indicated from top to bottom)

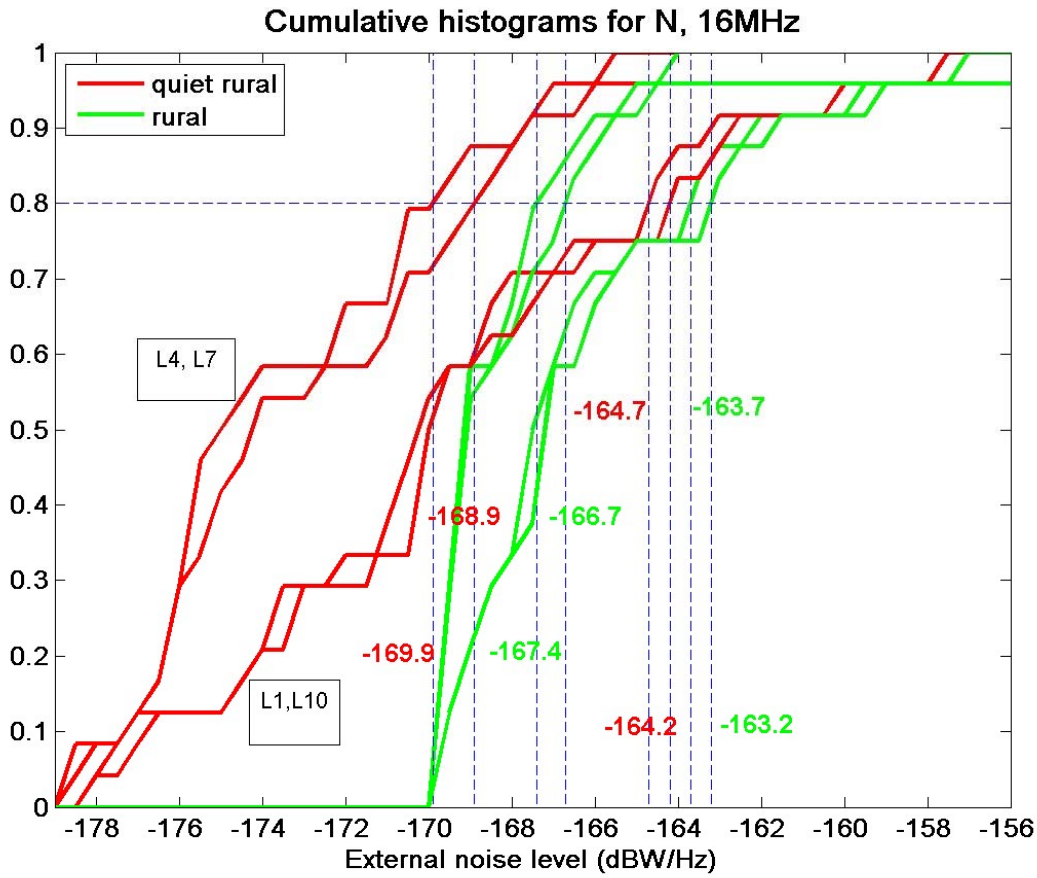

3-5 25 MHz

At 25 MHz, considering an oceanographic radar emitter in western Brittany, France, the locations where the path losses are lowest (with values around 150 dB) are the following:

$(L,G)_1$=(5.5°E, 32.25°N)

$(L,G)_4$= $(L,G)_1$

$(L,G)_7$= (22.75°E, 32,25°N)

$(L,G)_{10}$= (17,75°E, 41,5°N).

At this location, the median atmospheric noise follows the values indicated Table 28.

TABLE 28

Atmospheric noise (dBW/Hz) at 25 MHz for the 3 locations

Time block	Winter	Spring	Summer	Autumn
L1				
0000-0400	−217.5	−206.6	−204.6	−209.6
0400-0800	−209.1	−207.3	−207.2	−205.6
0800-1200	−203.9	−208.8	−207.4	−201.3
1200-1600	−193.7	−200.9	−209.6	−191.5
1600-2000	−192.5	−194.0	−199.9	−183.1
2000-2400	−203.8	−199.6	−198.8	−195.1
L7				
0000-0400	−220.6	−206.5	−204.8	−208.2
0400-0800	−210.0	−207.5	−209.0	−205.9
0800-1200	−206.9	−210.0	−207.0	−202.9
1200-1600	−199.5	−198.5	−204.3	−189.6
1600-2000	−195.5	−194.7	−197.7	−183.1
2000-2400	−208.8	−199.0	−200.2	−194.4
L10				
0000-0400	−217.3	−206.4	−203.2	−210.4
0400-0800	−210.6	−210.6	−206.2	−207.2
0800-1200	−206.8	−208.4	−205.7	−202.5
1200-1600	−200.5	−198.6	−201.8	−193.7
1600-2000	−196.8	−194.8	−194.7	−186.6
2000-2400	−205.3	−198.5	−195.9	−196.4

Man-made noise is −190.4 dBW/Hz for “quiet rural” environment and −175.5 dBW/Hz for “rural” environment. The galactic noise is −184.2 dBW/Hz.

Figure 46 shows the cumulative histograms of the resulting external noise for the “rural” (green) and the “quiet rural” (red) environments which are quite similar for the three locations. It can be seen that whatever the location, N_{20} is −175 dBW/Hz and −183 dBW/Hz respectively for the “rural” and the “quiet rural” environments.

FIGURE 46

Cumulative histogram of external noise (dBW/Hz) at 25 MHz for 4 locations

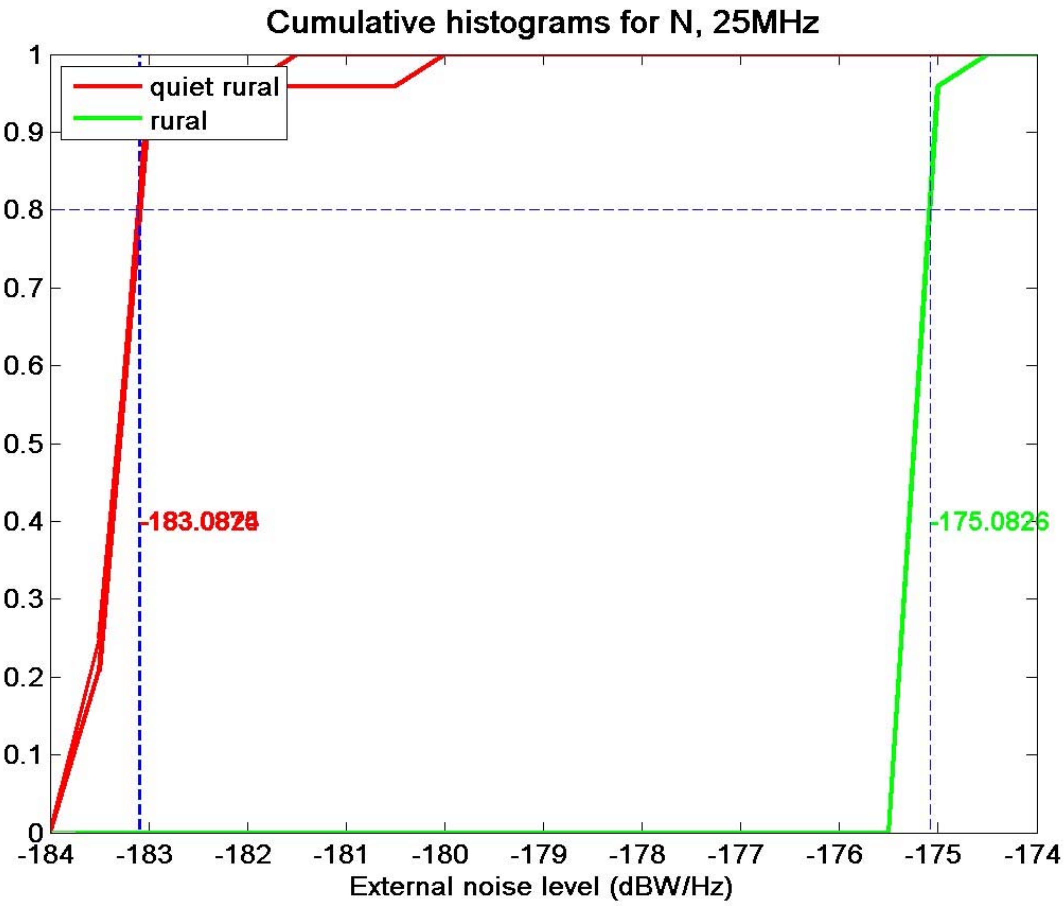

Attachment 4

Results from RECAREA sky-wave analysis worldwide

Calculation results of RECAREA simulation described in § 6.5 are shown in following tables.

TABLE 29

Ratio of time interference occurs for 4.5 MHz Poleward emission with oceanographic radar peak power 50 W

Local Time / Month	0:00–3:00	3:00–6:00	6:00–9:00	9:00–12:00	12:00–15:00	15:00–18:00	18:00–21:00	21:00–24:00	AVERAGE
Jan	0.031	0.032	0.023	0.000	0.000	0.002	0.028	0.032	0.019
Feb	0.037	0.037	0.017	0.000	0.000	0.001	0.028	0.037	0.020
Mar	0.034	0.037	0.008	0.000	0.000	0.000	0.021	0.036	0.017
Apr	0.037	0.036	0.005	0.000	0.000	0.000	0.012	0.036	0.016
May	0.037	0.026	0.004	0.000	0.000	0.000	0.006	0.030	0.013
Jun	0.031	0.022	0.003	0.000	0.000	0.000	0.005	0.023	0.010
Jul	0.031	0.023	0.003	0.000	0.000	0.000	0.005	0.025	0.011
Aug	0.031	0.030	0.004	0.000	0.000	0.000	0.008	0.030	0.013
Sep	0.036	0.038	0.008	0.000	0.000	0.000	0.015	0.037	0.017
Oct	0.036	0.038	0.021	0.000	0.000	0.000	0.021	0.037	0.019
Nov	0.035	0.037	0.031	0.001	0.000	0.001	0.028	0.036	0.021
Dec	0.029	0.030	0.027	0.000	0.000	0.001	0.027	0.030	0.018
AVERAGE:	0.034	0.032	0.013	0.000	0.000	0.001	0.017	0.032	0.016

TABLE 30

Ratio of time interference occurs for 4.5 MHz Equatorward emission with oceanographic radar peak power 50 W

Local Time / Month	0:00–3:00	3:00–6:00	6:00–9:00	9:00–12:00	12:00–15:00	15:00–18:00	18:00–21:00	21:00–24:00	AVERAGE
Jan	0.000	0.002	0.006	0.000	0.000	0.001	0.013	0.003	0.003
Feb	0.002	0.004	0.005	0.000	0.000	0.001	0.014	0.004	0.004
Mar	0.002	0.006	0.004	0.000	0.000	0.000	0.016	0.005	0.004
Apr	0.003	0.007	0.003	0.000	0.000	0.000	0.009	0.006	0.004
May	0.003	0.008	0.002	0.000	0.000	0.000	0.004	0.006	0.003
Jun	0.001	0.007	0.002	0.000	0.000	0.000	0.003	0.004	0.002
Jul	0.001	0.007	0.002	0.000	0.000	0.000	0.003	0.003	0.002
Aug	0.001	0.007	0.003	0.000	0.000	0.000	0.006	0.003	0.002
Sep	0.001	0.004	0.004	0.000	0.000	0.000	0.006	0.003	0.002
Oct	0.001	0.004	0.010	0.000	0.000	0.000	0.009	0.003	0.003
Nov	0.000	0.004	0.011	0.001	0.000	0.001	0.011	0.003	0.004
Dec	0.001	0.002	0.007	0.001	0.000	0.001	0.013	0.003	0.004
AVERAGE:	0.001	0.005	0.005	0.000	0.000	0.000	0.009	0.004	0.003

TABLE 31

Ratio of time interference occurs for 9 MHz Poleward emission with oceanographic radar peak power 50 W

Local Time / Month	0:00–3:00	3:00–6:00	6:00–9:00	9:00–12:00	12:00–15:00	15:00–18:00	18:00–21:00	21:00–24:00	AVERAGE
Jan	0.007	0.002	0.007	0.004	0.002	0.006	0.024	0.002	0.007
Feb	0.017	0.014	0.013	0.003	0.002	0.004	0.031	0.018	0.013
Mar	0.025	0.020	0.016	0.002	0.000	0.002	0.026	0.027	0.015
Apr	0.028	0.025	0.010	0.002	0.000	0.003	0.017	0.030	0.014
May	0.031	0.024	0.010	0.002	0.000	0.003	0.010	0.030	0.014
Jun	0.028	0.020	0.009	0.001	0.000	0.002	0.010	0.024	0.012
Jul	0.028	0.021	0.009	0.001	0.000	0.002	0.011	0.026	0.012
Aug	0.024	0.023	0.011	0.002	0.000	0.003	0.013	0.028	0.013
Sep	0.024	0.020	0.015	0.002	0.000	0.003	0.020	0.029	0.014
Oct	0.017	0.018	0.024	0.003	0.001	0.003	0.026	0.022	0.014
Nov	0.014	0.013	0.025	0.004	0.002	0.004	0.030	0.018	0.014
Dec	0.009	0.004	0.013	0.003	0.002	0.004	0.029	0.009	0.009
AVERAGE:	0.021	0.017	0.013	0.002	0.001	0.003	0.021	0.022	0.013

TABLE 32

Ratio of time interference occurs for 9 MHz Equatorward emission with oceanographic radar peak power 50 W

Local Time / Month	0:00–3:00	3:00–6:00	6:00–9:00	9:00–12:00	12:00–15:00	15:00–18:00	18:00–21:00	21:00–24:00	AVERAGE
Jan	0.005	0.006	0.007	0.004	0.002	0.004	0.013	0.005	0.006
Feb	0.009	0.008	0.007	0.003	0.001	0.003	0.014	0.008	0.007
Mar	0.010	0.011	0.009	0.002	0.000	0.002	0.018	0.011	0.008
Apr	0.011	0.012	0.007	0.002	0.000	0.002	0.013	0.011	0.007
May	0.011	0.014	0.007	0.001	0.000	0.002	0.009	0.011	0.007
Jun	0.008	0.012	0.008	0.001	0.000	0.001	0.008	0.009	0.006
Jul	0.008	0.012	0.007	0.001	0.000	0.002	0.009	0.009	0.006
Aug	0.008	0.011	0.009	0.001	0.000	0.002	0.012	0.011	0.007
Sep	0.011	0.013	0.009	0.002	0.000	0.002	0.012	0.009	0.007
Oct	0.010	0.011	0.013	0.003	0.001	0.003	0.013	0.009	0.008
Nov	0.007	0.009	0.013	0.004	0.001	0.003	0.014	0.009	0.008
Dec	0.007	0.008	0.009	0.003	0.002	0.003	0.013	0.007	0.007
AVERAGE:	0.009	0.011	0.009	0.002	0.001	0.002	0.012	0.009	0.007

TABLE 33

Ratio of time interference occurs for 13 MHz Poleward emission with oceanographic radar peak power 50 W

Local Time / Month	0:00–3:00	3:00–6:00	6:00–9:00	9:00–12:00	12:00–15:00	15:00–18:00	18:00–21:00	21:00–24:00	AVERAGE
Jan	0.000	0.000	0.001	0.007	0.004	0.008	0.005	0.000	0.003
Feb	0.000	0.000	0.002	0.007	0.005	0.007	0.015	0.001	0.004
Mar	0.006	0.002	0.011	0.005	0.003	0.005	0.018	0.012	0.008
Apr	0.014	0.012	0.012	0.005	0.003	0.006	0.015	0.015	0.010
May	0.014	0.012	0.011	0.004	0.001	0.005	0.014	0.016	0.010
Jun	0.014	0.011	0.010	0.002	0.000	0.003	0.011	0.014	0.008
Jul	0.014	0.011	0.010	0.002	0.000	0.003	0.011	0.015	0.008
Aug	0.010	0.009	0.010	0.003	0.000	0.005	0.013	0.014	0.008
Sep	0.004	0.001	0.012	0.005	0.003	0.006	0.016	0.012	0.007
Oct	0.000	0.000	0.013	0.006	0.004	0.006	0.015	0.003	0.006
Nov	0.000	0.000	0.007	0.007	0.004	0.007	0.013	0.001	0.005
Dec	0.000	0.000	0.003	0.006	0.004	0.007	0.012	0.000	0.004
AVERAGE:	0.006	0.005	0.008	0.005	0.003	0.006	0.013	0.009	0.007

TABLE 34

Ratio of time interference occurs for 13 MHz Equatorward emission with oceanographic radar peak power 50 W

Local Time / Month	0:00−3:00	3:00−6:00	6:00−9:00	9:00−12:00	12:00−15:00	15:00−18:00	18:00−21:00	21:00−24:00	AVERAGE
Jan	0.003	0.001	0.003	0.007	0.004	0.005	0.007	0.004	0.004
Feb	0.008	0.002	0.003	0.006	0.003	0.005	0.010	0.007	0.005
Mar	0.012	0.008	0.010	0.005	0.002	0.005	0.017	0.012	0.009
Apr	0.015	0.012	0.009	0.005	0.002	0.004	0.014	0.012	0.009
May	0.013	0.014	0.011	0.004	0.002	0.003	0.012	0.012	0.009
Jun	0.012	0.010	0.009	0.002	0.001	0.004	0.010	0.012	0.007
Jul	0.011	0.011	0.009	0.002	0.001	0.004	0.011	0.012	0.007
Aug	0.012	0.010	0.009	0.004	0.002	0.004	0.013	0.013	0.008
Sep	0.012	0.009	0.010	0.005	0.002	0.004	0.012	0.010	0.008
Oct	0.012	0.006	0.012	0.005	0.003	0.005	0.012	0.011	0.008
Nov	0.006	0.004	0.010	0.006	0.004	0.006	0.013	0.010	0.007
Dec	0.006	0.003	0.005	0.005	0.005	0.005	0.008	0.005	0.005
AVERAGE:	0.010	0.008	0.008	0.004	0.002	0.005	0.012	0.010	0.007

TABLE 35

Ratio of time interference occurs for 16 MHz Poleward emission with oceanographic radar peak power 50 W

Local Time / Month	0:00−3:00	3:00−6:00	6:00−9:00	9:00−12:00	12:00−15:00	15:00−18:00	18:00−21:00	21:00−24:00	AVERAGE
Jan	0.000	0.000	0.000	0.006	0.005	0.007	0.000	0.000	0.002
Feb	0.000	0.000	0.000	0.007	0.006	0.007	0.005	0.000	0.003
Mar	0.000	0.000	0.003	0.006	0.004	0.006	0.012	0.002	0.004
Apr	0.002	0.000	0.008	0.006	0.004	0.007	0.011	0.006	0.006
May	0.004	0.000	0.007	0.002	0.000	0.004	0.009	0.009	0.004
Jun	0.007	0.001	0.004	0.000	0.000	0.000	0.006	0.008	0.003
Jul	0.007	0.000	0.004	0.000	0.000	0.000	0.007	0.009	0.003
Aug	0.001	0.000	0.003	0.001	0.000	0.002	0.009	0.007	0.003
Sep	0.000	0.000	0.006	0.005	0.002	0.006	0.010	0.002	0.004
Oct	0.000	0.000	0.005	0.007	0.006	0.007	0.009	0.000	0.004
Nov	0.000	0.000	0.003	0.008	0.005	0.008	0.003	0.000	0.003
Dec	0.000	0.000	0.000	0.006	0.005	0.006	0.003	0.000	0.002
AVERAGE:	0.002	0.000	0.004	0.004	0.003	0.005	0.007	0.004	0.004

TABLE 36

Ratio of time interference occurs for 16 MHz Equatorward emission with oceanographic radar peak power 50 W

Local Time / Month	0:00−3:00	3:00−6:00	6:00−9:00	9:00−12:00	12:00−15:00	15:00−18:00	18:00−21:00	21:00−24:00	AVERAGE
Jan	0.001	0.000	0.000	0.006	0.005	0.006	0.005	0.003	0.003
Feb	0.004	0.000	0.000	0.007	0.004	0.006	0.009	0.006	0.004
Mar	0.009	0.004	0.005	0.006	0.003	0.005	0.013	0.011	0.007
Apr	0.011	0.007	0.007	0.006	0.003	0.005	0.013	0.011	0.008
May	0.011	0.008	0.008	0.003	0.003	0.004	0.011	0.010	0.007
Jun	0.008	0.006	0.005	0.000	0.001	0.004	0.009	0.008	0.005
Jul	0.007	0.006	0.004	0.000	0.001	0.004	0.010	0.008	0.005
Aug	0.007	0.005	0.005	0.002	0.002	0.005	0.012	0.010	0.006
Sep	0.009	0.004	0.006	0.005	0.004	0.004	0.011	0.008	0.006
Oct	0.007	0.002	0.006	0.006	0.004	0.006	0.010	0.009	0.006
Nov	0.003	0.001	0.005	0.007	0.005	0.007	0.011	0.008	0.006
Dec	0.003	0.000	0.002	0.006	0.006	0.006	0.006	0.004	0.004
AVERAGE:	0.007	0.004	0.005	0.005	0.003	0.005	0.010	0.008	0.006

TABLE 37

Ratio of time interference occurs for 24.5 MHz Poleward emission with oceanographic radar peak power 50 W

Local Time / Month	0:00–3:00	3:00–6:00	6:00–9:00	9:00–12:00	12:00–15:00	15:00–18:00	18:00–21:00	21:00–24:00	AVERAGE
Jan	0.000	0.000	0.000	0.000	0.000	0.000	0.000	0.000	0.000
Feb	0.000	0.000	0.000	0.000	0.000	0.000	0.000	0.000	0.000
Mar	0.000	0.000	0.000	0.000	0.000	0.000	0.000	0.000	0.000
Apr	0.000	0.000	0.000	0.000	0.000	0.000	0.000	0.000	0.000
May	0.000	0.000	0.000	0.000	0.000	0.000	0.000	0.000	0.000
Jun	0.000	0.000	0.000	0.000	0.000	0.000	0.000	0.000	0.000
Jul	0.000	0.000	0.000	0.000	0.000	0.000	0.000	0.000	0.000
Aug	0.000	0.000	0.000	0.000	0.000	0.000	0.000	0.000	0.000
Sep	0.000	0.000	0.000	0.000	0.000	0.000	0.000	0.000	0.000
Oct	0.000	0.000	0.000	0.000	0.000	0.000	0.000	0.000	0.000
Nov	0.000	0.000	0.000	0.001	0.000	0.000	0.000	0.000	0.000
Dec	0.000	0.000	0.000	0.000	0.000	0.000	0.000	0.000	0.000
AVERAGE:	0.000	0.000	0.000	0.000	0.000	0.000	0.000	0.000	0.000

TABLE 38

Ratio of time interference occurs for 24.5 MHz Equatorward emission with oceanographic radar peak power 50 W

Local Time / Month	0:00–3:00	3:00–6:00	6:00–9:00	9:00–12:00	12:00–15:00	15:00–18:00	18:00–21:00	21:00–24:00	AVERAGE
Jan	0.000	0.000	0.000	0.000	0.000	0.001	0.000	0.000	0.000
Feb	0.000	0.000	0.000	0.000	0.000	0.002	0.002	0.000	0.000
Mar	0.000	0.000	0.000	0.000	0.000	0.001	0.001	0.000	0.000
Apr	0.000	0.000	0.000	0.000	0.000	0.000	0.002	0.000	0.000
May	0.000	0.000	0.000	0.000	0.000	0.000	0.001	0.000	0.000
Jun	0.000	0.000	0.000	0.000	0.000	0.000	0.000	0.000	0.000
Jul	0.000	0.000	0.000	0.000	0.000	0.000	0.000	0.000	0.000
Aug	0.000	0.000	0.000	0.000	0.000	0.000	0.001	0.000	0.000
Sep	0.000	0.000	0.000	0.000	0.000	0.000	0.001	0.000	0.000
Oct	0.000	0.000	0.000	0.000	0.000	0.002	0.000	0.000	0.000
Nov	0.000	0.000	0.000	0.002	0.000	0.002	0.001	0.000	0.001
Dec	0.000	0.000	0.000	0.001	0.000	0.001	0.000	0.000	0.000
AVERAGE:	0.000	0.000	0.000	0.000	0.000	0.001	0.001	0.000	0.000

Attachment 5

Results of CW propagation measurements within the frequency band 3-50 MHz

5-1 Measurement objectives, system and methodology

5-1.1 Measurement objectives

The objective of the measurements reported in this document were to characterize the pass loss within the 26 ± 4 MHz and 43 ± 4 MHz frequency range and to compare those path losses to the path losses that were computed using Recommendations ITU-R P.368-9 (GRWAVE) and ITU-R P.1546-4 in order to resolve discrepancies in path loss values that were used for 42 MHz oceanographic radar compatibility and interference studies. Transmitter locations, terrain type, operating frequencies and transmitted signal power levels can be found in Table 39.

TABLE 39

Site locations, terrain types and operational frequency

Location	Terrain Type	26 ± 4	43 ± 4
Mountain View California, USA	Flat Land Suburban-Rural	25 MHz 12 W	40.18 MHz 12 W
Crissy Field SF Bay Area, USA	Land Urban	N/A	43.69 MHz 12 W
Mikawa Bay, Japan	Urban Land Saline Sea	N/A	41.9 MHz 25 W

5-1.2 Measurement system

The measurement system for this project was simple as the measurement itself was a relative, not absolute one. The system will consist of a single or possibly several antennas that are tuned to operate in the 26 and 45 MHz frequency ranges. In order to detect low signal levels the spectrum analyser should have a minimum resolution bandwidth of at least 10 Hz and a DANL (Displayed Average Noise Level) that assures that any low level measurements will not be masked by the noise floor of the measurement system. In cases where the desired signal level was extremely low and additional high-level signals are present, an amplifier and/or filter was needed in the measurement path in order to assure that the desired signal was detectable and that the front end of the spectrum analyser was not over driven into a non-linear mode of operation. Figure 47 is a simple block diagram of the test setup.

FIGURE 47

Measurement system block diagram

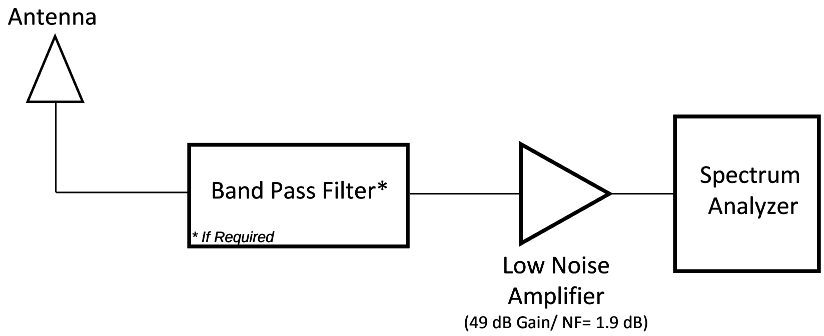

Figure 48 shows the filter, the amplifier and the spectrum analyser that was used to take the measurements.

FIGURE 48

Measurement system filter, low noise amplifier and spectrum analyzer

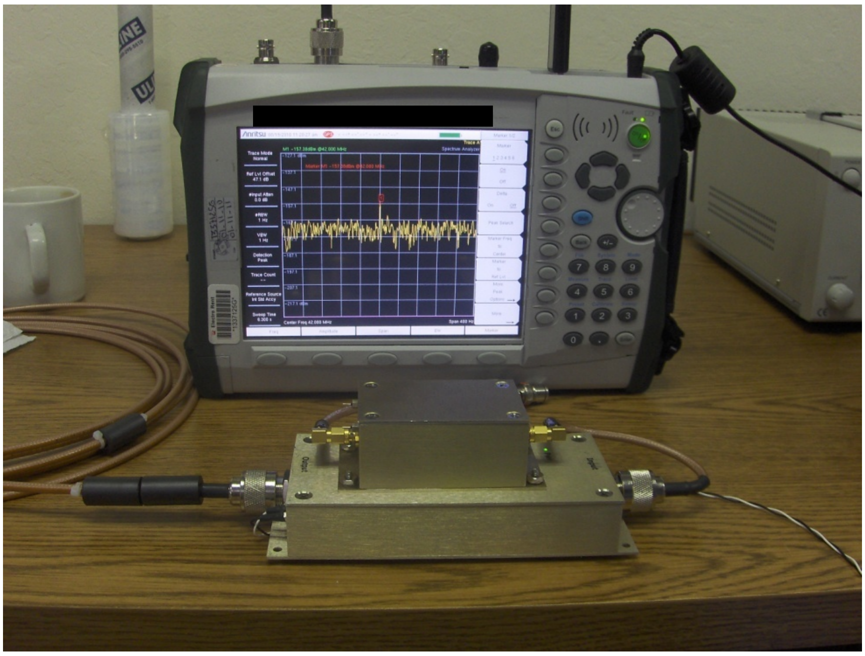

The primary measurement device that was be used to measure the received signal was the spectrum analyser. At the fringes of the geography over which the test signal was radiated they approached the theoretical noise floor limit. The maximum interference level acceptable for a fixed or mobile receiver is –152 dBm. The measurement system needed to measure at least 10 dB below that level in order to insure that the received signal was below the interference threshold but above the noise floor of the spectrum analyser.

Since the measurement of low-level signals is limited by the noise generated inside the spectrum analyser, the spectrum analyser's sensitivity needs to be maximized in order to effectively measure low-level signals. This can be accomplished by: 1) minimizing the input attenuator, 2) narrowing the resolution bandwidth (RBW) filter, and 3) using a preamplifier. Applying these techniques will effectively lower the displayed average noise level DANL, revealing signals that otherwise would be lost in the noise.

The DANL of the spectrum analyser used for these measurements was –140 dBm/Hz. Use of the spectrum analysers internal pre-amplifier lowered the DANL to –163 dBm. Further improvements in the DANL could be achieved by by-passing the internal pre-amplifier and inserting an external high gain low noise figure pre-amplifier at the input to the spectrum analyser. Inserting a preamplifier with a gain of 40 dB and a noise figure of 1 dB before the input to the spectrum analyser reduced the DANL –168 dBm/Hz. With a DANL of this magnitude, the noise floor margin was high enough to insure that the noise floor of the spectrum analyser did not limit measurements (Table 40).

TABLE 40

Noise floor measurement margin

Frequency	Units	25 MHz	42 MHz
Maximum interference level (Rural)	dBm	–146	–152
Measurement DANL with spectrum analyser internal pre-amplifier	dBm	–163	–163
Noise floor margin w/internal pre-amp	dB	17	11
Measurement DANL with spectrum analyser internal pre-amplifier	dBm	–169	–169
Noise floor margin w/external pre-amp	dB	23	17

Although the spectrum analyser's DANL with the internal pre-amplifier would have been adequate for these measurements, bypassing the built-in preamplifier and using an external pre-amplifier at the higher frequencies could, depending upon the pre-amplifiers' gain and noise figure, improve the noise floor margin. A pre-amplifier with a gain of 49 dB and a noise figure of 1.9 dB was selected for use at the measured frequency. Using this LNA as a pre-amplifier along with and by-passing the spectrum analyser's internal pre-amplifier resulted in lowering the measurement DANL to –168 dB, increasing the noise floor margin to 16.7 dB at 42 MHz[15].

5-1.3 Measurement methodology

The receiver antenna and the GPS antenna were be mounted on the vehicle (Fig. 49).

[15] This level is 18 dB below the maximum interference threshold (–152 dB) that is acceptable for interference free operation of fixed or mobile systems.

FIGURE 49

Test vehicle with receiver and GPS antenna

The measurement equipment described in § 5-1.2 wwa placed in the vehicle. A CW signal will be transmitted from an oceanographic radar system at 40.18 and 25 MHz (Fig. 50).

FIGURE 50

Transmitter antenna

The vehicle was driven along a pre-determined drive path. At fixed intervals along the drive path the signal level was measured, the distance of each measurement point from the transmitter site was determined, the GPS coordinates of the measurement location will be noted and the type of terrain and ground type was noted. The signal level, spectrum analysers scan data, the GPS coordinates of the measurement location, the drive path and the elevation was stored to digital media and saved as data files on a PC. The duration and distance travelled was a function of how far one would travel along the drive path until the signal level approached and fell below the measurement system noise floor. At that point in time travel along the path was reversed and additional data was collected on the return leg of the trip. In some cases the path was travelled in one direction only.

5-2 Analysis methodology

Drive path data extracted from the GPS system and a detailed graphic depicting the drive path over which the data was taken was developed. The data that was taken at each of the "test points" along the drive path was tabulated and a plot of signal strength versus distance was created. A plot of the path loss as a function of distance was derived from this data. A regression analysis was conducted and the path loss plotted using this analysis. Additional frequency specific plots of path loss data that is based upon Recommendation ITU-R P.368-9 (GRWAVE) and Recommendation ITU-R P.1546-4 were developed and overlaid on top of the path loss data that was derived from the signal strength data acquired during the propagation measurements. Comparisons were made between the results from the models and the results from the measurements in order to see which, if any, of the models correlated well with the measurement results.

5-3 Measurements

Several sets of measurements were taken in the San Francisco Bay Area. One of these measurements used an operational oceanographic radar site whose transmitter was set to the CW mode. Two other sets of measurements used a CW signal that was located in Mountain View, California as the transmitting source. In all of the cases, drive paths were selected that extended to the fringes of the transmissions. An initial measurement was made within a wavelength of the transmitting antenna in order to assure that terrain or any anomalous propagation effects would not impact the determination of the power level of the transmitted signal. Drive Path 1 followed a route between Mountain View and Morgan Hill California and traversed a generally flat terrain that varied from suburban to rural over dry land. Figure 51 illustrates the drive path that was followed for these measurements.

The other set of measurements were taken in the Mikawa Bay Area, Japan. The transmitter of an oceanographic radar had been set in 137 deg 18' 32" (E) and 34 deg 46' 45" (N).

FIGURE 51

25 MHz and 40.18 MHz signal level measurement drive paths 1 and 2

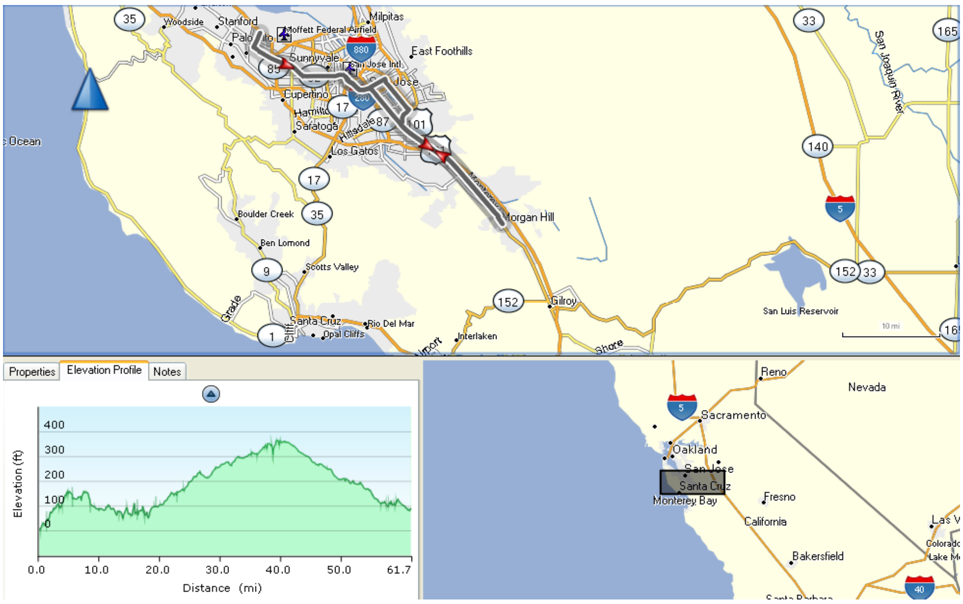

Drive Path 2 followed the same route in the opposite direction (Morgan Hill to Mountain View California) and traversed a generally flat terrain that varied from rural to suburban over dry land.

Drive Path 3 followed a route between Crissy Field, San Francisco and Mountain View California. The route traversed a hilly terrain that varied from urban to suburban over dry land. Figure 52 illustrates the drive path that was followed for these measurements.

FIGURE 52

43.69 MHz signal level measurement drive path 3

Additional measurements were taken in the Mikawa Bay Area, Japan where the transmitter of oceanographic radar was located at 137 deg 18’ 32” (E) and 34 deg 46’ 45” (N). The land and sea paths that were associated with these measurements are illustrated in Fig. 53.

FIGURE 53

41.9 MHz measurement points

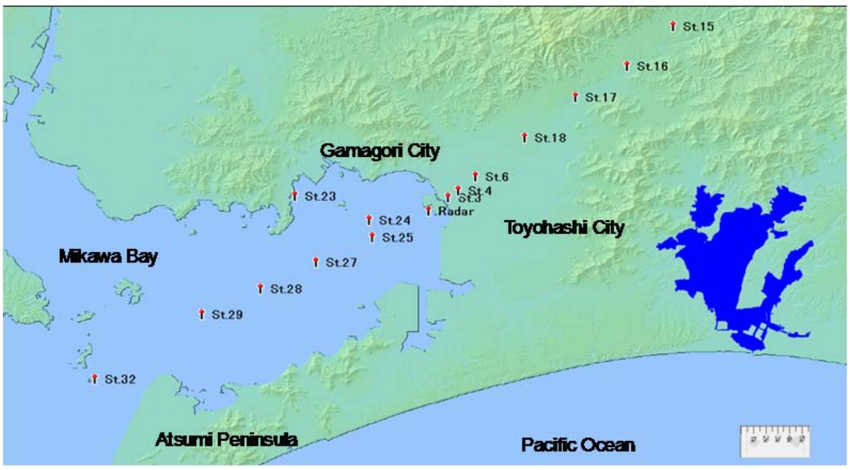

5-3.1 40.18 and 43.689 MHz measurements

The 40.18 MHz and 43.689 MHz measurements were based upon a CW transmission of 12 Watts and followed drive Path 1 between Mountain View, California and Morgan Hill, California.

Data was collected randomly at 53 points along the route. At distances within 1 km of the transmitter, data was taken more frequently in order to assure that an adequate representation of the rapid drop in signal level that occurs close in to the transmitter site could be captured. The data was transferred to a spreadsheet where signal level versus distance was plotted (Fig. 54).

FIGURE 54

40.18 MHz propagation measurements (signal level vs. distance – path 1)

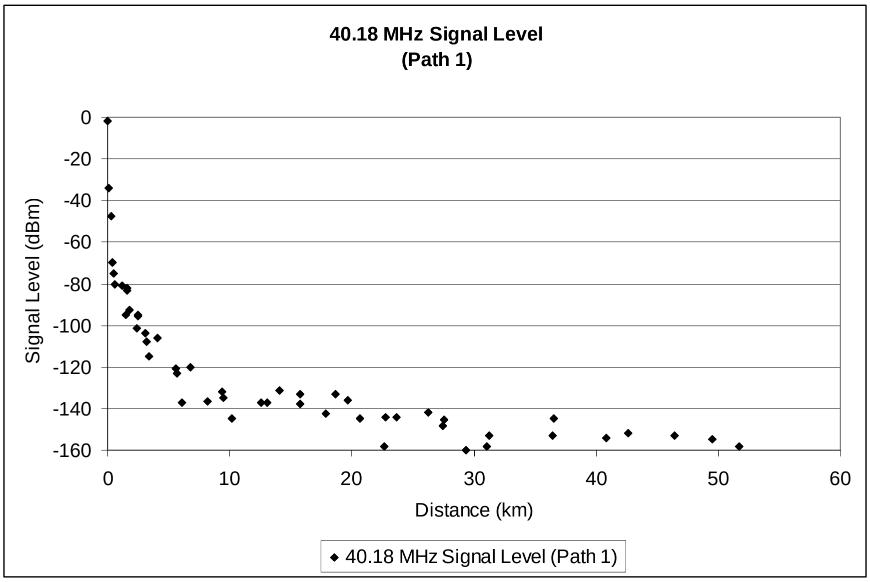

The path loss was derived from the signal strength data and is plotted in Fig. 55, where it is represented by the black diamonds.

FIGURE 55

Comparison of measured and predicted path losses (path 1)

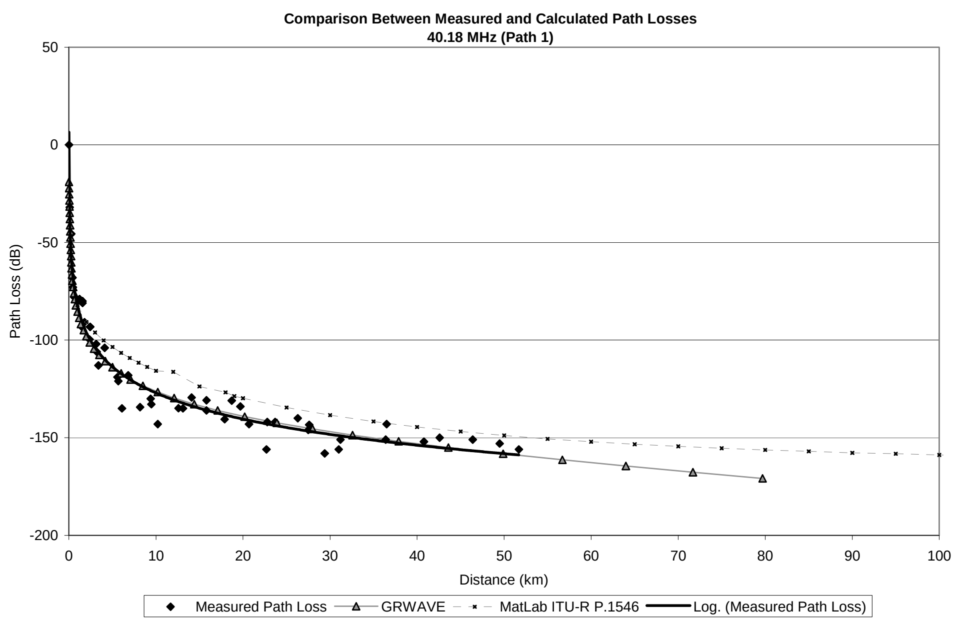

A logarithmic regression was performed on the path loss data that was derived from the measured signal levels. The results of that regression analysis appear as the dark black line. The path loss as predicted by GRWAVE (Recommendation ITU-R P.368-9) appears as light gray triangles that are traced through by a light gray line. As can be seen from the graph, the correlation between the path losses as predicted by GRWAVE and the logarithmic fit to the path losses that were derived from the measured signal levels is excellent.

The dotted light gray line represents the path loss as predicted by a computer simulation implementation of Recommendation ITU-R P.1546-4. As can be seen from the graph, there is very little correlation between the path losses as predicted by Recommendation ITU-R P.1546-4 and the logarithmic fit to the path loss that was derived from the measured signals.

Similar results were obtained for Paths 2 and 3 and can been seen in Figs 56 and 57.

FIGURE 56

Comparison of measured and predicted path losses (path 2)

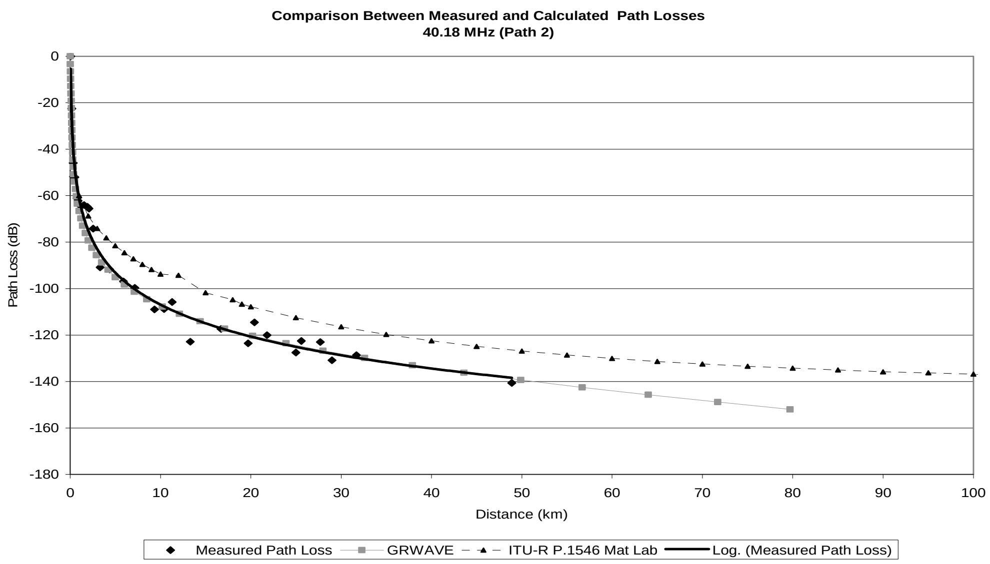

The received signal level data in Fig. 56 differs from the signal level data is more widely dispersed then the data that appeared in previous figures. This is due to terrain and multi-path effects that were encountered in the hilly urban environment in which the measurements were taken. As a result a logarithmic regression could not be directly applied to this data. For this particular data set the path loss prediction that was provided by GRWAVE was subjectively fitted to the data points prior to making comparisons to the predicted path loss values that were derived from Recommendation ITU-R P.1546-4.

FIGURE 57

Comparison of measured and predicted path losses (path 3)

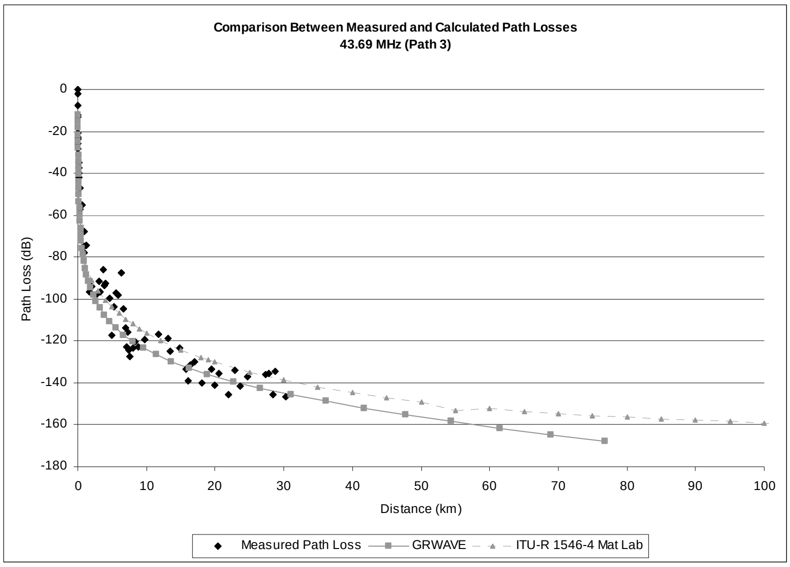

A simulation that incorporated an implementation of Recommendation ITU-R P.1546-4 was run on a commercially available software package in order to plot the signal strength over the geography that surrounded drive paths 1 and 2. The output of that simulation can be seen in Fig. 57.

FIGURE 58

Output of simulation for signal strength levels along path 1

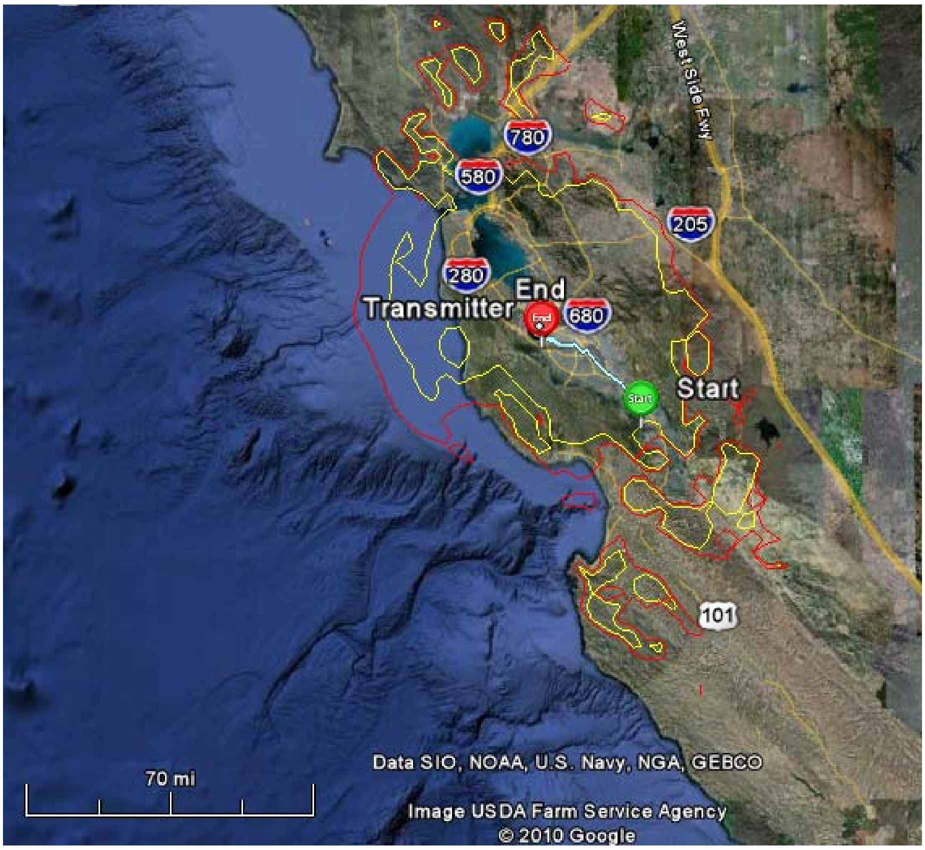

The light blue line represents the drive path. The light yellow lines represent the points at which the signal level is equal to or less than –141 dBm. The red lines represent the points at which the signal level is equal to or less than –146 dBm.

Figure 58 is a plot of the signal levels that were received while driving along drive path 1.

FIGURE 59

Measured signal levels along path 1

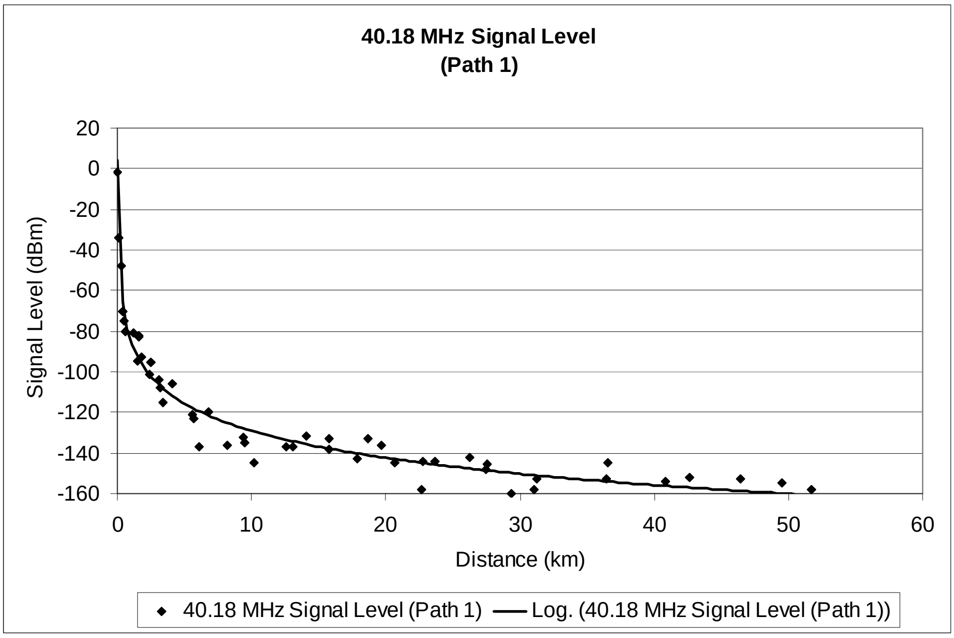

Table 41 compares the distances at which the measured signal levels and the signal levels that were derived from the simulations implementation of Recommendation ITU-R P.1546-4 reached levels less than or equal to –141 dBm and –146 dBm.

TABLE 41

Distance at which the received signal level is equal to or less than a given value

Signal level	(dBm)	–141	–146
Distance as derived from signal level measurements	(km)	20	28
Distance as derived from simulation	(km)	74	75

The results of the simulation and the results of the path loss data that was derived from a computer simulation implementation of Recommendation ITU-R P.1546-4 are consistent and show that use of path loss data that was derived from Recommendation ITU-R P.1546-4 results in an overestimation of the distances at which various signal levels are reached. The data also shows that as the distance increases the differences between the measured and the signal levels that are predicted by Recommendation ITU-R P.1546-4 also increases.

5-3.2 25 MHz measurements

The 25 MHz measurements were based upon a CW transmission of 12 Watts and followed drive path 1 between Mountain View, California and Morgan Hill, California. Data was collected randomly at 53 points along the route. At distances within 1 km of the transmitter, data was taken more frequency in order to assure that an adequate representation of the rapid drop in signal level that occurs close in to the transmitter site could be captured. The data was transferred to a spreadsheet where signal level versus distance was plotted (Fig. 60).

FIGURE 60

25 MHz propagation measurements (signal level vs. distance)

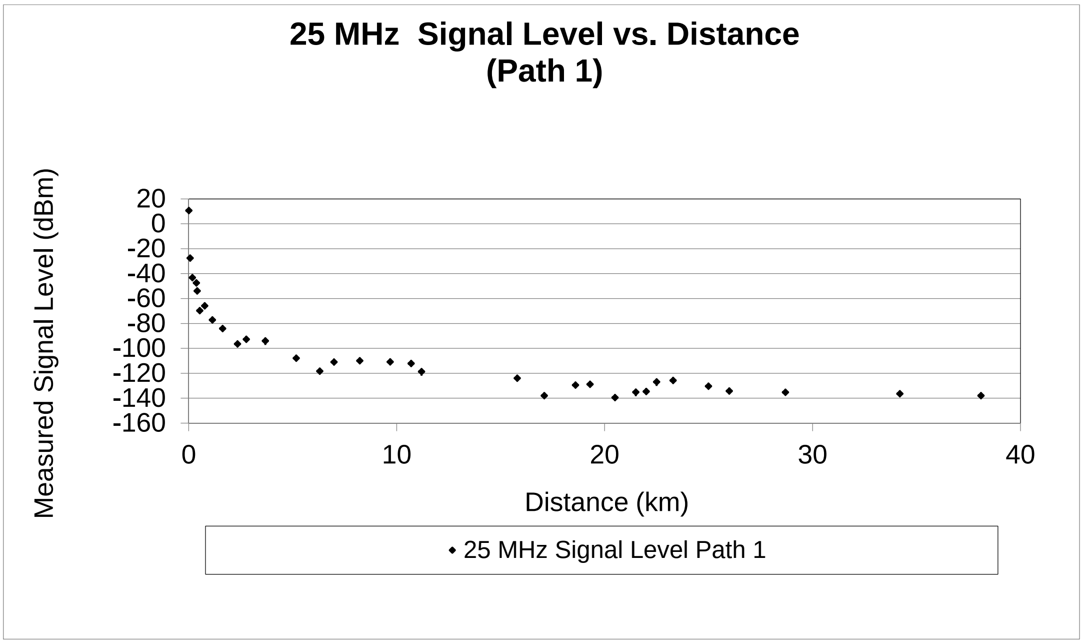

The path loss was derived from the signal strength data and is plotted in Fig. 61, where it is represented by the black diamonds.

FIGURE 61

Comparison between measured and calculated path losses

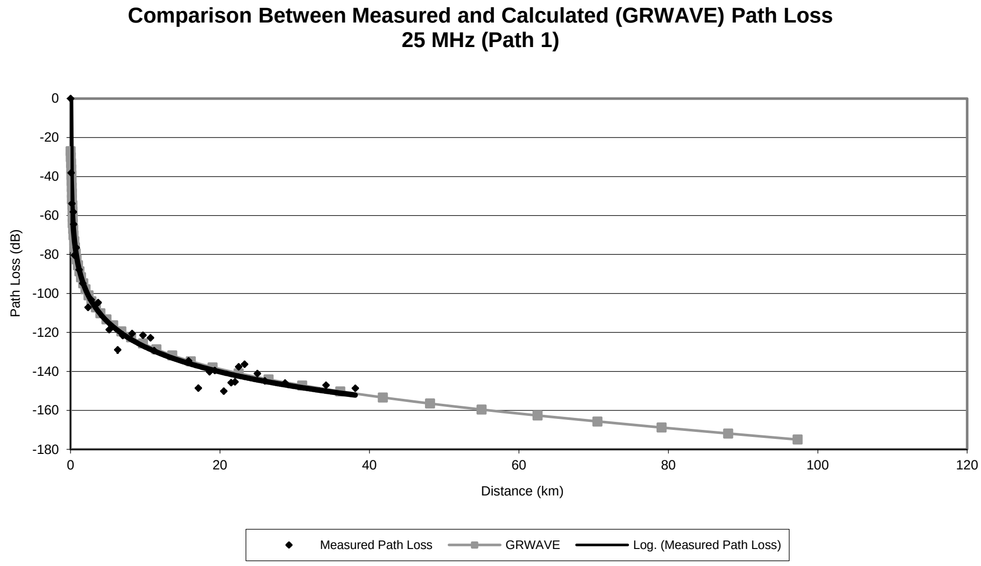

A logarithmic regression was performed on the path loss data that was derived from the measured signal levels. The results of that regression analysis appear as the dark black line. The path loss as predicted by GRWAVE (Recommendation ITU-R P.368-9) appears as light gray triangles that are traced through by a light gray line. As can be seen from the graph, the correlation between the path losses as predicted by GRWAVE and the logarithmic fit to the path losses that were derived from the measured signal levels is excellent.

5-3.3 41.9 MHz measurements

These measurements were made using a 25 W (peak emission) oceanographic radar system that was operating at a centre frequency of 41.9 MHz. The oceanographic radar used a ground plane transmitting antenna with 1/4 wavelength elements and was located on the coast. Field strength was measured by using a mobile receiver equipped with measuring antennas. Results of those measurements and their comparison to predicted field intensity levels that were derived from GRWAVE and Recommendation ITU-R P.1546-4 are shown in Fig. 62.

FIGURE 62

Measured signal levels along land path and sea path

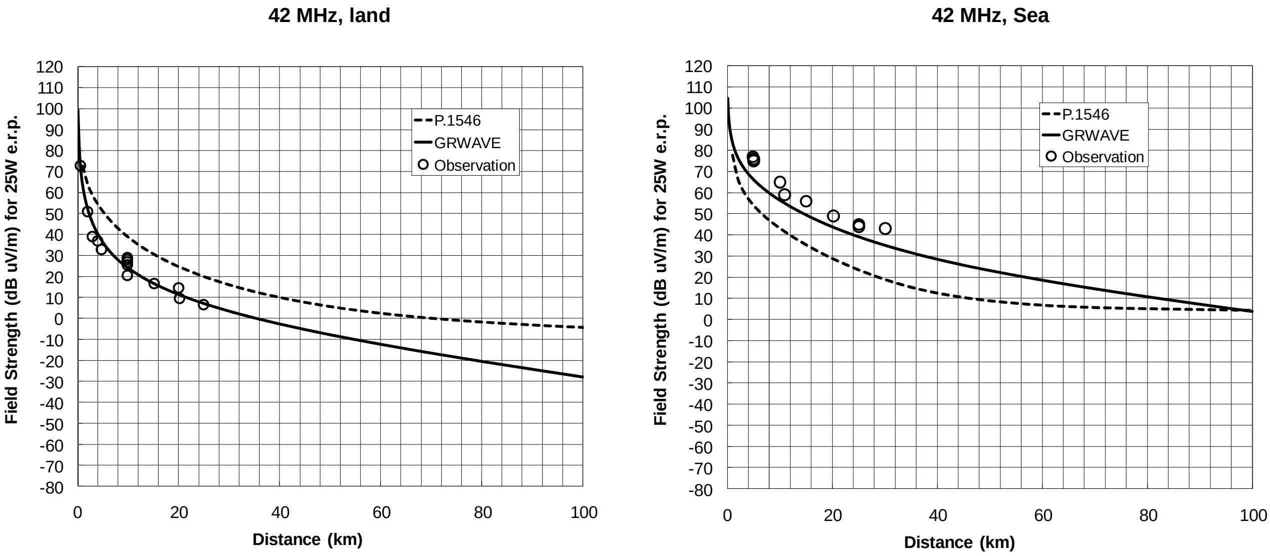

These measurement results also showed the poor correlation between the actual path loss measurements and the path loss that was calculated using Recommendation ITU-R P.1546-4. They also showed that there is good correlation between the measured path loss and the path loss that was calculate using GRWAVE (Recommendation ITU-R P.368-9) confirming the results of measurements that were described in § 5-3.1.

5-4 Conclusions

There is excellent correlation between the path loss values that were derived from the signal level measurements at 25 MHz, 40.18 MHz, 40.9 MHz and 43.69 MHz and those that were derived from Recommendation ITU-R P.368-9 (GRWAVE) indicating that GRWAVE provides a reliable and accurate prediction of path loss values at frequencies equivalent to and below 43.689 MHz.

There is very little correlation between the path loss values that were derived from the signal level measurements at 40.18 MHz and 43.789 MHz and those that were derived from Recommendation ITU-R P.1546-4. The reasons for this lack of correlation are:

1) Recommendation ITU-R P.1546-4 was designed for high-to-low paths (e.g. broadcast tower to receiver modelling). As a result, the recommendation is not good at predicting field intensity levels for low-to-low antenna height paths. In particular, the Recommendation itself states that, "if both terminals are below the levels of clutter in their respective vicinities, then this Recommendation will not give accurate predictions to the problem at hand" The recommendation goes on to state that "This Recommendation is not valid when the transmitting/base antenna is below the height of surrounding clutter"; and

2) the Recommendation has been shown to generate errors in predicted field-strength levels under conditions in which antenna heights are low (< 10 m) and terrain clearance angles are not defined properly[16].

[16] Peyman Hesami and Narges Noori, IEEE Transactions on Antenna and Propagation, "Evaluation and Improvement of the Field Prediction Method in Recommendation ITU-R P.1546-3", March 2009.

5-5 Summary

In summary, the data has shown:

1) that use of path loss data that was derived from Recommendation ITU-R P.1546-4 results in an overestimation of the distances at which various signal levels are reached;

2) that the use of Recommendation ITU-R P.1546-4 for interference and compatibility studies for systems with low antenna heights will result in an underestimation of the path loss that will in turn result in an overestimation of separation distances. As such Recommendation ITU-R P.1546-4 should not be used for interference or compatibility studies for systems whose antenna heights and terrain angles are low (e.g. oceanographic radars); and

3) that Recommendation ITU-R P.368-9 provides a reliable and accurate assessment of path losses up to 43.789 MHz[17] and as such should be used for any interference or compatibility studies where the systems that are under investigation have low antenna heights and low terrain angles (e.g. oceanographic radars).

[17] The implementation of GRWAVE that was used in this analysis, GWPS V2.0, is a program for estimating ground wave range value under specified ground and operating conditions, for transmitter frequencies between 10 kHz and 50 MHz.

Attachment 6

Observation of the radio environment in the frequency band 3-50 MHz

6-1 Purpose

The objectives of this Attachment are to:

1) assess and quantify the potential for interference effect of oceanographic radars and allocated services when operating co-channel within frequency bands 4.5 MHz ± 1 MHz, 9 MHz ± 2 MHz, 13 MHz ± 1 MHz, 16 MHz ± 2 MHz, 26 MHz ± 4 MHz and 43 MHz ± 4 MHz; and

2) review compatibility of oceanographic radars with incumbent allocated users within the above frequency bands.

In addition, the test results could facilitate the consideration of available frequency bands for a new allocation to radiolocation service.

6-2 System overview

In order to investigate the number of radio signals which are being introduced at coastal area of Korea, the mobile measuring system was used for the observation test of the radio environment in the frequency band 3-50 MHz.

Figure 63 shows an overview of the observation system used for this test. The system consists of two HF antennas for reception of radio signals in the range of 3-50 MHz, antenna selector for switching the frequency, vector analyser for data processing, personal computer for saving data and a monitor. Two types of HF antennas were used to fully cover the frequency band 3-50 MHz. One is HE010 antenna covering the lower frequency band of 3-20 MHz, and the other is HE309 antenna for the 20-50 MHz range.

This equipment was mounted on a vehicle for monitoring the radio environment at Korean Radio Monitoring Office, and the tests were carried out after selecting proper test sites along the coastal border in Korea.

FIGURE 63

Observation system mounted on board vehicle

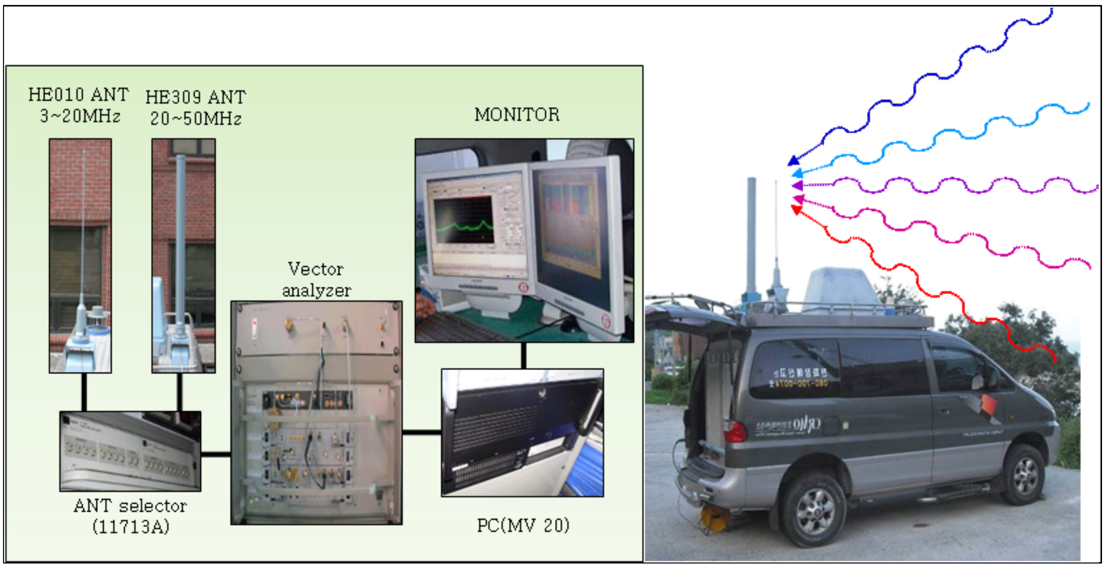

Korea is located in the North-Eastern part of Asia and is close to Japan and China across the sea. Thus the test sites were considered for three parts of the coastal area, East, South and West. Finally 4 sites were selected as shown in Fig. 64; one site in the Western and Eastern areas, and two sites in the Southern area.

FIGURE 64

Observation sites for radio environment test

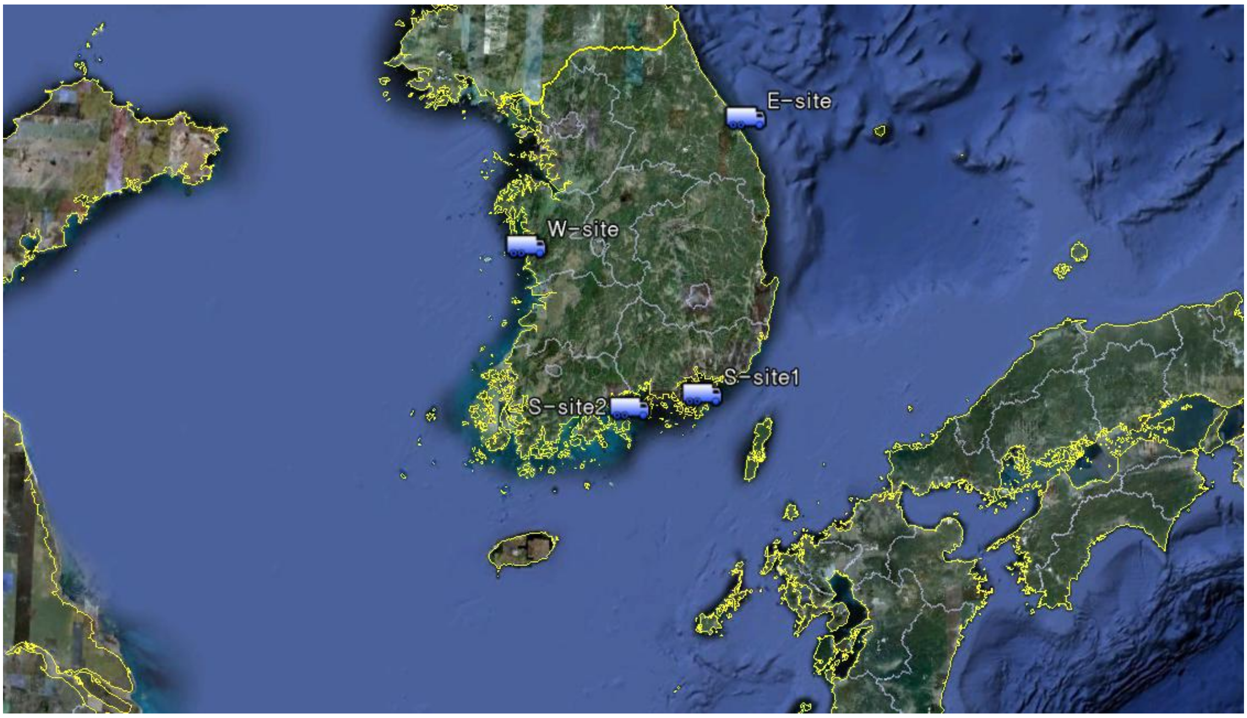

6-3 Test and results

The tests were carried out several times from July to September 2009, each observation test for scanning radio environment in the frequency band 3-50 MHz was made for 2 hours.

Two measurement steps are applied to these tests, one is broadband measurement for observing radio signals at the input of measurement system in the range of 3-50 MHz with resolution bandwidth (RBW) of 1 kHz, the other was a narrowband measurement in the concerned sub-band with RBW of 10 Hz.

6-3.1 3 to 10 MHz range

4.5 MHz ± 1 MHz and 9 MHz ± 2 MHz frequency bands were considered. These frequency bands encompass several sub-bands considered as suitable frequency bands for the operation of oceanographic radars.

The characteristics of received spectrum at each site in these frequency bands are illustrated in Fig. 65.

As shown in Fig. 65, it was determined that these frequency bands have been widely used by existing terrestrial radiocommunication services. Therefore, it is very hard to find available spectrum satisfying the bandwidth requirements for oceanographic radars in these frequency bands.

FIGURE 65

Observed radio spectrum in the frequency range of 3-10 MHz

4 438-4 650 kHz at W-Site

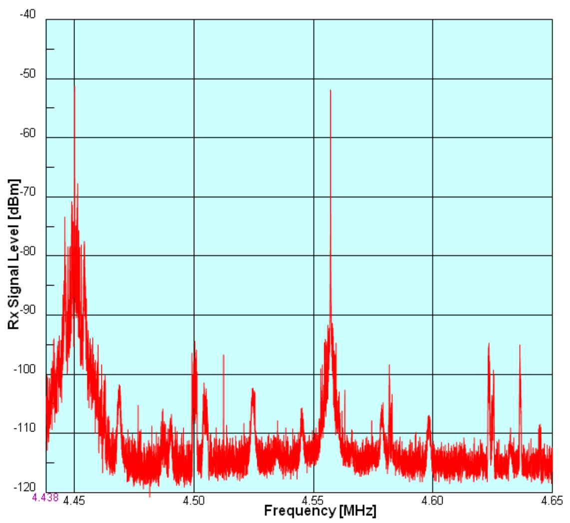

5 060-5 450 kHz at E-Site

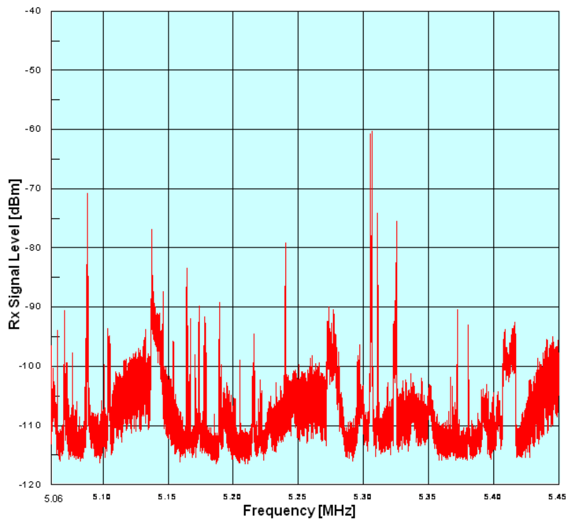

7 450-8 100 kHz at S-Site 1

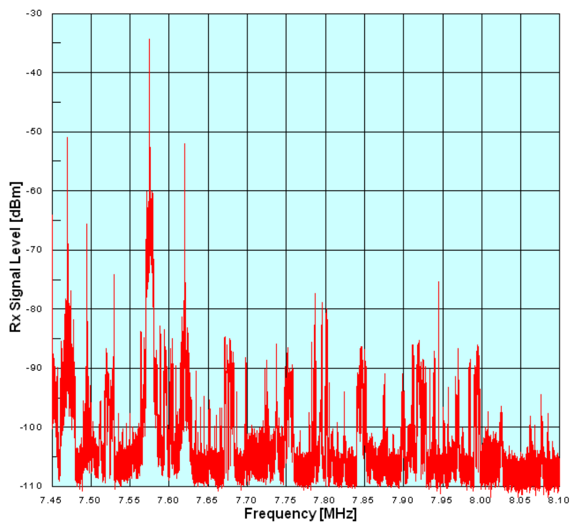

9 040-9 400 kHz at S-Site 2

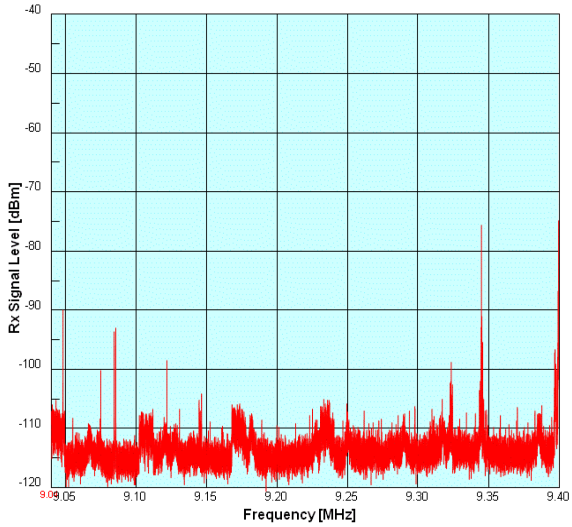

6-3.2 10 to 20 MHz range

13 MHz ± 1 MHz and 16 MHz ± 2 MHz frequency bands were considered. These frequency bands encompass several sub-bands considered as suitable frequency bands for the operation of oceanographic radars.

The observed results at each site in these frequency bands are illustrated in Figs 66 and 67.

Korea and its adjacent country currently use 13 MHz band for oceanographic radars as experimental stations, as shown in the observation. The observation indicated that the frequency band has not been extensively used by the existing terrestrial radiocommunication services. Thus this frequency band may be considered as a suitable frequency band for oceanographic radars with proper selection of geographical location.

However, the observation indicated that the 16 MHz frequency band has been extensively used by the existing terrestrial radiocommunication services. Thus, it may be difficult to practically find available spectrum for the oceanographic radars.

FIGURE 66

Observed radio spectrum in a sub-band of 13 870-14 000 kHz range

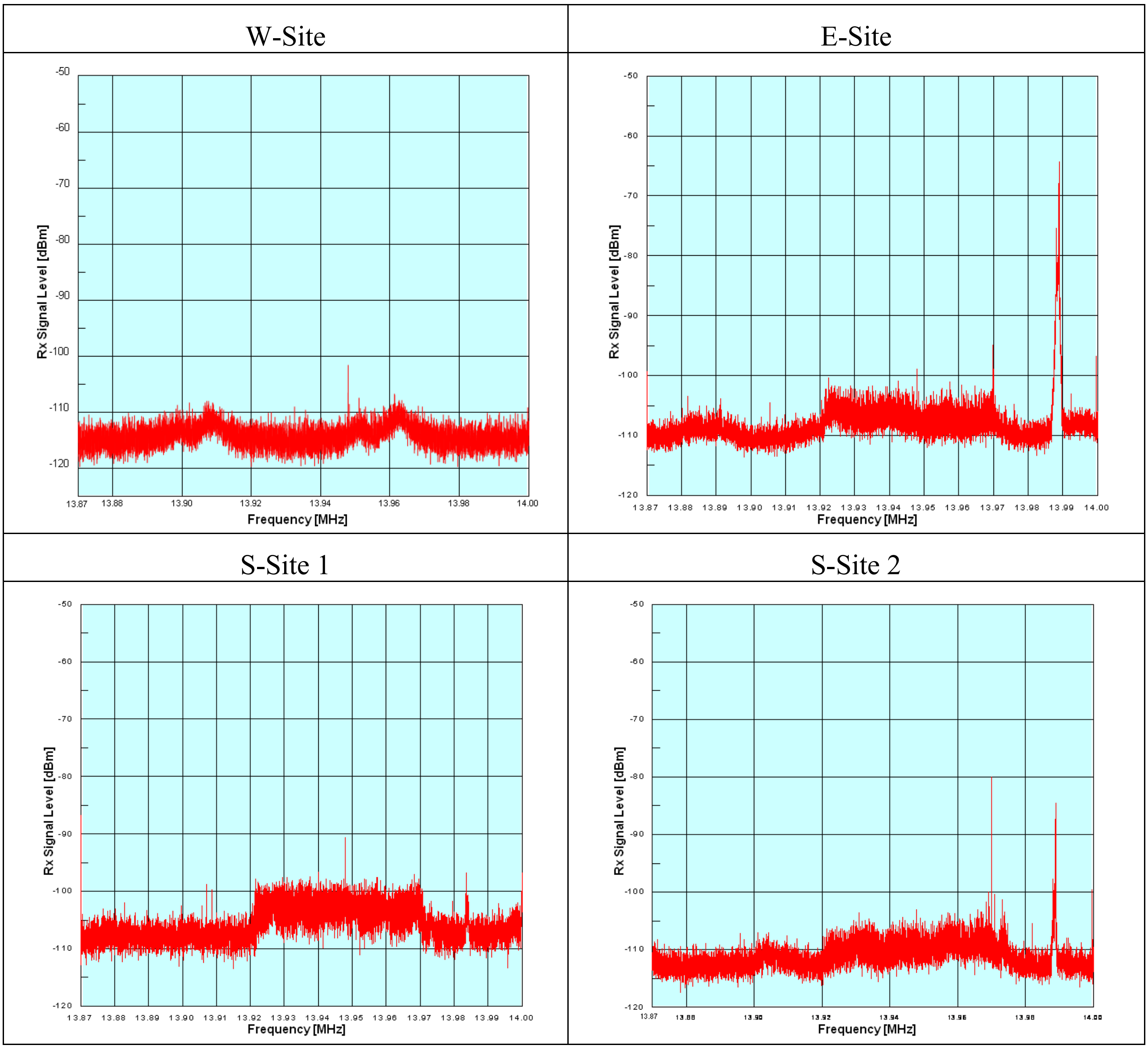

FIGURE 67

Observed radio spectrum in other sub-bands within the 10-20 MHz range

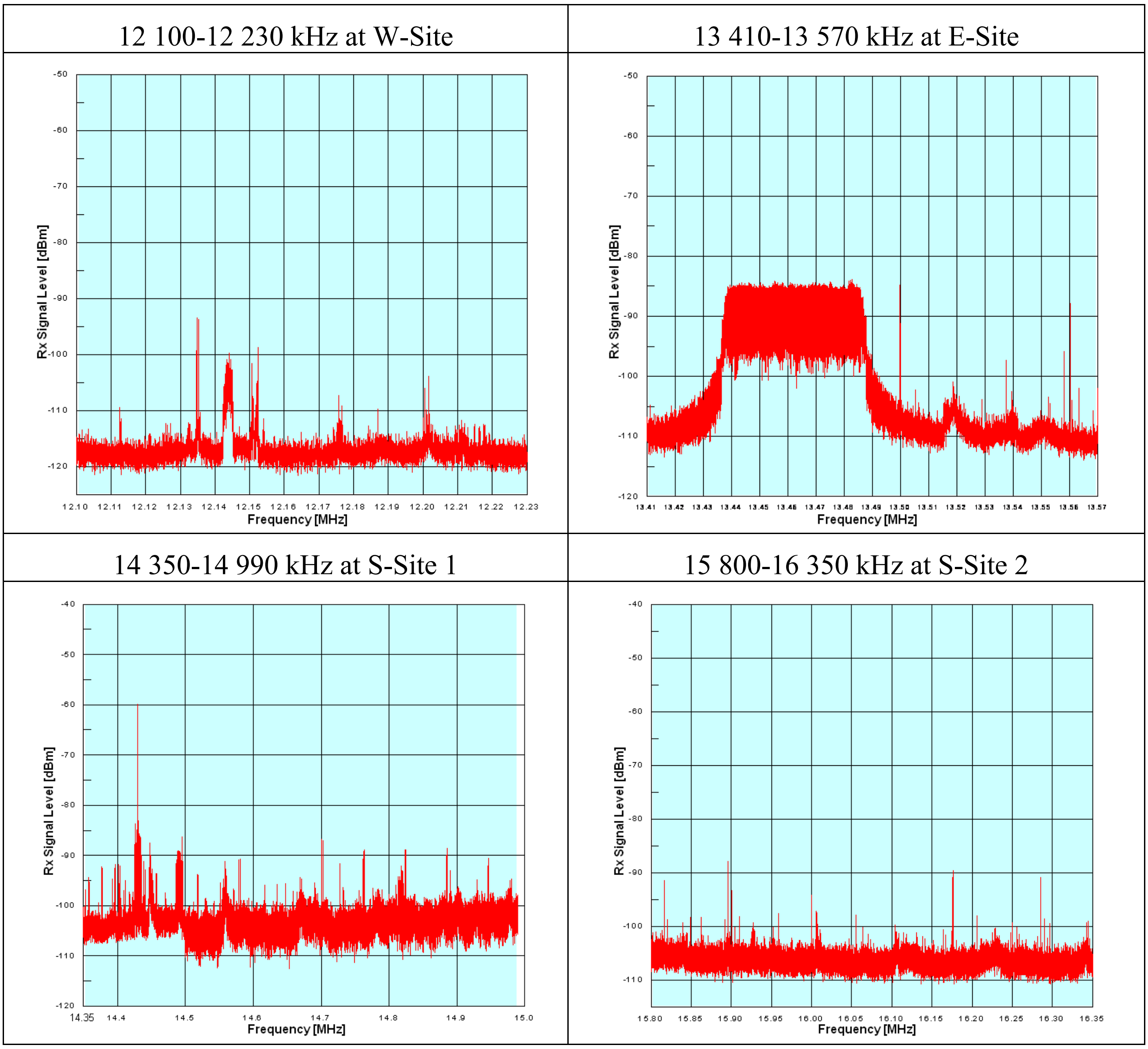

6-3.3 20 to 50 MHz range

26 MHz ± 4 MHz and 43 MHz ± 4 MHz frequency bands were considered.

These frequency bands can be considered as a suitable band for oceanographic radars since there was no indication of spectrum usage. The results of spectrum measurement for each site are illustrated in Figs 68 and 69.

As shown in Fig. 68, Korea currently uses the frequency band 24 000-24 890 kHz for two oceanographic radars as experimental stations. These oceanographic radars use the same centre frequency on a shared basis.

Although Korea uses the frequency band 25 010-25 070 kHz for oceanographic radars as experimental stations, the oceanographic radar signals were not monitored by the measurement system as a result of the distance and blockage due to geographic obstacles. Thus it is possible to allow other oceanographic radar systems in this frequency band with frequency reuse on a shared basis.

FIGURE 68

Observed radio spectrum in a sub-band of 24 000-24 890 kHz range

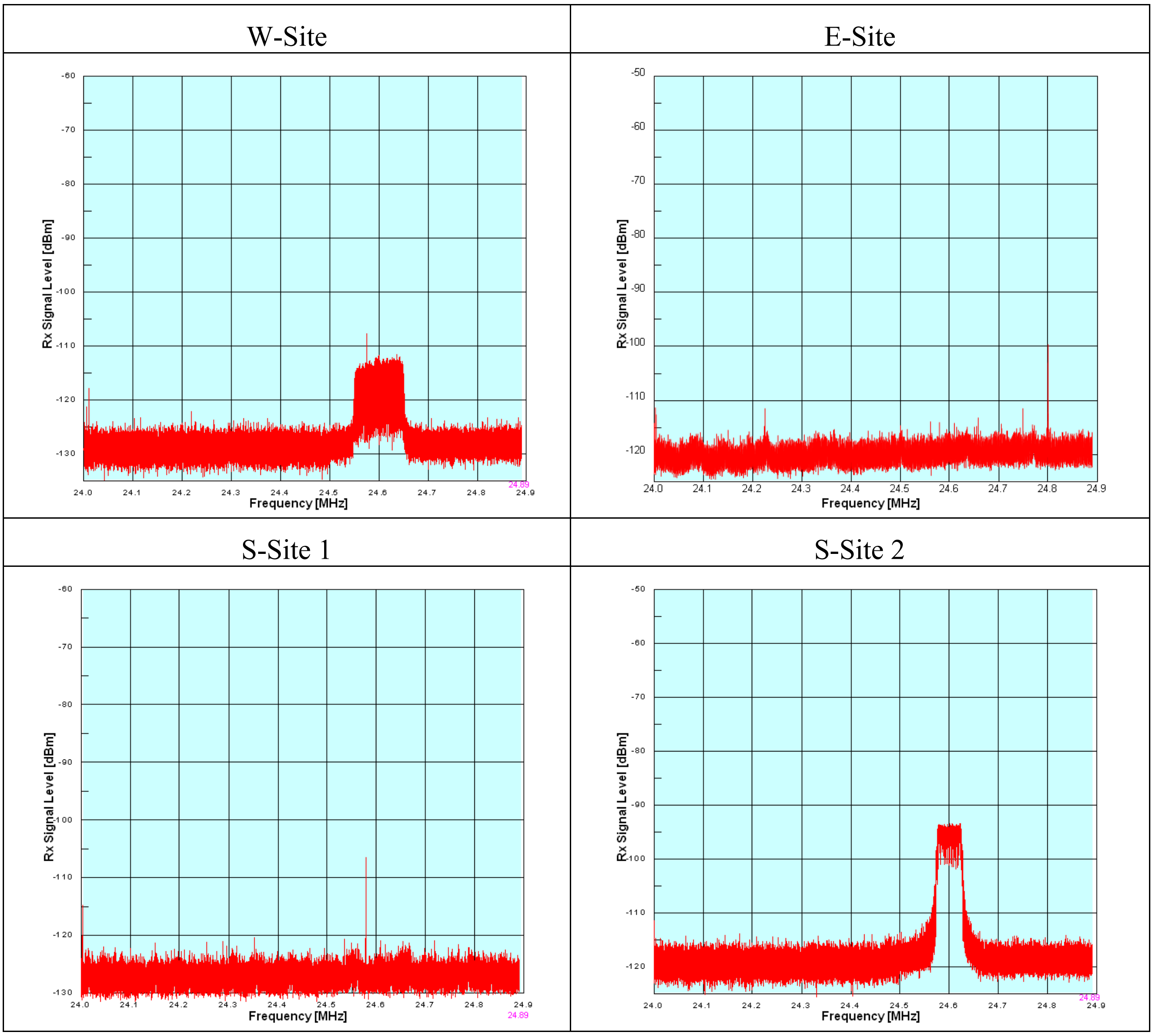

FIGURE 69

Observed radio spectrum in other sub-bands within the 20-50 MHz range

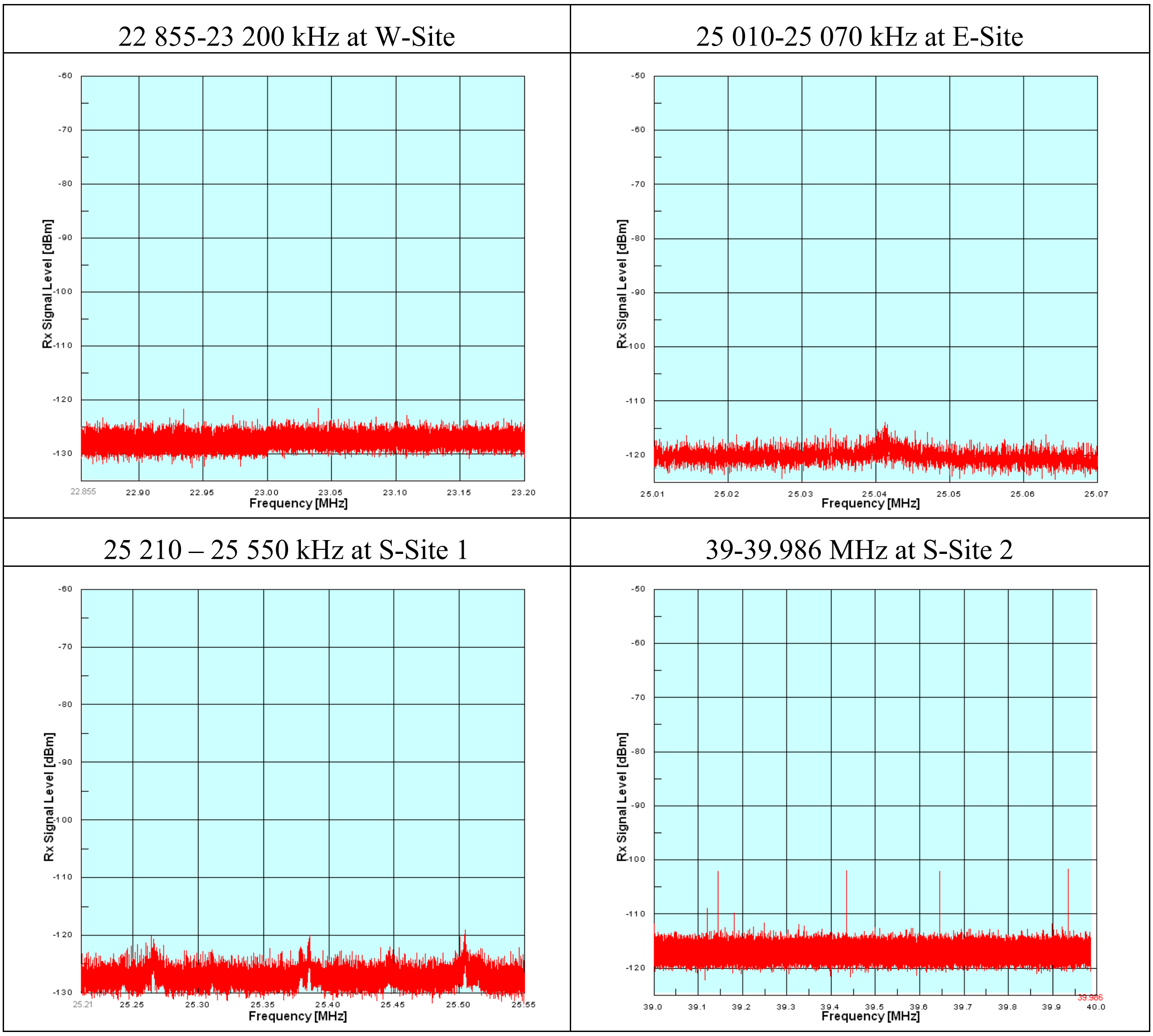

6-4 Calculations and analysis

Administrations around Korean Peninsula are operating some oceanographic radars on an experimental basis. The measurement results as shown in previous section show that oceanographic radars in the frequency bands 13 MHz and 24 MHz are currently operating.

This section provides comparisons between measurement results and calculation results. The calculations were carried out by the ground-wave propagation model.

6-4.1 Calculations

Ground-wave analysis for path loss calculation, derivation of noise and maximum interference levels are provided in § 5 (ground-wave analysis) of the main text.

Based on the analysis, interference to noise ratio (*I/N*) due to the emission of oceanographic radar is given by:

$$I/N = P_{radar} + P_L - N$$

where,

P_{radar} : transmission power of oceanographic radar

P_L : path loss (see Rec. ITU-R P.368-9)

N : available noise power in 1 kHz resolution bandwidth (see Rec. ITU-R P.372-10).

6-4.1.1 Oceanographic Radar location and characteristics

Geographical locations of oceanographic radars and 4 measurement sites (Rx sites) are given in Fig. 70.

Table 42 shows the characteristics of oceanographic radars as provided in Table 1.

FIGURE 70

Oceanographic Radar locations

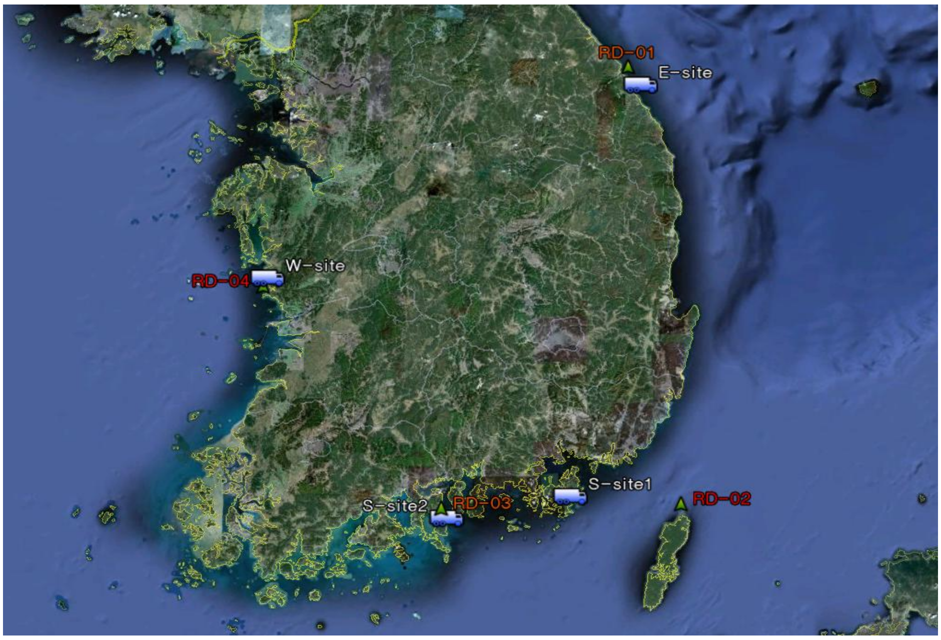

TABLE 42

Information of oceanographic radars

Oceanographic Radars		Rx Sites			Comments
Name	Characteristic	Name	Distance (km)	Propagation	
RD-01	13 MHz (System 2)	W-site	277.7	Land	1)
		E-site	7.8	Land	2)
		S-site1	298.6	Land	1)
		S-site2	335.9	Land	1)
RD-02	13 MHz (System 6)	W-site	309.4	Mixed	3)
		E-site	304.6	Mixed	3)
		S-site1	70.8	Mixed	3)
		S-site2	150.0	Mixed	3)
RD-03	24.5 MHz (System 3)	W-site	209.5	Land	1)
		E-site	339.8	Land	1)
		S-site1	79.7	Land	3)
		S-site2	0.6	Land	2)
RD-04	24.5 MHz (System 3)	W-site	4.3	Land	2)
		E-site	280.7	Land	1)
		S-site1	250.0	Land	1)
		S-site2	207.7	Land	1)

1) No calculation is required since the Rx site exceeds the separation distance recommended in main text.

2) No calculation is required since the Rx site is very close to the oceanographic radar.

3) Calculation would be required for verifying the measurement results.

6-4.1.2 Calculation results in 13 MHz frequency band

Calculation of Interference level for RD-02

Even though this oceanographic radar (RD-02) was being operated in a neighbouring country, the oceanographic radar signal in the 13 MHz frequency band was monitored at 3 receiving sites, as shown in Fig. 66. While the oceanographic radar signal was measured at W-site, the measured *I/N* levels shows 5 to10 dB at E-site, 8 to 13 dB at S-site1, and 5 to 10 dB at S-site2.

According to Recommendation ITU-R SM.1753-1, the geographical categories for the measurement sites are classified as follows:

− W-site: Residential

− E-site: Rural

− S-site1: City

− S-site2: Residential

Using the above geographical categories, the calculated results of received *I/N* values at each measurement site from RD-02 emissions are given in Table 43. Since the main beam of RD-02 was assumed to be directed toward E-site in these calculations, received signal was considered to be from the side-lobe pattern in Recommendation ITU-R M.1874 for other 3 sites.

In addition, all the calculations were performed with procedures for propagation over sea path.

TABLE 43

Calculation results for RD-02 oceanographic radar

Tx Oceanographic Radar (RD-02)		Rx site		P_L (dB)	N (dB)	I/N	
Tx Power (W)	Tx Gain (dBi)	Name	Category			Calculated (dB)	Measured (dB)
30	–2	W-site	Residential	–137.4	–132.2	7.6	None
30	8	E-site	Rural	–136.8	–137.1	23.1	5 to 10
30	–12	S-site1	City	–98.7	–128.0	32.1	8 to 13
30	–12	S-site2	Residential	–113.5	–132.2	21.5	5 to 10

As seen in the above table, the differences between calculated and measured values are more than 10 dB. All the paths are assumed to propagate over sea path in the calculations, but the real paths constitute mixed propagation over sea and land. Therefore, mixed path has more propagation loss than sea path, as much as 15 dB.

Calculation of Interference level for RD-03

This oceanographic radar (RD-03) is being operated in the Republic of Korea on an experimental basis using 24.5 MHz frequency band in the vicinity of S-site 2.

As shown in Fig. 68, the oceanographic radar signal at S-site 2 is very high, but there is no signal at S-site1, 80 km away from this oceanographic radar.

Using the same method as the RD-02 cases, the calculated results of received *I/N* values for S-site 1 due to RD-03 emissions are given in Table 44.

TABLE 44

Calculation results for RD-03 oceanographic radar

Tx Oceanographic Radar (RD-03)		Rx site		P_L (dB)	N (dB)	I/N	
Tx Power (W)	Tx Gain (dBi)	Name	Category			Calculated (dB)	Measured
80	8	S-site1	City	–170.0	–135.6	–7.4	None

Based on the above results, RD-03 is compatible with existing terrestrial services in the areas of S-site 1.

6-4.2 Analysis

6-4.2.1 3 to 10 MHz range

According to the Recommendation ITU-R M.1874, oceanographic radars in this frequency band require two separate frequency bands with bandwidth more than 25 kHz each.

However, considering the geographical features in the Korean Peninsula, surrounded by sea and closely located to neighbouring countries, it is undesirable to allocate bandwidth more than 50 kHz for oceanographic radars due to the potential interference from existing radiocommunication systems taking into account measurement results.

Since oceanographic radars within this frequency range are implemented for the purpose of long range observation in the order of 150 km, it is noted that the responsible administrations of close neighbouring countries must carefully evaluate geographic information, which may lead to avoiding operations in coastal area, and the status of fixed and mobile stations, to which the use of the frequency band can be possible with caution.

6-4.2.2 10 to 20 MHz range

In the 13 MHz frequency band, the observation indicated that the frequency band has not been extensively used by the existing terrestrial radiocommunication services. Therefore, it may be considered that the frequency spectrum for the oceanographic radars is available in this sub-band.

However, considering long range propagation characteristics in this frequency band, it is necessary to consider that coordination between concerned countries is required for stable operation of oceanographic radars without causing interference problems in 13 MHz frequency band.

In the 16 MHz frequency band, it is estimated that spectrum is not available for the oceanographic radars based on measured results.

6-4.2.3 20 to 50 MHz range

As for this frequency range, although frequency allocations for land mobile and fixed services are throughout, the measured results show that there was no indication of spectrum usage. Hence, it is possible to provide spectrum for oceanographic radars, including high resolution oceanographic radars.

However, even though spectrum is available, it is not desirable to allocate the frequency bands excessively, considering the demand for mobile and fixed services

6-5 Conclusion and remarks

In order to accomplish the sharing studies under the WRC-12 Agenda item 1.15, more information on compatibility within the suggested sub-bands was needed to make reasonable allocations in the portion of the 3-50 MHz frequency band. By informative and practical reasons, some observations were made through the whole candidate sub-band.

From the measurement results, it was demonstrated that spectrum is available for oceanographic radars in the frequency bands above 20 MHz. And it was also noted that candidate sub-bands below 20 MHz are extensively used by terrestrial radiocommunication services in geographical areas surrounded by sea. In these areas, it is difficult to deploy and operate oceanographic radars in the sub-bands below 20 MHz except for the 13 MHz frequency band.

Attachment 7

Observation of ground-wave oceanographic radar emission impact into HF receivers

Measurements to determine potential interference to mobile stations in the frequency band 10 to 13.5 MHz from oceanographic radars

7-1 Scope

This document gives an overview of measurements on the impact of oceanographic radars to the mobile service in the frequency band 10 to 13.5 MHz. The objectives of the campaign were

1) to detect oceanographic radar signals;

2) to measure the field strength; and

3) to record the influence on a HF radio communication link.

7-2 Introduction

In this document the measurements performed by the Federal Office of the Bundeswehr for Information Management and Information Technology and the Radio Monitoring Service of Technical Center for Information Technology and Electronics supported by a manufacturer of oceanographic radars are presented.

The measurements were carried out at the German North Sea Coast, Fig. 71, and took place between the 19th of July 2010 and the 23rd of July 2010.

7-3 Oceanographic radar system

System overview

Two oceanographic radar systems (System 6 Recommendation ITU-R M.1874) were studied located in Wangerooge and Büsum, Germany.

Table 45 shows the technical parameters of the systems.

TABLE 45

Location	Units	Wangerooge	Büsum
Site of operation		LAT 53° 47’ 23.79” N LON 07° 55’ 11.60” E	LAT 54° 07’ 10.00’’ N LON 08° 51’ 28.57’’ E
Frequency range	(MHz)	12 132 – 13 534	10 650 MHz – 10 950
Bandwidth	(kHz)	100	100
Power ERP	(W)	30	14
Direction of max. radiation		360°	259°

FIGURE 71

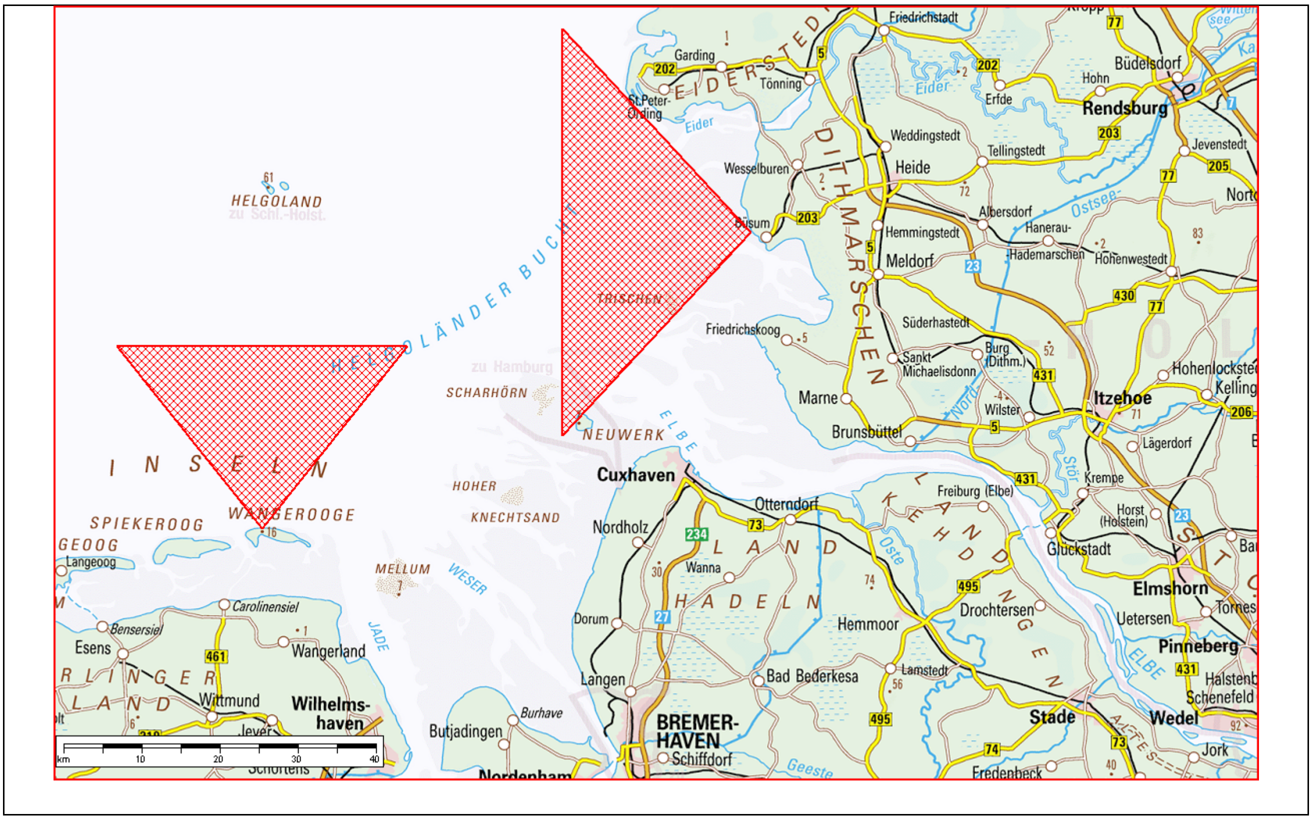

7-4 HF radio system

System overview

An HF receiver was used for the tests. Table 46 illustrates the deployed mobile radio equipment and technical parameters.

TABLE 46

Power	SSB	0,1-5 W
Sensitivity	SSB (10 dB S/N)	0,16 µV
Antenna gain	–	–3 dBi
Bandwidth	–	3 kHz

7-5 Measurement set-up

The measurements were taken at three different sites. One set of measurements was carried out in Büsum, one 5 km away from Meldorf and the last on the isle of Helgoland (Figs 72, 73, 74).

FIGURE 72

Measurement location Büsum

FIGURE 73[18]

Measurement location Meldorf

18 Reference: OpenStreetMap.

FIGURE 74[19]

Measurement location Helgoland

Figure 75 show the place of installation of the fixed service station.

FIGURE 75[19]

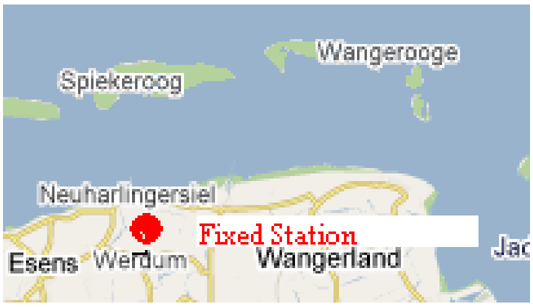

In Fig. 76 the measurement set-up of the electric field strength is depicted.

FIGURE 76

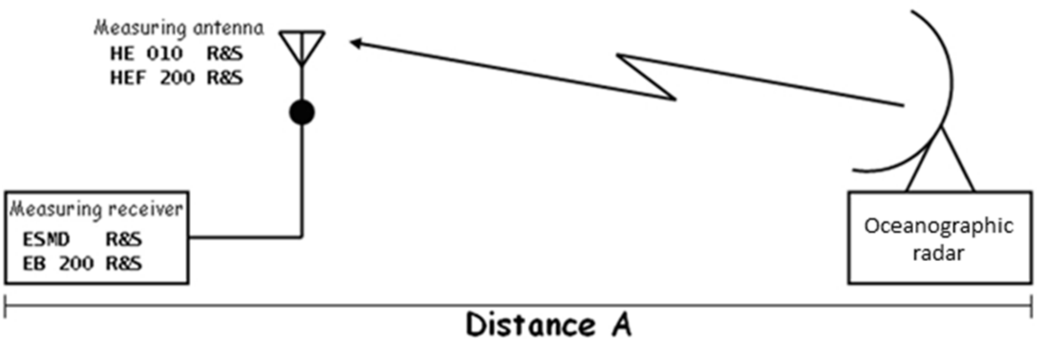

[19] Reference: OpenStreetMap.

The general measurement configuration to record the effect of oceanographic radar signals on the transmission quality of a radio communication link is shown in Fig. 77.

FIGURE 77

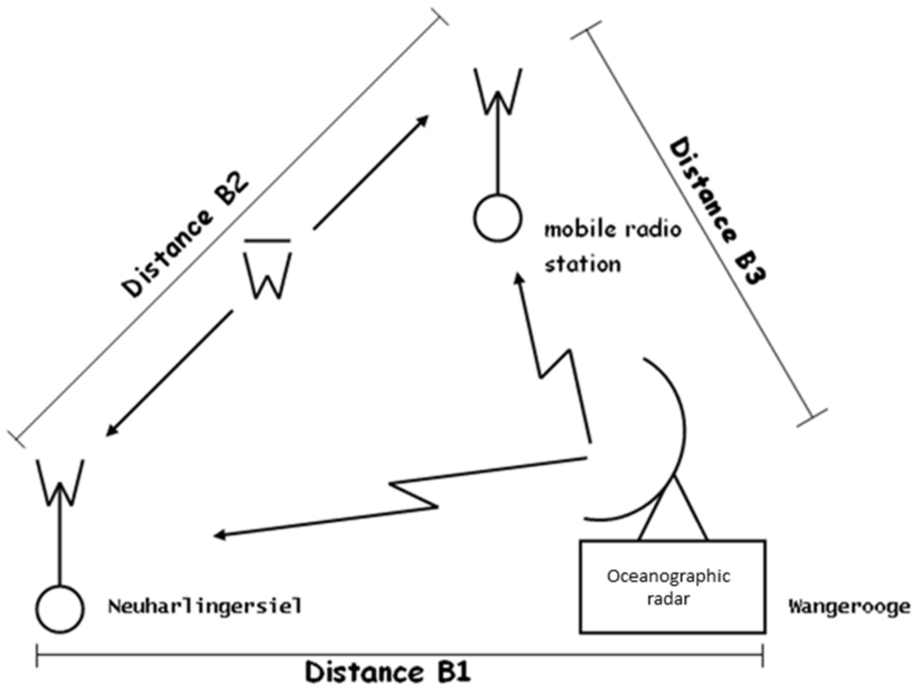

A fixed radio station, located in NEUHARLINGERSIEL, was used to establish a radio link to the mobile station at the measurement sites. The various distances are listed as per particulars given below. Field-strength measurement values are listed in Table 47.

Measurement 1 (Büsum)

Field strength:

Distance A – Tx/Rx:	Büsum/Büsum	290 m
	Wangerooge/Büsum	73 km

Radio link:

Distance B2 – Tx/Rx:	Fixed station/Büsum	87 km
Distance B3 – Tx/Rx:	Wangerooge/Büsum	73 km

Measurement 2 (Coastline 5 km west of Meldorf)

Field strength:

Distance A – Tx/Rx:	Büsum/Meldorf	9 km
	Wangerooge/Meldorf	75 km

Radio link:

Distance B2 – Tx/Rx:	Fixed station/Meldorf	89 km
Distance B3 – Tx/Rx:	Wangerooge/Meldorf	75 km

Measurement 3 (Helgoland)

Field strength:

Distance A – Tx/Rx:	Büsum/Helgoland	63 km
	Wangerooge/Helgoland	43 km

Radio link:

Distance B2 – Tx/Rx:	Fixed station/Helgoland	45 km
Distance B3 – Tx/Rx:	Wangerooge/Helgoland	43 km

7-6 Measurements results

Field strength:

TABLE 47

Site	BÜSUM	Wangerooge
Helgoland	48 dBµV/m	51 dBµV/m

Figure 78 shows a snapshot of the oceanographic radar FMCW signal radiated from Wangerooge in the frequency domain and the waterfall chart of the signal in the frequency range 12.2 to 12.3 MHz. The measurement reading was recorded at a distance of 73 km. FMCW signal was measured in the time domain (measuring time 500 µs) and transformed by FFT into the frequency domain. The bandwidth of the signal is 100 kHz and the sweep time 260 m/s.

FIGURE 78

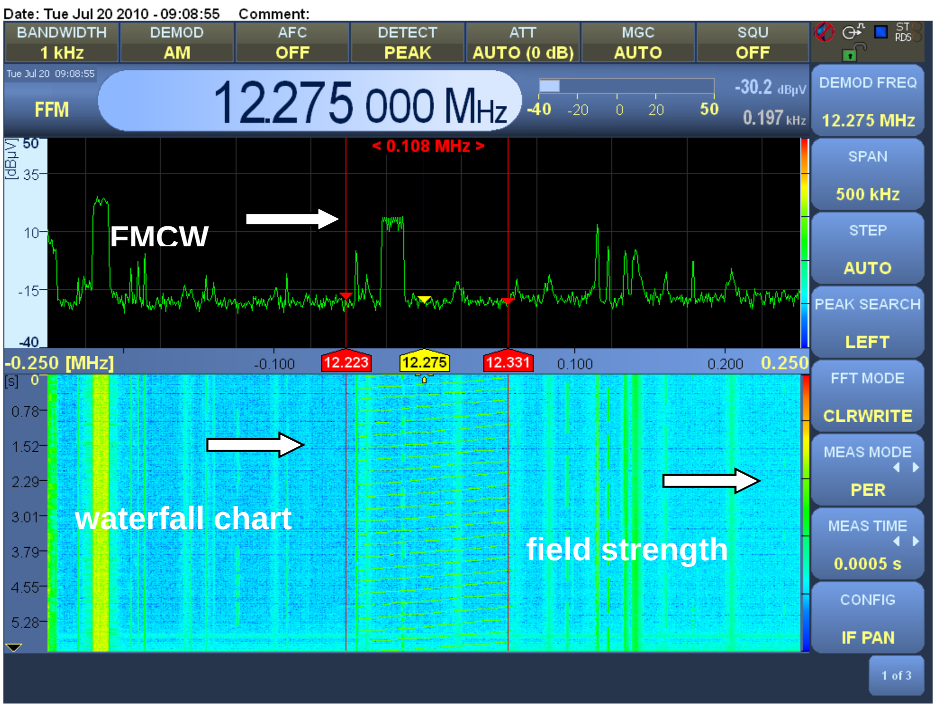

Figure 79 shows a snapshot of the FMCW oceanographic radar signal (System 6 Recommendation ITU-R M.1874) from Wangerooge and the voice signal in a 3 kHz channel transmitted by a radio station in Neuharlingersiel on a frequency of 12.255 MHz (SSB, UB). The measurement reading was recorded at a distance of 73 km (Wangerooge) and 87 km (Fixed Station Neuharlingersiel). Figure 79 shows that the field strength of the oceanographic radar signal is stronger than the radio voice signal.

FIGURE 79

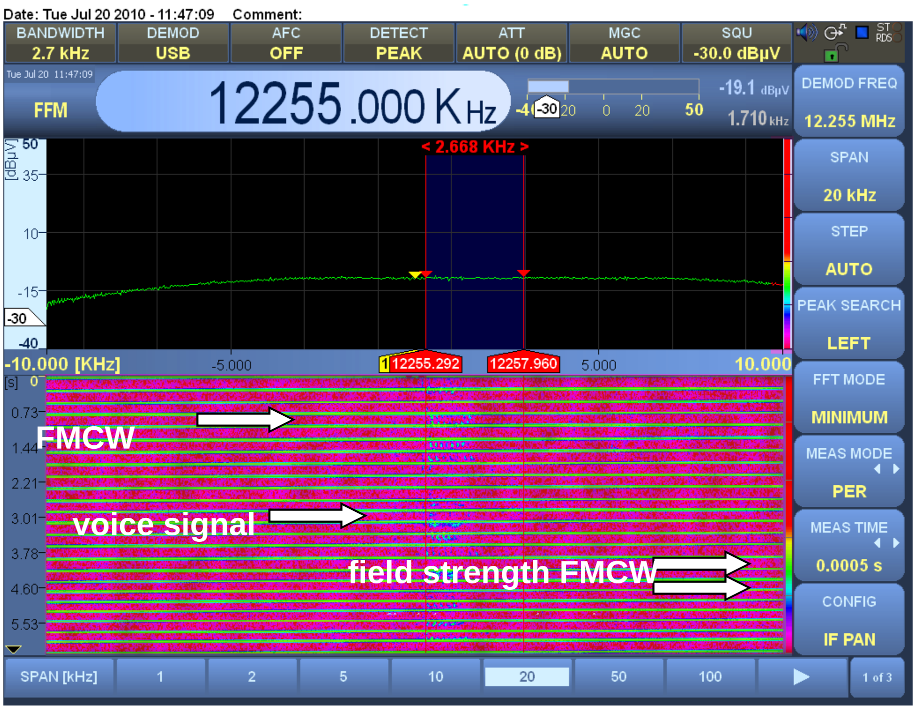

Figure 80 shows a snapshot of the FMCW oceanographic radar signal radiated from Wangerooge.

FIGURE 80

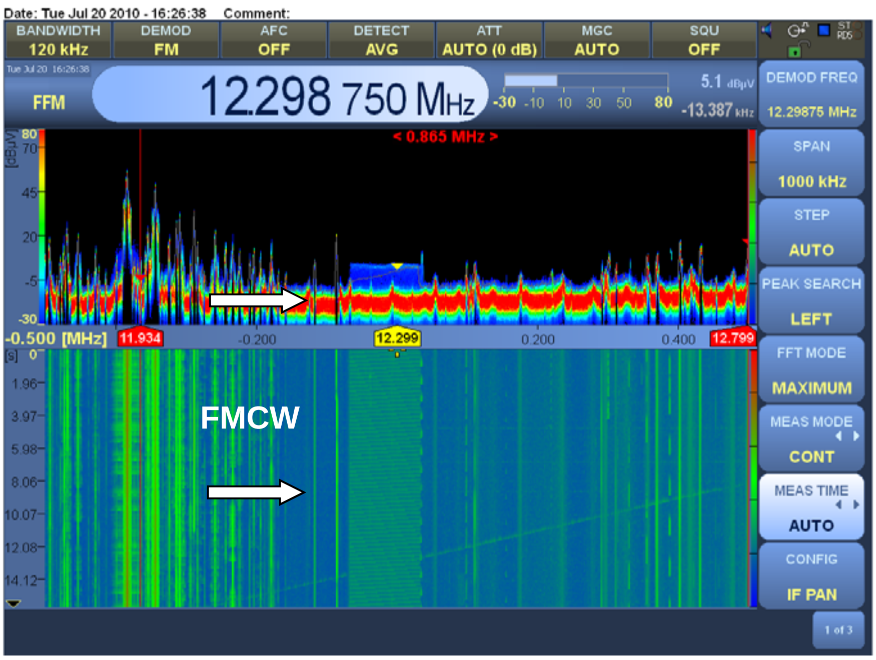

Figure 81 shows the peak levels of a FMCW oceanographic radar signal in a 3 kHz (zero span) voice channel radiated from Wangerooge and received in Helgoland at a distance of 43 km.

FIGURE 81

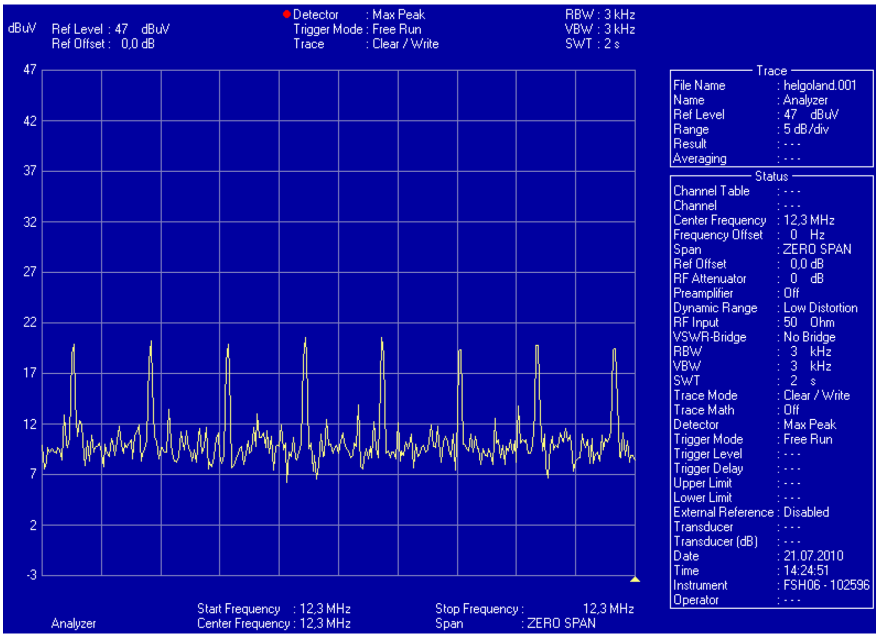

At all measurement sites the effect of the FMCW oceanographic radar signal on a voice channel was recorded on a digital audio data device.

7-7 Conclusions

The tests have shown that a receiver with a bandwidth of 3 kHz will be affected within the separation distances as detailed in Table 7 for System 6.

The oceanographic radar signal manifests itself as repetitive interference to the 3 kHz received signal; this indicates that the peak signal may be important as the source of interference.

In case of operation of an oceanographic radar, occupants within the 100 kHz bandwidth would be affected. The impact on digital transmission was not subject of the current measurement campaign.

The results of the measurement confirm the need for separation between existing services and oceanographic radar operating under the radiolocation service.

Attachment 8

Observation of sky-wave oceanographic radar emission into HF receivers

8-1 Introduction

During a campaign (Attachment 7) to measure the interference effect of the ground-wave of oceanographic radars to a station of the mobile service a signal from an unidentified radio transmitter was detected, the field strength was measured and the audio signal was recorded. According to the characteristic of the emission it seems very likely that the source was an oceanographic radar.

8-2 Measurements of potential interference via sky-wave

This document gives a short overview about measurements performed by the Federal Office of the Bundeswehr for Information Management and Information Technology and the Radio Monitoring Service of Technical Center for Information Technology and Electronics.

During a campaign to measure the interference effect of the ground wave of oceanographic radars to the mobile service a signal from an unidentified radio transmitter was detected, the field strength was measured and the audio signal was recorded.

The technical characteristics of the signal and the fact that signal was discovered at different sites with nearly the same field strength indicate that it was most likely an emission of a oceanographic radar was received via sky-wave.

The location of the radio transmitter could be identified near Brest, France by the monitoring service of the BNetzA.

Table 48 shows the site, the geographical coordinates and the date of the measurement as well the measured field strength of the signal.

TABLE 48

Site	Geographical coordinates North	Geographical coordinates East	Date and time of measurement	Field strength (dBμV/m)
Brokzetel	53° 28’ 17”	7° 38’ 34”	09/30/2010 15:18 h UTC	31
Leer	53° 13’ 25”	7° 28’ 51”	09/30/2010 13:34 h UTC	31
Greding	49° 03’ 22”	11° 20’ 41”	10/04/2010 09:36 h UTC	30

Figure 82 shows the measurement sites on a map.

FIGURE 82

In Fig. 83 the measurement setup of the electric field strength is depicted. Following adjustments were done at test receiver, RBW 3 kHz and demodulation AM USB. The noise figure reached 16 dB(μV/m).

FIGURE 83

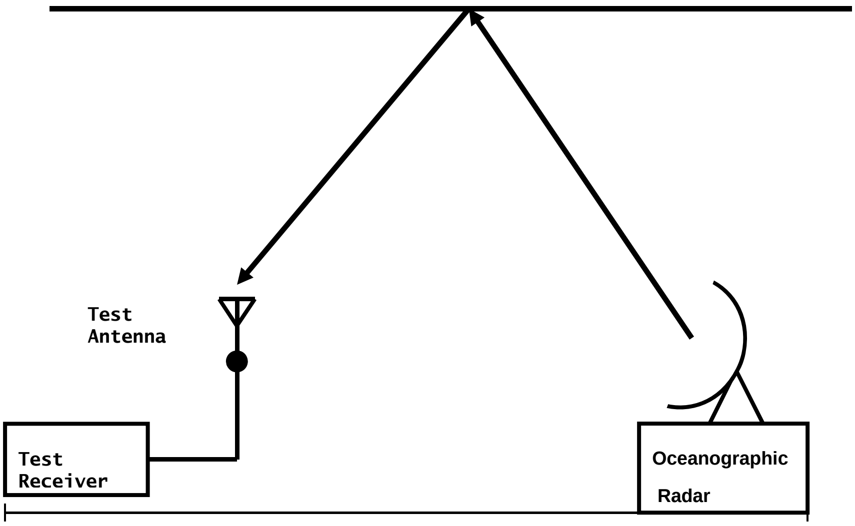

8-3 Conclusions

The observation shows the physical presence of sky-wave signals. The effect on HF receivers could not be quantified at this time.

Attachment 9

Oceanographic radar interference mitigation techniques and spectrum efficiency improvements – Technical and operational considerations

9-1 Introduction

This attachment examines potentially interfering signals produced by oceanographic radars used for continuous, real-time, operational ocean-current monitoring. The subject was examined from the following three standpoints:

1) consider and examine possible methods that might be used to mitigate interference effects;

2) how effective are these likely to be in eliminating any interference into others' receivers;

3) what are their impacts on performance effectiveness of an oceanographic radar network.

Experience has been gained within the oceanographic radar community since the 1970s. With over 25 licensed HF/VHF frequencies and a total of 120 oceanographic radars in the U.S., and 8 frequencies and 51 oceanographic radars in Japan. More than 250 licensed oceanographic radars are operating worldwide (as of 2010). The fact that these oceanographic radars have operated on an experimental, non-interference basis is an indicator that the radiolocation allocations for such surface wave oceanographic applications may have little or no effect on incumbent users of the frequency bands in 3 to 50 MHz. In the few cases where an interference problem has been identified, it has typically been resolved by assigning a different frequency to the oceanographic radar system. Operational experience alone indicates that shared use of the spectrum where the radiolocation service is co-allocated should be feasible given accurate, carefully evaluated frequency assignments.

9-2 Geometry of problem

The oceanographic radars are located on the coasts and transmit using vertical polarization, intended for surveillance of the ocean surface. Locations of the victim receivers potentially seeing the oceanographic radar signals are predominantly behind, i.e. back over land as shown in Fig. 84.

FIGURE 84

Schematic image of oceanographic radar location

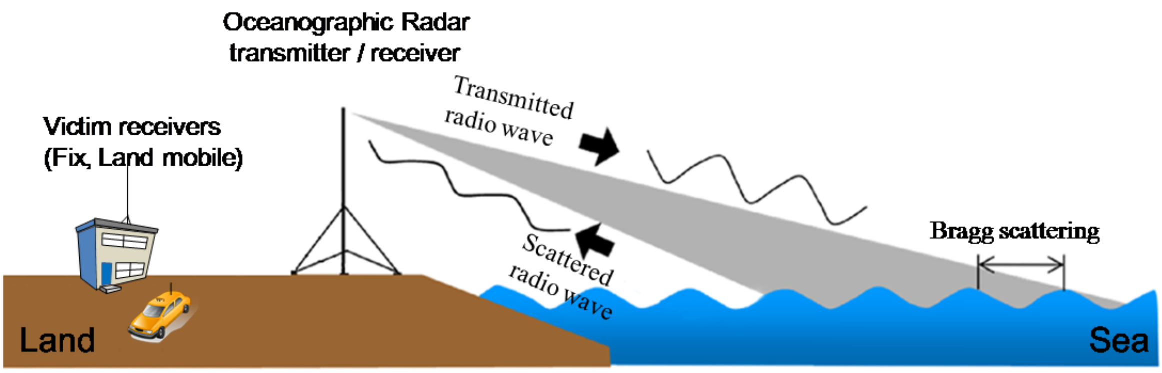

9-3 List of potential interference mitigation techniques

1) On-channel interference (both oceanographic radar and victim receivers are on the same frequency):
   - time multiplex:
     i) oceanographic radar systems listen before transmit; don't transmit on that frequency if other signal is heard;
     ii) oceanographic radar systems shut down (or change frequency) on command when other frequency band occupier needs to transmit;
   - reduce oceanographic radar spectral occupancy:
     i) eliminate multiple occupied frequency channels as much as possible;
     ii) reduce bandwidth required for each channel;
   - keep energy into others' receivers low:
     i) use directive transmit antennas to:
        – keep ground wave energy low;
        – keep sky wave energy low;
     ii) spread signal bandwidth so energy density into receiver channel is low;
     iii) reduce oceanographic radar radiated power.
2) Out-of-band interference (oceanographic radar signal due to pulsing, waveform discontinuities, or transmitter nonlinearity spills outside of authorized frequency band).
   - Pulse shaping and filtering.

9-3.1 Time multiplexing

9-3.1.1 Listen before transmit

Three U.S. over-the-horizon radars operate in this mode under secondary licenses. Using this methodology becomes more complex and perhaps unmanageable as the number of radars increases (already there are perhaps 220 operating worldwide, and this number continues to increase). The concept is this: at periodic intervals, the radar transmitter shuts off and the receiver listens at that frequency, attempting to detect a radio signal above the background noise. Here are some scenarios, trade-offs, and requirements if this is to be effective for both parties.

- The radio receiver being interfered with is most likely seeing sky-wave signals in the low part of the HF frequency band. Higher-frequency signals are used less often for sky-wave paths, and then only for shorter periods of time. Ground-wave distances for higher frequency signals are much shorter.
- Many oceanographic radars within a local network are likely to be sharing the same frequency at the same time, using GPS modulation multiplexing. Therefore, listen-before-transmit means that several oceanographic radars must cease transmitting at the same time, otherwise the oceanographic radar listen mode will be hearing another HF transmitter within the same network.

There are two ways or times when the oceanographic radars can be shut down without destroying their ability to extract coherent Doppler information needed for current and wave information.

Pulsing occurs with a 50% duty factor (square wave), with a pulse repetition period between 0.03 and 2 milliseconds. This is done so that the local oceanographic radar receiver will not be impaired by its strong transmit signal. The pulsing of multiple oceanographic radars is timed using GPS synchronization. Why not listen during the off-period of this square-wave cycle?

1) First of all, this is the period during which the sea-echo information is being received. This echo is strong, and typically lies as much as 20 dB above the background external noise. The other radio signal is therefore very likely to fall below the sea echo signal, and hence would not be heard.

2) Secondly, signals from the other transmitters 100 or more kilometres away will still be heard due to their time delay, even though they are simultaneously off. These are strong enough to mask a weaker radio signal being sought.

Therefore, this method does not show promise that it could effectively detect another radio signal transmission during gaps between pulses, even if processed over several off-cycles.

The next option is to wait until the end of the coherent echo time series that is required for the Doppler processing to get ocean current and wave velocities. Below 10 MHz (e.g. 5 MHz), this period is 1 024 seconds (17 minutes).

– The 17 minute uninterruptible duration is based on the relation between the time series length, the corresponding frequency resolution, and thence, the velocity resolution obtainable for currents. The velocity resolution corresponding to 17 minutes is 3 cm/s, which is considered to be at the threshold of utility for the oceanographic radar output products; this is the reason for the 17 minute interval.
– If the time series is interrupted (by shutting off the transmitter) during these 17 minutes, the coherence of the entire sample is destroyed and Doppler information cannot be extracted.
– We suggest that the utility of waiting 17 minutes to listen is questionable for the following reasons:
  i) Suppose the other user of this frequency wants to transmit a message. Most likely he will hear the oceanographic radar transmitter, because he will initiate his transmission during the 17 minute oceanographic radar transmit period. So he will shut off and wait for a while, then try again.
  ii) The oceanographic radar listens for one minute at the end of its 17minute cycle, hears no radio signal, and so resumes transmitting. The other user tries again, and hears the oceanographic radar transmitter. Understandable frustration and impatience sets in during this game of tag.
  iii) The other option is for the other radio user to continue transmitting for at least 30 minutes. That way, the oceanographic radar spectral processor – in its listen mode – will hear the signal and can cease transmission for an appropriate duration (e.g. another 15 minutes), listen again, and if finished, continue.
  iv) However, when listening at the oceanographic radar, perhaps the radio is only temporarily off the air, and will return, only to hear the oceanographic radar again.
  v) As mentioned earlier, it will hear several oceanographic radars on this frequency, because they will all turn on and off in synchronization.

To allow a proper interval for two-way communication for the other user, probably a 15 minute interval should be reserved with oceanographic radars off. However, these global oceanographic radar networks are used for emergency applications, such as tsunami detection, search and rescue, and vessel detection. Having oceanographic radars off for this length of time can render these applications less effective or even totally useless for the intended purpose.

Any “listen before transmit” system has dissymmetrical geographic sitting scenarios that may render it ineffective. A distant transmitter may not be heard distinctly above the noise by the oceanographic radar during its listen period. Therefore, the oceanographic radar continues to operate. But a receiver listening to this signal that is geographically near the oceanographic radar transmitter would be deafened by the oceanographic radar signal coming from close by. Even a few cases like this could be unacceptable to the other license holder sharing that frequency, especially in case of emergency.

This frustrating game of hide-and-seek among oceanographic radar and radio user of the same frequency will most likely render this well-intentioned mitigation technique unacceptable to the radio user, not to mention the degradation in oceanographic radar performance for the output ocean products or denial of key oceanographic radar data needed in emergencies.

9-3.1.2 Oceanographic radar shuts down on command

If the other authorized radio user sharing the same frequency needs to have access in cases of emergency, another option is a control system whereby that user commands the oceanographic radars to turn off their transmitters. This would free up the channel for exclusive use, for a period of time. Here are some considerations and trade-offs.

1) A scheme such as this could be implemented, with some software programming on both sides. Because several oceanographic radars (as mentioned earlier) are operating on the same channel, all of these must cease transmitting together. Although not insurmountable, such a control system for both radio and oceanographic radar user will take some time and resources to develop and optimize.
2) Such a system should command the oceanographic radar transmitters back on at the end of the radio use period, to allow resumption of normal operation.
3) If the oceanographic radar network has interruptions to allow radio transmissions longer than 15 minutes, this will seriously degrade several missions, including Coast Guard search and rescue; tsunami detection; oil spill clean-up; and vessel surveillance. It will also decrease the accuracy of surface current mapping accuracy.
4) In some cases, the radio user needing these channels does not want to divulge certain information for military or security reasons (exact frequencies, time of intended broadcast, etc.). Such a sharing scenario may be felt to compromise desired security.

Therefore, this suggested scenario imposes constraints and degradation of performance to all parties, compared to finding a way that each can occupy separate frequency channels exclusively.

9-3.2 Reduce oceanographic radar spectral occupancy

9-3.2.1 Eliminate multiple frequency channels

When oceanographic radars were first being developed and tested for ocean current mapping and wave monitoring, their number was so few that each could ask the FCC (or appropriate agency) for an experimental license to use a separate frequency. As the number increased and lower frequencies were needed for longer ranges, separate frequencies for each were no longer possible. A couple ways to mitigate this proliferation and lower-frequency use were tried:

1) Distance spacing is sufficient that two oceanographic radars no longer interfere with each other. This is especially helped if there is a stretch of land between the two oceanographic radars, rather than an all-over-sea path. And it becomes much less serious at higher frequencies where the surface-wave path loss attenuates an adjacent oceanographic radar’s signal. This becomes less effective at lower frequencies needed for long-range oceanographic radar coverage.

2) Time multiplexing, whereby one only one oceanographic radar in a nested group operates at a time (e.g. for 10-15 minutes) on a given frequency. This impacts current-mapping quality. Accuracy is greatest for continual signal-on processing. It seriously limits or negates performance for applications where timely data are needed; e.g. tsunami detection/warning, search and rescue, vessel surveillance, oil spill clean-up. As mentioned earlier, longer uninterrupted on-times are needed at lower frequencies in order to achieve acceptable current velocity resolution.

3) Frequency sharing, whereby several adjacent oceanographic radars can operate on the same frequency at the same time without mutually interfering. A specific oceanographic radar design has been employed using a timed modulation synchronization technique that makes this possible, and its international patents allow licensing this technology. This, along with varying the linear frequency sweep direction among oceanographic radar groups and distances between groups, allows large numbers (order of tens) of oceanographic radars to share the same frequency with no mutual interference.

FIGURE 85

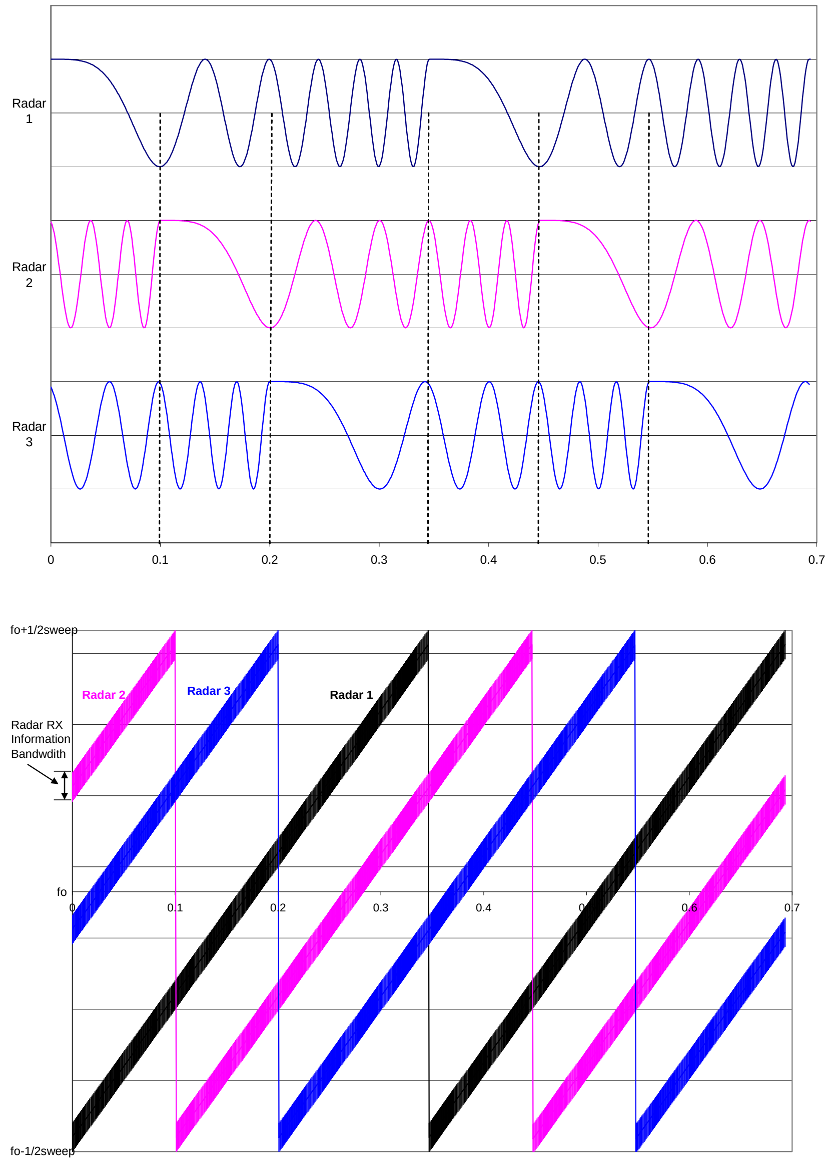

These methods that allow large numbers of oceanographic radars – even at the lowest frequencies – to share the same frequency channel have proven highly effective at reducing their required spectral footprint, even as the numbers of oceanographic radars continually increase.

9-3.2.2 Reduce channel bandwidth

The question is often asked: for over 100 years, an AM radio broadcast has required only 3-5 kHz spectral bandwidth for simple analogue voice transmission, why does oceanographic radar use up to 150 kHz or more, in some cases? That amount wipes out many potential AM radio channels (although FM generally uses much more bandwidth). The answer has to do with the oceanographic radar's spatial resolution. Regardless of oceanographic radar signal format employed, the radar cell size in range is inversely proportional to signal bandwidth. For example 150 kHz corresponds to a 1 km range cell; 25 kHz corresponds to 6 km. So ultimately the trade-off between utility of the current data vis-a-vis attempting to be a "good neighbour" by keeping spectral occupancy to a minimum has resulted in the following established practices over the past 30 years.

1) Lower frequency bands (9 MHz and lower) that are required to reach distances up to 200 km, 25 kHz is typically used, producing a 6 km oceanographic radar cell. A larger cell than this is deemed unacceptable to the ocean user community, and hence a smaller bandwidth cannot be considered. Although a smaller range cell is desired by many users (entailing greater bandwidth), a compromise has been struck that keeps the signal bandwidth lower than 30 kHz to minimize interference potential while providing useful ocean surface data.

2) At higher frequency bands like 25 and 42 MHz, with shorter ranges (and less interference potential), signal bandwidths used are typically 150 and 300 kHz, respectively. This allows 1 km and 500 m range cells, respectively. Thus the amount of information gathered in the smaller coverage area remains commensurate with that from the long range lower-frequency systems with larger range cells and reduced signal bandwidths. The "percent bandwidth" remains the constant over the frequency band 3 to 50 MHz. This has proven an acceptable compromise to the ocean user community and to the licensing authorities.

Therefore, established practice over the past 30 years has produced a compromise that keeps the oceanographic radar signal bandwidth as low as possible so as to minimize interference to others, while still providing an acceptable spatial resolution needed by the ocean user community.

9-4 Reduce interfering energy density

9-4.1 Directive transmit radiation patterns

An effective oceanographic radar network for ocean monitoring requires that the antennas be located at the coast (within ~100 m from the water). It also requires that the view over the sea extend from shore to shore, typically 180°. Transmit, as well as receive, antennas must be designed with this requirement in mind. Radio receivers seeing the oceanographic radar signal as potential interference are predominantly located behind the oceanographic radars, back over land. This is true for both surface wave and sky-wave propagation modes. This section reviews the questionable interference-reducing potential of directive transmit arrays vis-a-vis their disadvantages, and compares with the natural directive suppression offered by the land vs. sea electrical properties.

9-4.2 Transmit antenna arrays to minimize ground-wave signals back over land

A single vertical monopole or dipole is frequently used as the oceanographic radar transmit antenna; it has an omnidirectional pattern on the horizon (in free space or over perfect ground). Often an array of two or four such elements is used to direct the radiation more over the ocean and suppress energy back over land. However, no matter how an array is designed (e.g. number of elements, spacings, etc.), radio physics dictates that only limited backward suppression is possible if the entire seaward sector is to be viewed with an array of only a few elements. The resulting patterns for two dipoles fed as a Yagi at 13 MHz over a perfect ground plane are shown in Fig. 86. The green curve is the omnidirectional pattern of a single dipole over perfect ground, i.e. 6.5 dB. The blue curve has the reflector element adjusted in position and height so as to give a nearly uniform coverage over the sea (toward the right) and realizes a gain about 3.5 dB higher in this direction with a drop over land about 5 dB down from the seaward side. The red is adjusted to give slightly more gain seaward, with two nulls landward. In both cases, power over land can only be suppressed on average by 4 to 5 dB. Four transmit elements will suppress on average another 3 to 4 dB, but at the expense of a narrower field of view over the sea, which is not desirable. Also, the size, inconvenience, and expense of the transmit array becomes a significant factor that precludes its use at most desirable coastal locations.

FIGURE 86

Gains of single-element and two-element dipole arrays over perfect ground

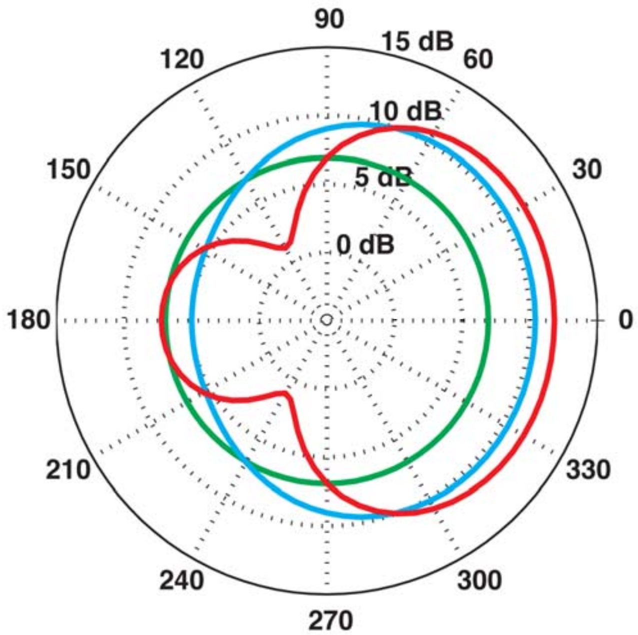

In summary, use of transmit antenna arrays to provide landward ground-wave interference suppression is not very effective, if the wide seaward view is to be maintained; 3 to 4 dB will provide little mitigation.

9-4.3 Directive effect of land to minimize ground-wave signals back over land

Let us look at “pseudo-gain” patterns of HF transmit antennas at the coast; i.e. the interface between land and sea. These are referred to as “pseudo-gain”, because the normal gain definition assumes a far-field power decrease with inverse range squared. Over a surface with reduced dielectric constant and conductivity, the ground-wave field decreases at least as fast as inverse range-to-the-fourth, and further away, even more rapidly than this as the view point drops below the spherical-earth horizon. We calculate these exact fields over finite ground using industry-standard codes such as “NEC (Numerical Electromagnetic Code (Defence Technical Information Center)” and "GRWAVE (Rec. ITU-R P.368)". Hence we define a “pseudo-gain” as the power in dB on the surface at specific distances over land but normalized with respect to the gain over the highly conducting sea (assumed a perfect conductor). The “pseudo-gain” plots over land thus depend on distance from the transmit antenna. An omnidirectional radiating element is assumed for clarity. The next three figures show these "pseudo-gain" patterns for three HF frequency bands. In all cases, assumed ground dielectric constant is 8 and conductivity 0.005 mho/m, considered typical. Note that this considered dry ground.

FIGURE 87

"Pseudo-gains" on the horizon at 4.5 MHz for dipole above surface at land-sea interface

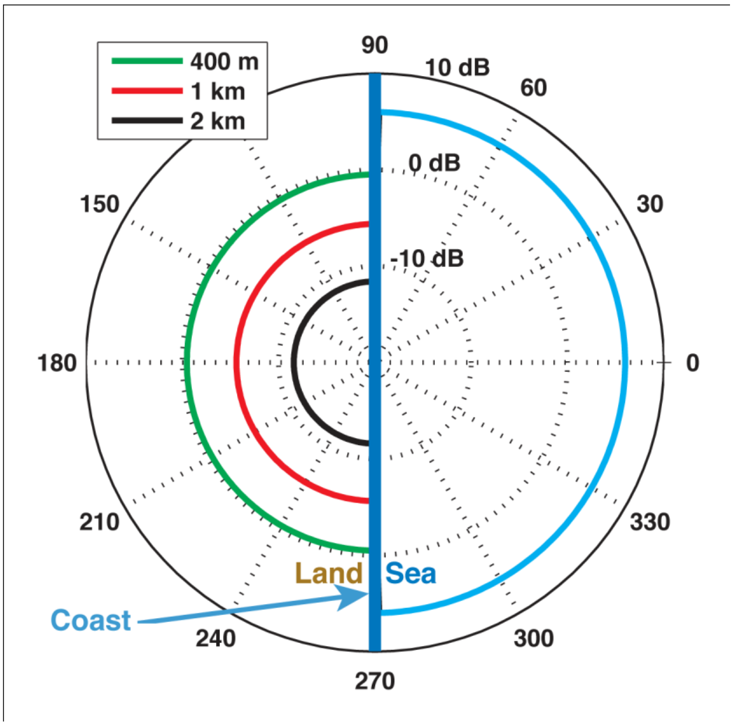

FIGURE 88

"Pseudo-gains" on the horizon at 13 MHz for dipole above surface at land-sea interface

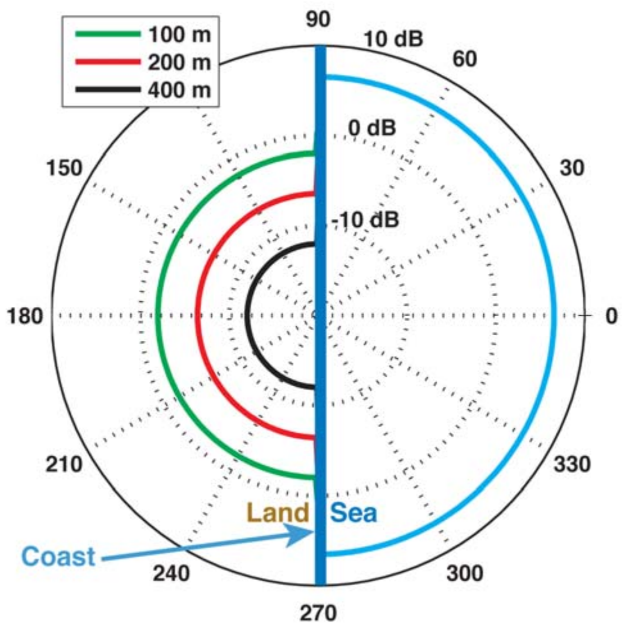

FIGURE 89

“Pseudo-gains” on the horizon at 25 MHz for dipole above surface at land-sea interface

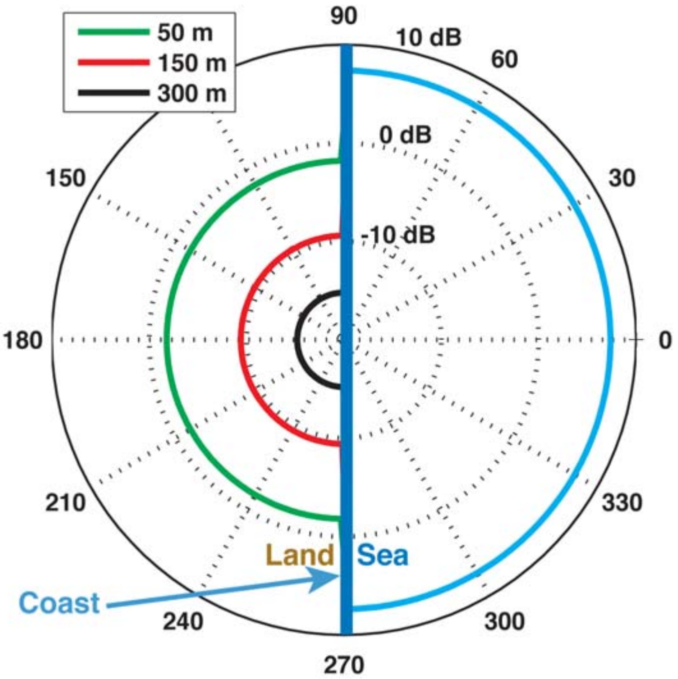

The point of Figs 87, 88 and 89 is the following. Compared with using arrays of elements to achieve horizon directivity to mitigate landward interference (see Fig. 86), the ground land attenuation is shown to provide much greater mitigation against interference into receivers. Even at the lowest frequency bands, the signal drops 6 dB at a distance of 400 m, which is what four transmit elements might have achieved (averaged over the 180° coastal sector). At 2 km back, the signal drops by 18 dB from that directed seaward. At the higher frequency bands, landward attenuation is considerably more severe. We do not show figures for 42 MHz..

9-4.4 Directive effect of land to minimize sky-wave signal interference back over land

Sky-wave propagation of oceanographic radar signals below 10 MHz has resulted in few interference complaints over the past two decades. Such ionospherically propagated signals are most significant in evening hours, and at elevation angles to the horizon of 20° or less. Signals higher than this in angle are more attenuated. Although transmit arrays can be conceived to partially reduce this low-angle sky-wave directivity, the array size requirements would increase. On the other hand, the low dielectric/conductive properties of ground on the landward side have the same effect as discussed above, i.e. they attenuate low-angle signals from vertical dipoles that would normally have a maximum on the horizon.

This is plotted in Fig. 90 below, which shows the gain pattern of such a dipole vs. elevation angle (horizontal axis).

FIGURE 90

Elevation pattern gain over ground showing low-angle attenuation caused by land

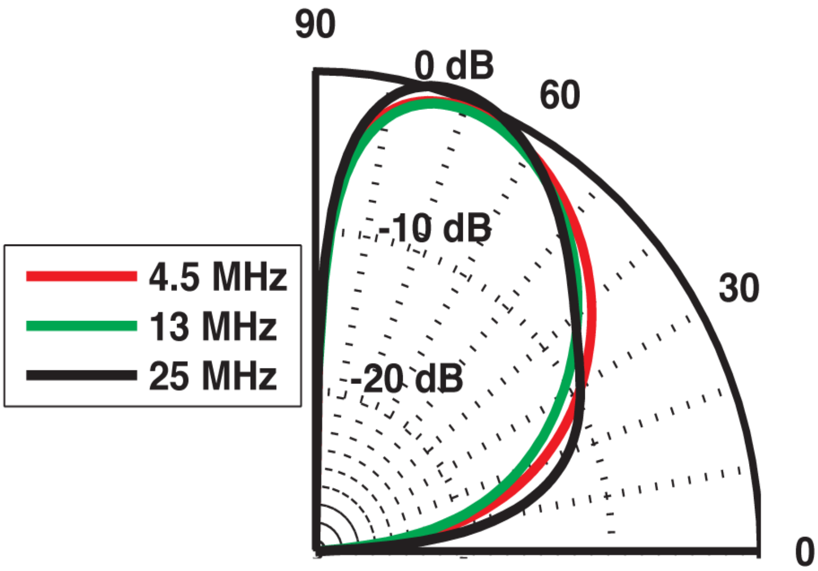

This study shows that at all frequency bands, sky-wave-propagated oceanographic radar signals below 20° are attenuated more than 10 dB below what would be obtained over perfect ground (or over the sea). Resorting to transmit arrays, as noted earlier, to achieve low-angle sky-wave signal attenuation could at best buy only another 3 to 4 dB, while driving up costs and objections to unsightly structures at pristine coastal locations where the oceanographic radars must be sited.

9-4.5 Added horizon attenuations not included in above studies

The above analyses leading to Figs 4 to 7 must be considered conservative: i.e. attenuation will always be even greater than these idealized plots show. These studies were done using NEC for perfectly flat ground behind the antenna. A spherical earth that slopes away always attenuates ground-wave signals further. But most important, trees, buildings, hills, and other irregular terrain will add considerably to the path loss. The oceanographic radar antennas are always at sea level, the lowest point of the land path. Although one can study specific terrain/building/foliage attenuation scenarios, it is difficult to give a number for this signal reduction that fits all situations. Such terrain/foliage effects offer greater attenuation at the higher frequency bands. Therefore, in the real world, added attenuation due to hills, foliage, buildings will further reduce both ground-wave and sky-wave signals propagating landward that can potentially interfere with other radio receivers.

9-5 Reduce interfering energy occurrence

9-5.1 Use spread-spectrum techniques

Earlier we talked about reducing the bandwidth of oceanographic radar signals as a way to minimize their spectral usage, and we discussed trade-offs and compromises with that approach. At the opposite extreme is the "spread-spectrum" approach used by some UHF communication and data systems. The idea here is to spread the signal over such a wide bandwidth, that within a narrow-band communications receiver channel, the energy density is so low that it is not seen above the noise. Because of a cleverly designed signal format, this spread-spectrum signal can be reconstructed in its receiver to convey the information intended.

In a sense, the oceanographic radars already realize this effect by spreading their energy over many small-bandwidth communications channels, thereby reducing the portion of the overall radiated oceanographic radar signal power that each observes. Spreading their energy further in bandwidth for this purpose will ultimately impact oceanographic radar complexity and performance adversely. Hence it is believed the practices arrived at for present oceanographic radars achieve the best mix of compromises for both oceanographic radar users and those who might be impacted by interference from the oceanographic radar signals.

9-5.2 Lower oceanographic radar radiated power

As with all trade-offs, lower radiated power implies less interfering signal strength into other receivers. However, oceanographic radar coverage distance is reduced by lower power. This must be weighed against increased oceanographic radar capital and operating costs if power is increased. Although experimental military-intended oceanographic radars have temporarily operated at average radiated power levels above 100 kW, oceanographic radars have a very modest average radiated power level of 40 Watts or lower. This 40-watt compromise allows a network of oceanographic radars to produce valuable information to the oceanographic radar user community.

9-6 Reducing out-of-band interference

9-6.1 Pulse shaping, filtering and signal gating

This document up to now has discussed potential interference only within the frequency band of the modulation on the radiated carrier signal. Every radio or oceanographic radar emits energy outside of this designed signal bandwidth. The source of this in oceanographic radars is the abrupt periodic changes in the waveform, including pulsing and discontinuities in the frequency sweep (e.g. at the end of the sweep when the cycle restarts), as well as nonlinearities in the transmit amplifier channels. Pulsing with sharp edges is known to produce sin(x)/x-type side lobes that fall off slowly away from the modulation spectral edges. Inevitable nonlinearities in the transmit channels generate second and third harmonics of the intended signal. Even if the main signal spectrum is not a problem, this unintended, spurious out-of-band radiation can often be the source of interference to others. Most oceanographic radars apply several methods to suppress this out-of-band radiation.

9-6.2 Low-pass filtering

After the last stage of transmit power amplification, a low-pass filter is used to suppress the higher harmonics of the radiated signal frequency. The 3 dB cutoff is set to about 15% higher than the carrier frequency. This has the effect of reducing second and third harmonics to 70 dB or more below the carrier. Natural antenna filtering and the propagation medium add several additional dB to this suppression.

9-6.3 Band-pass filtering

The final tool used by oceanographic radars is band-pass filtering. This is usually applied before final amplification. It is meant to suppress out-of-band interference that flares out from the intended edges of the signal frequency spectrum.

These techniques have proven highly effective in reducing out-of-band interference, such that this has never been a source of interference complaints.

9-6.4 Pulse shaping

The sharp on-off edges of a pulse are the source of adjacent channel spectral side lobes that can interfere with others. This can be drastically reduced by shaping the edges so that they are rounded at top and bottom and sloped in the middle. Many systems have used pulse shaping for many years. This shaping is designed digitally and stored as a look-up table, to be read out and applied during signal generation. The shape is programmable, so that it can be changed when appropriate. Such pulse shaping reduces out-of-band interference.

Figures 91 and 92 demonstrate the effects of pulse shaping by finite rising. Figure 91 shows wave form and its spectrum occupancy for pulse repetition interval T_p=1 ms, pulse width T_w=0.5 ms and pulse rise/fall time T_r=0 ms. Pulse edges are abruptly stepped, and the spectrum is widely spread. On the contrary, as shown in Fig. 92, a smooth-gated CW signal with a T_p=1 ms, T_w=0.5 ms and a T_r=0.2 ms has is represented by a spectrum that has steeply converged sidebands.

FIGURE 91

Waveform and spectrum of gated CW signal without pulse shaping. (The waveform between upper and lower envelops in pulse-on durations are filled by sinusoidal waveform of the carrier)

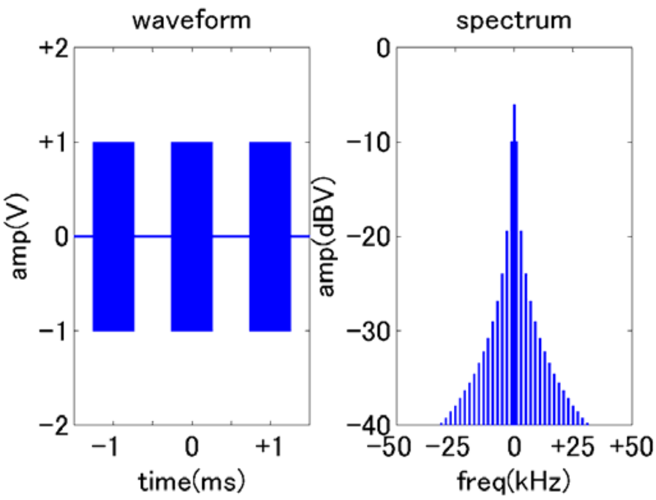

FIGURE 92

Waveform and spectrum of gated CW signal with pulse shaping. (The waveform between upper and lower envelops in pulse-on durations are filled by sinusoidal waveform of the carrier)

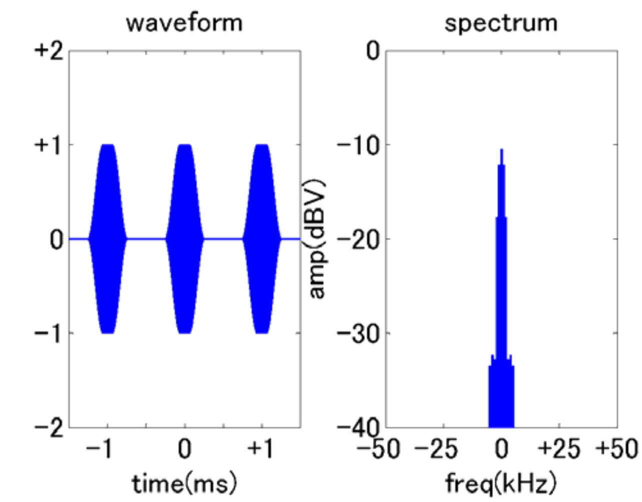

9-6.5 Signal gating

For FMICW modulation, higher order sidebands of pulse repetition frequency are generated. Interfered radars can avoid these sidebands by use of a synchronization technique. To apply this technique, propagation delays between radars should be considered.

Example of the generation of sidebands is illustrated in Fig. 93 where the pulse repetition interval (T_p) = 1 ms and the pulse width (T_w) = 0.5 ms. In this case, sidebands are generated at 1 kHz intervals and nulls occur at even order harmonics.

FIGURE 93

Waveform, spectrum and sweeping image of abrupt-gated CW signal. (The waveform between upper and lower envelops in pulse-on durations are filled by sinusoidal waveform of the carrier)

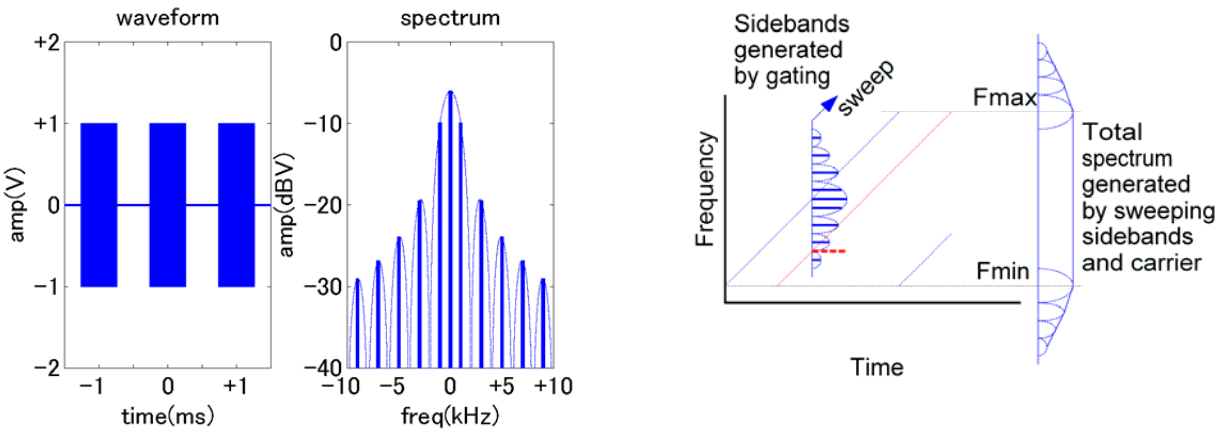

9-7 Conclusions

Starting with one or two oceanographic radars in 1970 that first measured current and waves, and increasing in number to over 250 worldwide today (most operating continuously in real time), this evolving experience under experimental licenses has produced much information about the impacts regarding interference to others. All of these oceanographic radars have operated on static frequencies. The most effective interference mitigation techniques are already being practiced. These include:

1) minimizing sweep bandwidth, without compromising the performance of the oceanographic radar mission, will reduce possible interference by reducing demand on the;

2) use of GPS to synchronize signal modulation allows many oceanographic radars to operate on the same frequency at the same time; this greatly reduces the spectral occupancy of networks;

3) keeping radiated power as low as possible without compromising data product utility;

4) use of pulse shaping and layers of filtering to reduce out-of-band interference;

5) using transmit antenna arrays to reduce gain in the backlobe over land (where susceptible receivers are located) was examined in light of the requirement that the seaward sector must be covered as uniformly as possible.

6) A "listen-before-transmit" operating mode for oceanographic radars was examined, so that multiple users with different missions could share the same channels. Several schemes were considered, including the ability of another licensed user to shut down co-channel oceanographic radars while transmitting needed messages. In all cases, compromises in performance to both other systems and oceanographic radars was deemed unacceptable.

Reducing out-of-band interference methods were examined in light of reducing the risk of interference without compromising oceanographic radar performance. Effectiveness of pulse shaping and filtering techniques were also described.

Experience has shown that the distances at which the oceanographic radar interference is received is less than those predicted in modelling studies. This is attributed primarily to two factors:

1) The external noise that is seen in practice is typically higher than the levels that are predicted from survey based models. This means that the noise into a receiver will mask any interfering signal below that level.

2) The assumption of flat ground behind the oceanographic radar antenna used in studies is not seen in practice. Trees and other foliage, terrain, hills that are higher than the coastal oceanographic radar's elevation, and buildings attenuate the potentially interfering signal, beyond that of the idealized flat or smooth spherical earth models of simulations.

Attachment 10

Study of sky-wave propagation interference impact in the Darwin region

10-1 Introduction

In this study the interference via sky-wave propagation of oceanographic radar transmissions on incumbent fixed and mobile service receivers is considered. Several model parameters can influence the assessment of interference. These include main and back lobe scenarios, peak or average interference levels, sunspot number, and geographic zone.

Characteristics of oceanographic radar transmission systems are represented by 13 generic systems as described in Recommendation ITU-R M.1874, and repeated here in § 3 Table 1. The system parameters and protection criteria for the incumbent service receivers were provided in ITU-R Document 5B/300 – Working Party 5C liaison statement to Working Party 5B, and are listed in § 2 of this Report. The measure of interference impact used here is based on the interference to noise ratio (INR) at the incumbent receiver.

10-2 Method

10-2.1 Incumbent receiver

The incumbent receiver parameters and protection criteria used in this study are:

- receiver bandwidth of 3 kHz;
- receivers externally noise limited by atmospheric, galactic and a “rural” noise environment;
- threshold INR = –6 dB;
- receiver antenna gain of 0 dBi.

10-2.2 Sky-wave propagation model

The recommended HF sky-wave propagation model for ITU analysis is that provided by Recommendation ITU-R P.533. For the purposes of this study a software program called the Ionospheric Communications Enhanced Profile Analysis and Circuit Prediction Program (ICEPAC available from NTIA Institute for Telecommunication Services) was used to calculate the model estimates. ICEPAC is based on Recommendation ITU-R P.533. The prediction procedure applies ray-path analysis up to path lengths of 7 000 km, with an empirical formulation beyond 9 000 km, and a smooth transition between. In this study we used both “area” and “point-to-point” calculations. The model provides an estimate of the monthly median maximum useable frequency (MUF) taken as the maximum of the E-layer and F2-layer MUFs. The propagation path transmission loss P_{Loss} is also estimated and accounts for range, absorption loss, multi-hop ground reflection loss, auroral losses, miscellaneous losses, and an additional *above-the-MUF* loss (L_m). An example loss calculation for the arbitrary Darwin to Alice Springs (Australia) circuit is shown in Fig. 94. A diurnal cycle is evident, and the slow loss decay *above the MUF* (overlaid white line) is observed.

FIGURE 94

Example model calculation of the monthly median propagation path transmission loss. The estimate of monthly median operational MUF is overlaid in white (SSN = 100, SEP 2002, Darwin to Alice Springs circuit)

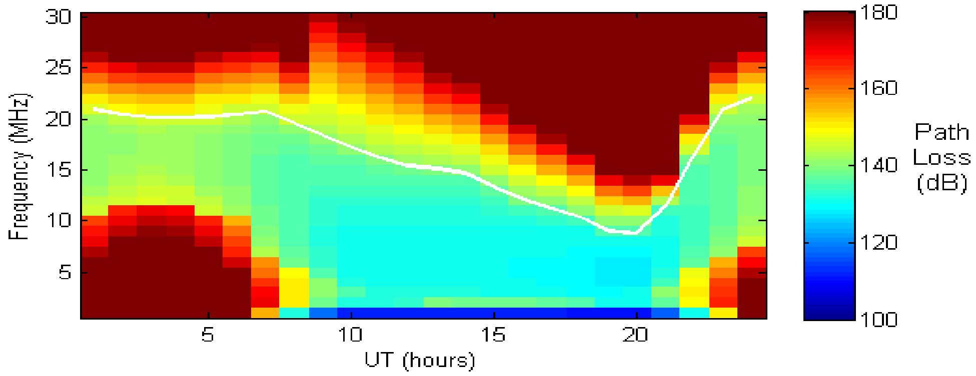

The interference power at the incumbent receiver location can be calculated as:

$$\begin{aligned} I(dBW) &= P_{Tx}(dBW) + G_{Tx}(dBi) - P_{Loss}(dB) + G_{Rx}(dBi) \\ &= EIRP(dBW) - P_{Loss}(dB) + G_{Rx}(dBi) \end{aligned}$$

where P_{Tx} is the transmission power, G_{Tx} is the transmitter antenna gain relative to an isotropic antenna, as defined in Table 1 of the main report body. In this study the elevation pattern of the transmitter is modelled as a half-wavelength vertical dipole (Fig. 95), with the gain normalised to G_{Tx}. This provides some realism as oceanographic radar are not required to achieve gain at high elevation, and although low elevation gain is desired it is difficult to achieve with vertically polarised signals. *E.i.r.p.* is the Effective Isotropic Radiated Power, and G_{Rx} is the receiver antenna gain relative to an isotropic antenna. For the purposes of this study, G_{Rx} = 0 dBi, and is dropped from further use. Figure 96 shows the interference power corresponding to the Fig. 94 loss example. In this example the transmit antenna is isotropic and an *e.i.r.p.* = 25 dBW was applied to match a sounder measurement system that will be shown in Fig. 97. The model propagation support above the MUF is evident. Below the MUF interference power is observed to increase at night (UT~15UT) as the absorption losses decrease; whilst the MUF decreases with reduced maximum ionospheric electron density.

FIGURE 95

Transmitter elevation pattern modelled as a vertical dipole of half-wavelength (ITS-78 Type 35)

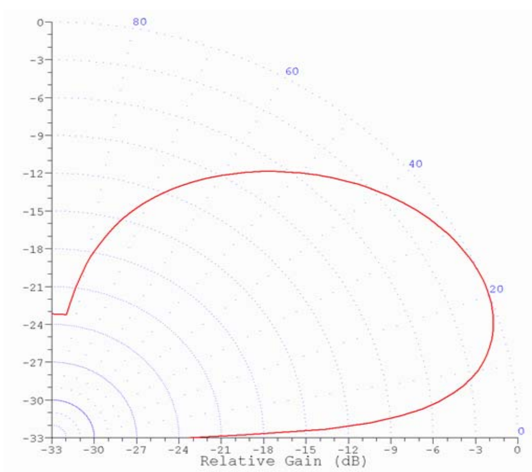

FIGURE 96

Example model calculation of the monthly median interference power (dBW). The estimate of monthly median operational MUF is overlaid in white (SSN = 100, SEP 2002, Darwin to Alice Springs circuit, *e.i.r.p.* = 25 dBW)

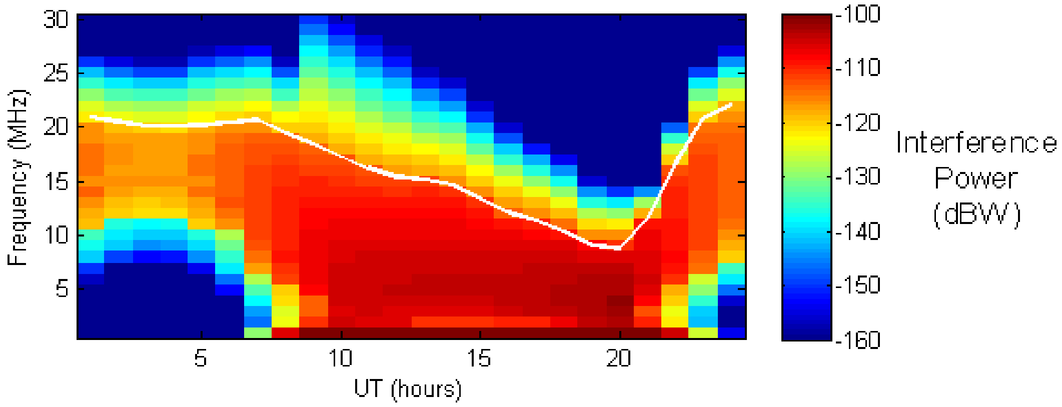

A spot check of the propagation model was made using oblique incidence sounder (OIS) measurements. Band availability (propagation support) may be calculated as the maximum signal power over all OIS group ranges (paths) as a function of frequency. Measurements from the OIS were collected for 20 days of September 2002, and the "monthly" median at each frequency and time-of-day calculated and plotted in Fig. 97. Sporadic-E contributions were rejected in this analysis. Figure 96 displays the comparative model estimate for the same month and a sunspot number reflecting that period. Note the OIS power and antenna gains are similar but not calibrated to the model. The general temporal characteristics between model and measurements are similar, apart from beyond the MUF where the model has unrealistic propagation support. The influence of support beyond the MUF will be to extend occurrence for any particular operating frequency.

FIGURE 97

Measured monthly median signal power (dBW) for the Darwin to Alice Springs circuit for September 2002 (sunspot maximum and ionospheric heights > 160 km)

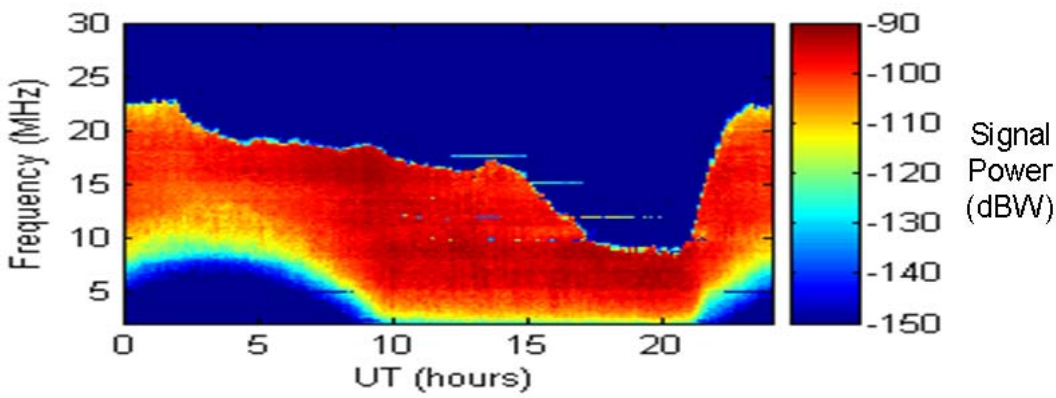

10-2.3 External noise model

The external noise energy is calculated as the sum of three sources, being atmospheric, man-made and galactic, as defined by Recommendation ITU-R P.372-10 – Radio Noise in terms of median values. The noise source standard deviations were not incorporated.

$$N_{Ext} = 10\log_{10}\left(10^{N_{man-made}/10} + 10^{N_{atmospheric}/10} + 10^{N_{galactic}/10}\right) \quad \text{dBW/Hz}$$

Here we consider the "rural" man-made noise environment. Galactic noise is assumed to contribute only above a frequency of 10 MHz, as specified in Fig. 10 of Recommendation ITU-R P.372-10.

Median atmospheric noise may be estimated from § 7 of Recommendation ITU-R P.372-10, which provides noise world charts at 1 MHz for each season and includes conversion curves to calculate noise levels at other frequencies. Software developed by ITU-R Study Group 3 named NOISEDAT was used. To avoid season confusion across hemispheres we refer only to months. An example estimate of monthly median atmospheric noise energy is shown in Fig. 98.

FIGURE 98

Atmospheric noise energy (dBW/Hz) estimate at 10 MHz for the month of December at 14 UT with correction to time-of-day error

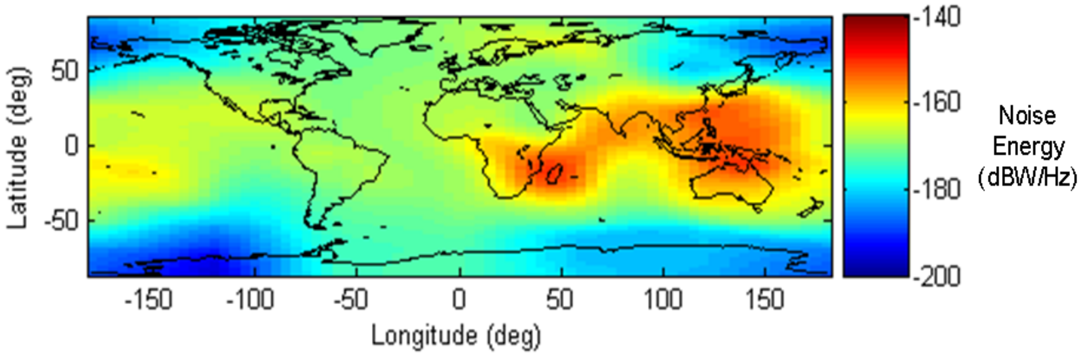

In this study we calculate the external noise energy at each incumbent receiver location using monthly median levels. This offers more protection to the incumbent service than the 80th percentile (over all time at a given location) used in § 6.4.3 and less protection than the 0.5 percentile (over all time and location) used in current PLT protection studies: Report ITU-R SM.2158-1 – Impact of power line telecommunication systems on radiocommunication systems operating in the LF, MF, HF and VHF bands below 80 MHz.

10-2.4 Calculation of INR

The interference on the incumbent service may be assessed using the INR metric. The noise power received depends on the external noise energy and the receiver bandwidth B_{Rx}:

$$N_{Rx}(dBW) = N_{Ext}(dBW/Hz) + 10Log_{10}B_{Rx}(Hz)$$

Hence the INR is calculated as:

$$INR(dB) = EIRP(dBW) - P_{Loss}(dB) - N_{Rx}(dBW)$$

The interference effect may be calculated in either the oceanographic radar transmitter's main lobe or back lobe directions, and if considered appropriate the average power level may be calculated rather than the peak power level. The average power level accounts for the waveform duty cycle and the short-term interference ratio. Measurement data provided in Attachment 7 suggests average power is not appropriate. Four cases of *EIRP* are thus considered in this study:

$$EIRP_{main}^{Peak} = P_{Tx} + G_{Tx}^{main}$$

$$EIRP_{back}^{Peak} = P_{Tx} + G_{Tx}^{back}$$

$$EIRP_{main}^{Avg} = P_{Tx} + G_{Tx}^{main} + 10Log_{10}\frac{B_{Rx}}{B_C} + 10Log_{10}D$$

$$EIRP_{back}^{Avg} = P_{Tx} + G_{Tx}^{back} + 10Log_{10}\frac{B_{Rx}}{B_C} + 10Log_{10}D$$

where *Peak* refers to the peak power, *Avg* the short-term average power, *D* denotes the oceanographic waveform duty cycle, and B_C denotes the oceanographic radar waveform bandwidth. The values for each of the *e.i.r.p.* cases for the generic oceanographic radar systems may be obtained from Table 1.

As an example geographic calculation, Fig. 99 shows *INR* for several times-of-day and frequencies for an oceanographic radar of *e.i.r.p.* = 12 dBW arbitrarily located near Darwin, Australia. The *INR* at the incumbent receiver was calculated for receiver locations at 1° increments within a ±30° latitude and longitude grid. We observe low INR at daytime low frequency due to D-layer absorption, and low INR at night time high frequency due to insufficient electron density to support ionospheric reflection.

FIGURE 99

INR calculations in Darwin region for a vertical dipole transmitter antenna with *e.i.r.p.* = 12 dBW during April with SSN = 100 in a rural environment

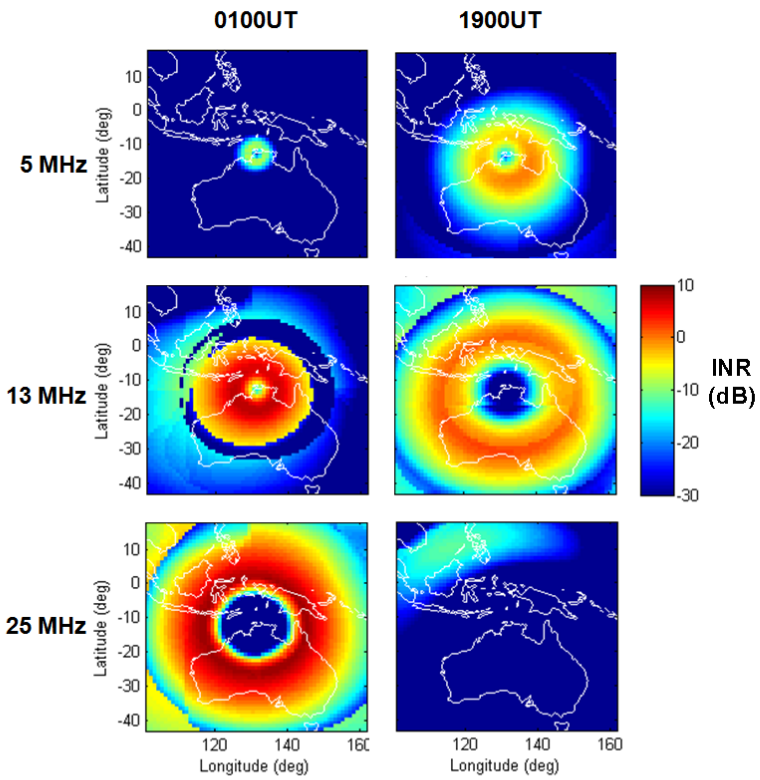

The *INR* geographic cumulative distributions (CDF) for each hour of the day, four seasonal months, and several operating frequencies can be calculated as shown in Fig. 100. A strong dependence is exhibited against time-of-day and operating frequency. The cumulative distribution is interpreted at the fraction of the analysed geographic region that does not exceed a given *INR*. A high CDF value at *INR* = –6 indicates a low level of interference. Calculation of the temporal average (sampled over month and time-of-day) provides the resultant CDF curves of Fig. 101 as a function of operating frequency, and based on a “rural” environment, sunspot number of 100, and an *e.i.r.p.* of 12 dBW.

From these curves the percentage of the time-region samples the INR exceeds the threshold level of –6 dB can be found.

FIGURE 100

Regional INR cumulative distributions for the Darwin region, as a function of time-of-day, month, in a rural environment, *e.i.r.p.* = 12 dBW, SSN = 100

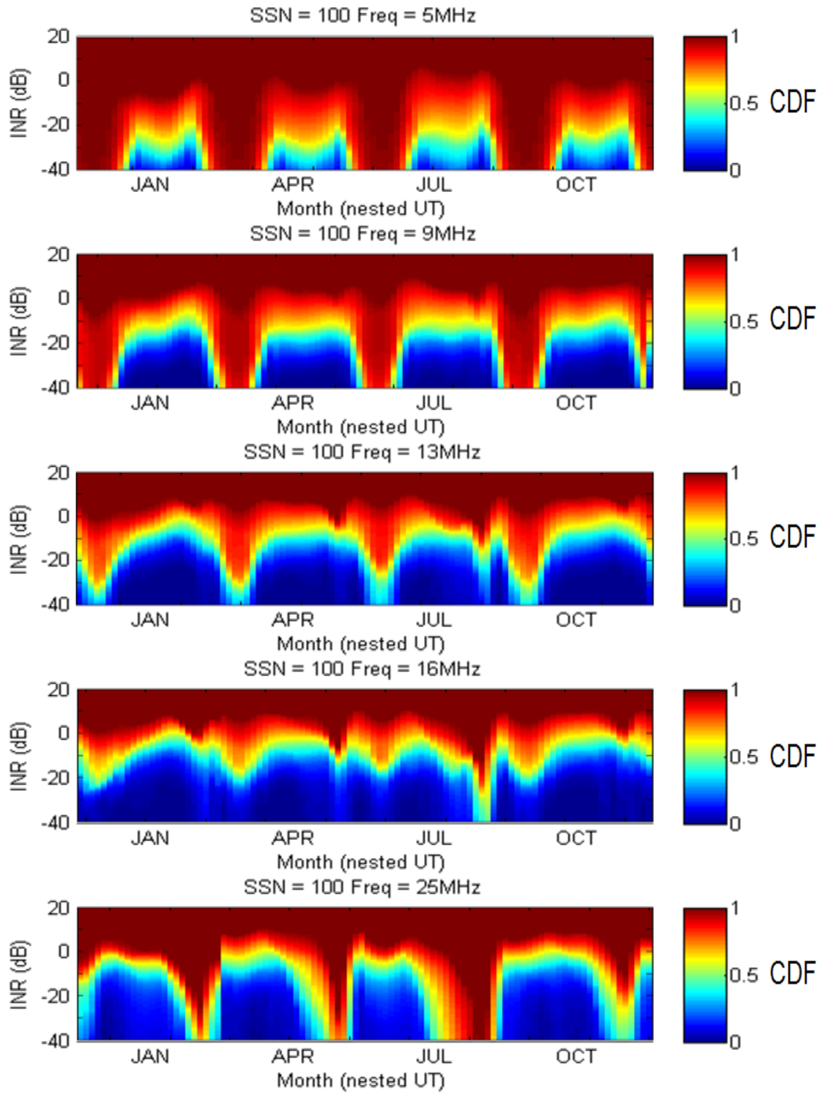

FIGURE 101

INR time-region cumulative distributions for Darwin ±30 deg region, at SSN = 100, rural environment, with an *e.i.r.p.* = 12 dBW

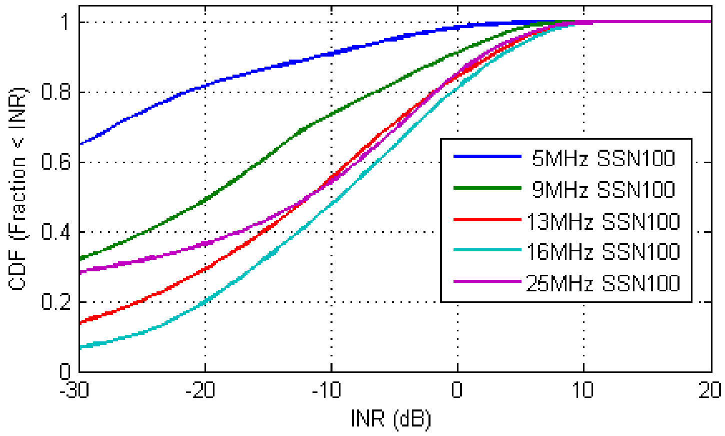

10-3 Results

10-3.1 Interference occurrence

The INR was calculated for the Darwin region (±30 deg), for each of the HF oceanographic systems of Table 1. The resulting percentage of time-region that exceeded a level of INR = –6 dB, termed interference occurrence, is listed in Table 49. The calculations assumed a "rural" noise environment together with galactic and atmospheric components, and were made at high and low sunspot number, for both peak and average interference levels, and both transmit antenna main and back lobe directions. The transmitter antenna was modelled as a vertical dipole.

The INR interference occurrence as a function of e.i.r.p. may be derived from the time-region CDFs, and are plotted in Figs 102 and 103 for SSNs=10 and 100 respectively. Overlaid on these plots are the values for the generic oceanographic radar systems. Interference occurrence is lower at 5 MHz and 25 MHz during low SSN.

TABLE 49

Percentage of time-region that INR exceeds –6 dB in a rural environment

Darwin ±30 deg, 1 deg resolution, rural environment									
Generic system	Freq band (MHz)	Signal peak level				Signal average level			
		Main lobe		Back lobe		Main lobe		Back lobe	
		SSN=10	SSN=100	SSN=10	SSN=100	SSN=10	SSN=100	SSN=10	SSN=100
1	5	18.6	16.0	18.6	16.0	7.2	5.5	7.2	5.5
2	13	61.8	66.6	61.8	66.6	15.1	22.7	15.1	22.7
3	25	24.2	61.1	24.2	61.1	2.5	14.0	2.5	14.0
4	42	–	–	–	–	–	–	–	–
5	9	44.8	43.3	13.3	13.4	28.7	27.6	3.6	3.6
6	13	57.7	63.8	15.2	22.8	19.0	27.8	0.0	0.2
7	16	53.9	72.3	14.4	27.8	18.6	34.0	0.0	0.4
8	25	22.9	59.4	5.1	23.5	5.1	23.6	0.0	0.0
9	42	–	–	–	–	–	–	–	–
10	9	75.1	68.0	31.7	30.4	49.0	47.2	8.8	9.2
11	25	33.2	71.1	15.8	48.5	15.5	47.9	0.0	1.5
12	25	28.8	66.7	7.5	30.9	7.3	30.1	0.0	0.0
13	42	–	–	–	–	–	–	–	–

FIGURE 102

Interference occurrence for Darwin ±30 deg region, SSN = 10, rural environment, months January, April, July and October, over all hours, calculated with INR threshold = –6 dB. The overlaid numbers locate the values for the generic oceanographic radar systems, assuming either peak main lobe or average back lobe power

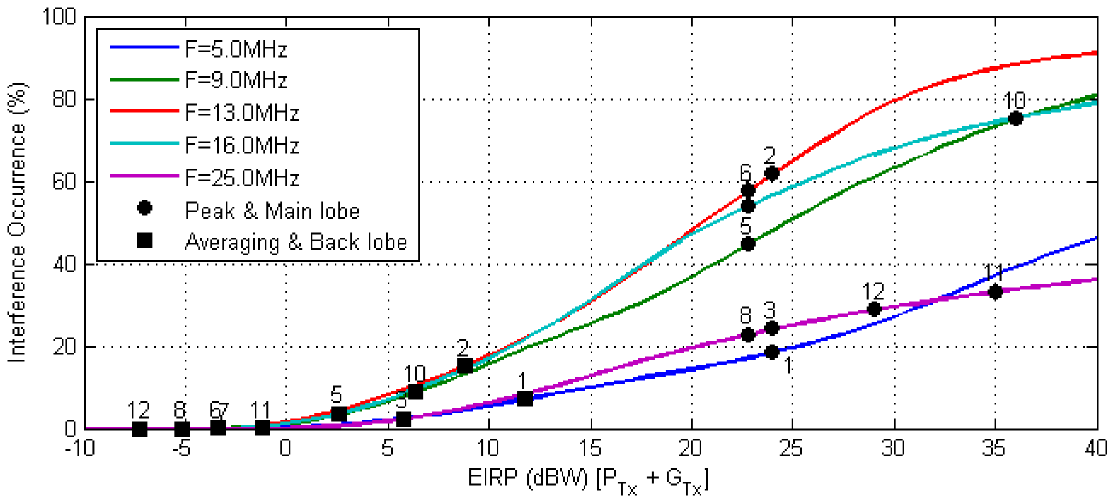

FIGURE 103

Interference occurrence for Darwin ±30 deg region, SSN = 100, rural environment, months January, April, July and October, over all hours, calculated with INR threshold = –6 dB. The overlaid numbers locate the values for the generic oceanographic radar systems, assuming either peak main lobe or average back lobe power

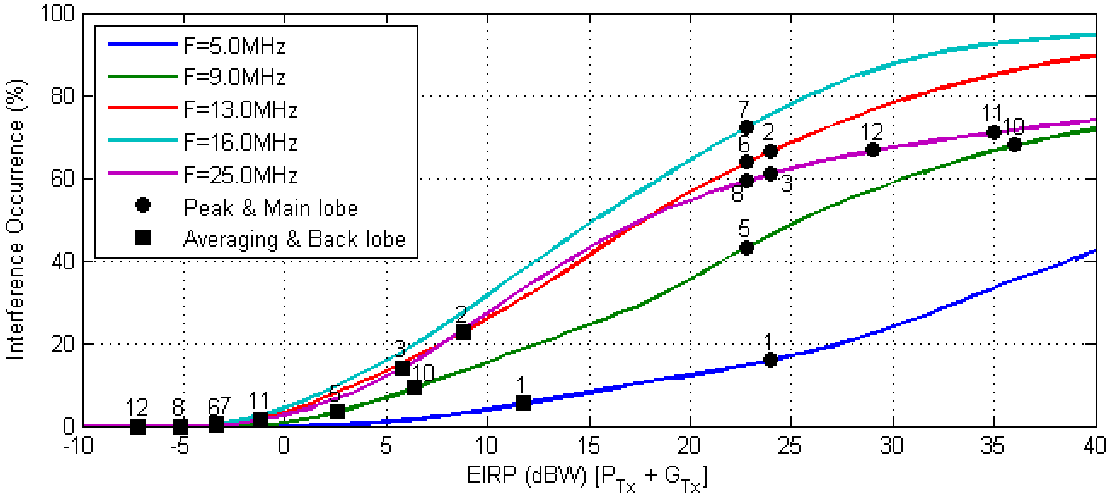

10-4 Conclusions

A study of the occurrence of sky-wave propagated interference on incumbent fixed and mobile service receivers as caused by generic oceanographic radar systems was conducted. The study assumed the oceanographic radar was arbitrarily located near Darwin Australia, and calculated the interference to noise ratio at the incumbent receiver using recommended ITU-R HF propagation and radio noise monthly median models. The transmitter elevation pattern was modelled as a rudimentary vertical dipole to provide low and high elevation attenuation. This provides some realism as oceanographic radars are not required to achieve gain at high elevation, and although low elevation gain is desired it is difficult to achieve with vertically polarised signals. The calculations assumed a "rural" noise environment together with galactic and atmospheric components, and were made for high and low sunspot number, both peak and average interference levels, and both transmit antenna main and back lobe directions. Interference occurrence was less than 20% when considering average level signals in the back lobe, but higher if the peak level signal in the forward direction is considered. Interference occurrence is less at 5 MHz and at 25 MHz during low SSN. Antenna back lobe gain attenuation provides some interference mitigation in that direction. Interference is significantly different between peak power and average power calculations. In this attachment, a transmitter antenna configuration has been used which matches that used by other oceanographic radar ITU-R studies to date, but there would be benefit from conducting further modelling studies utilising alternative, more effective, transmitter antenna configurations to properly gauge the impact of oceanographic radars on incumbent services.

Attachment 11

An experimental study for the evaluation of compatibility criteria between HF oceanographic radars and digital data systems

11-1 Introduction

Operating HF oceanographic radars within the radio spectrum of fixed and land mobile services will introduce interference to co-channel users of fixed and land mobile services, in particular to HF digital data systems. An experimental study was carried out in order to investigate interference effects and to establish the necessary set of operating parameters to enable the simultaneous operation of the oceanographic radar and digital data systems within the same radio spectrum. Details of the setup, process and findings are outlined below.

11-2 Description of experimental setup

The experimental setup shown in Fig. 104, a digital data error analyzer (source/sink) device is connected to a digital data modem which in turn is connected to the radio transmitter. The radio transmitter is connected to the radio receiver using a 3-port signal summation device Σ which combines the modulated RF signal with the additive white Gaussian noise (AWGN) source and simulated pulsed radar signals. The received radio signal is then passed to the receiving digital modem which in turn passes the data back to the data error analyser device for analysis and bit error ratio (BER) evaluation.

The digital data waveform parameters include 64-QAM modulation, data rate of 9 600 bps, 3 kHz bandwidth and long interleaver. The data modem used in this experiment is described in the Annex 6 of Recommendation ITU-R F.763-5 – Data transmission over HF circuits using phase shift keying or quadrature amplitude modulation. The oceanographic radar signal is simulated as described in Recommendation ITU-R M.1874 – Technical and operational characteristics of oceanographic radars operating in sub-bands within the frequency range 3-50 MHz. The typical oceanographic radar waveform parameters used are given in Table 50.

The simulated oceanographic radar waveforms used in the experiment are FMCW amplitude modulated signal. An amplitude modulated FMCW linear chirp waveform is used as the source of interference into the victim digital data link, with the pulse period and duty cycles given in Table 50. Figure 105 illustrates the waveform structure of typical oceanographic radars. The waveform at the top of the figure represents an FMCW signal. The waveform at the bottom is representative of amplitude modulated or a gated FMCW radar signal.

11-3 Description of experiment

In this experiment, the BER is monitored as digital data is passed through the AWGN HF channel (no fading) while the oceanographic radar signal is injected into the channel.

The experiment is conducted for the centre frequencies specified in Table 50. The 3 kHz bandwidth of the data waveform is centered on the centre frequency of the oceanographic radar centre frequency and the oceanographic radar sweep was adjusted to start at centre frequency – ½ (sweep bandwidth) and end at centre frequency + ½ (sweep bandwidth) for the three typical oceanographic radar waveforms. The oceanographic radar signal sweep time, pulse period and the duty cycle for each centre frequency are included in Table 50.

FIGURE 104

Experimental evaluation of spectrum compatibility between HF oceanographic radar and digital data link

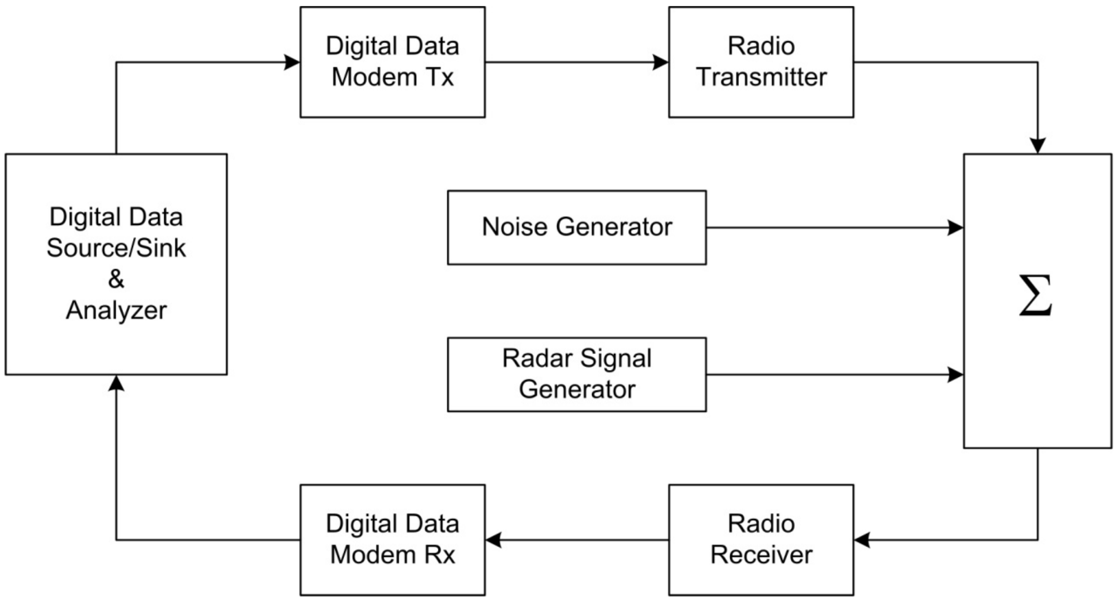

TABLE 50

List of typical oceanographic radar waveform parameters

Centre frequency (MHz)	Sweep bandwidth (kHz)	Sweep time T_{Sweep} (s)	Pulse period $T_{PulsePeriod}$ (s)	Duty cycle (%)	Measured PAPR (dB)
4.53	25.6	1	1 946	50	31
13.46	49.4	0.5	669	50	61
24.65	101	0.5	486	50	61

A 3-port signal summation device Σ is inserted into the radio link between the transmitter and receiver as shown in Fig. 104. The signal summation device combines the modulated RF signal with AWGN source and simulated oceanographic radar signal prior to receiver antenna input. The experiment is conducted for the centre frequencies specified in Table 50. The 3 kHz bandwidth of the data waveform is centered on the centre frequency of the oceanographic radar centre frequency and the oceanographic radar sweep was adjusted to start at centre frequency – ½ (sweep bandwidth) and end at centre frequency + ½ (sweep bandwidth) for the three typical oceanographic radar waveforms. The oceanographic radar signal sweep time, pulse period and the duty cycle for each centre frequency were as shown in the Table 50.

FIGURE 105

Typical oceanographic radar waveform structures

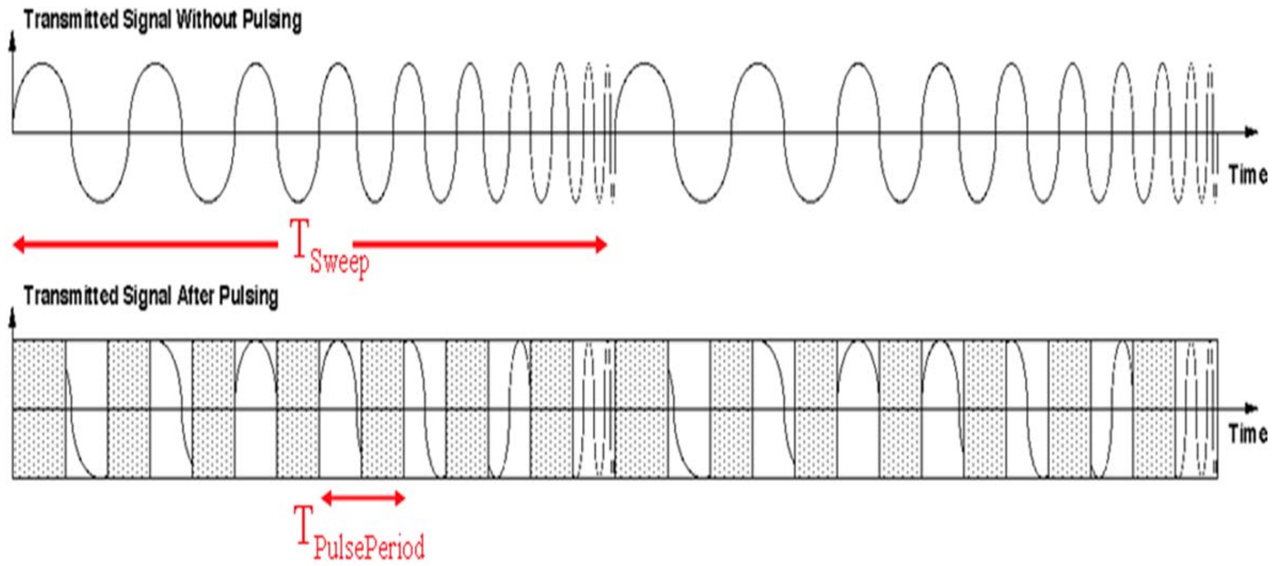

The digital HF radio link S/N is initially calibrated without the oceanographic radar signal for a BER of 1 in 10^5. After the noise level is determined, the oceanographic radar signal is introduced with interference to noise ratio (I/N) equal to –6 dB (i.e. 6 dB below the noise level) as compatibility criteria. This calibration allows for the results to be independent of the absolute strength of the oceanographic radar signal. The test was run with the peak power of the oceanographic radar signal set at the I/N level of –6 dB, and again with the average power of the oceanographic radar signal set at the I/N level of –6 dB. In the case of the average oceanographic radar power level set to 6 dB below the noise floor, the resulting peak power was well above the –6 dB I/N level. The experiment is repeated for the centre frequencies presented in Table 50.

Table 50 also shows the peak-to-average power ratios, (PAPR) is a measurement of the oceanographic radar waveform, measured from the peak amplitude of the waveform divided by the RMS value of the transmitted gated waveform.

11-4 Results and conclusion

The performance degradation observed for the digital data link was very small (degradation from 1×10^{-5} to less than 3×10^{-5}) when the oceanographic radar interference peak level was set to I/N = –6 dB with results within experimental error margins for the three oceanographic radar centre frequencies used. The experiment was repeated using the average of the oceanographic radar signal instead of the peak signal level for I/N = –6 dB setting. The observed BER increased to 1×10^{-1}, which is very severe degradation for digital data links, for all three oceanographic radar centre frequencies.

The compatibility studies for HF digital data links and oceanographic radars should use waveform's peak signal levels for interference calculations. In addition, degradation should not be scaled with the bandwidth ratio of data and oceanographic radar waveforms.

Attachment 12

Glossary

Glossary of Abbreviations

AM	Amplitude modulation
AWGN	Additive white gaussian noise
BER	Bit error ratio
BNetzA	Bundesnetzagentur
CDF	Cumulative distribution function
CW	Continuous wave
DANL	Displayed average noise level
dB	Decibel(s)
dBi	dB referred to the gain of an isotropic antenna
dBm	dB referred to one milliwatt
dBm/Hz	dB referred to one milliwatt per hertz
dBW	dB referred to one watt
e.i.r.p.	Effective isotropic radiated power
ENG	Electronic news gathering
FCC	Federal Communications Commission
FDR	Frequency dependent rejection
FFT	Fast fourier transform
FMCW	Frequency modulated continuous wave
FMICW	Frequency modulated interrupted continuous wave
FSL	Free space loss
FOT	Frequency of optimal transmission
GPS	Global positioning system
HF	High frequency
INR	Interference to noise ratio
ITS	Institute for Telecommunication
ITU	International Telecommunication Union
ITU-R	ITU Radiocommunication Sector
kHz	kilohertz
LNA	Low noise amplifier
LOS	Line-of-sight
MHz	Megahertz
MUF	Maximum useable frequency

NTIA	National Telecommunications and Information Administration
OIS	Oblique incidence sounder
OR	Oceanographic radar
PAPR	Peak to averager power ratio
PLT	Power line telecommunications
PPDR	Public protection and disaster relief
QAM	Quadrature amplitude modulation
RBW	Resolution bandwidth
RMS	Root mean square
Rx	Receiver
SNR	Signal-to-noise ratio
SSB	Single sideband
SSN	Sun spot number
Tx	Transmitter
UHF	Ultra high frequency
W	Watt
WRC	World Radiocommunication Conference
WRC-07	WRC 2007
WRC-12	WRC 2012